Computational strategies to characterize topological properties of pathologically altered functional brain networks

Darwin Eduardo Martínez Riaño

Universidad Nacional de Colombia
Facultad de Ingeniería, Departamento de Ingeniería de Sistemas e Industrial
Bogotá, Colombia
2022

Computational strategies to characterize topological properties of pathologically altered functional brain networks

Darwin Eduardo Martínez Riaño

Thesis submitted as requirement to obtain a:
Ph.D. en Ingeniería de Sistemas y Computación

Advisor:
Ph.D. Francisco Albeiro Gómez Jaramillo

Co-Advisor:
Ph.D. Fabio Augusto González Osorio

Research Field:
Applied computation

Research group:
Computational modelling of biological systems (COMBIOS)

Universidad Nacional de Colombia
Facultad de Ingeniería, Departamento de Ingeniería de Sistemas e Industrial
Bogotá, Colombia
2022

Dedication

To my loved family

They teach me with patient and love. They provide me the courage and strength that I need in this path.

To Sara and Yomara

The girls that improve my life.

Acknowlegments

I would like to thanks Francisco, my advisor, an awesome person who inspired me to believe, and to keep advancing, to bring opportunities to everyone because everyone has something unique to offer. To Fabio, my co-advisor, who boost the work with his rigour and perspectives. Also, I would like to thanks Jorge and Manuel "my pals" for the interesting discussions, insights and boosting to do and finish my PhD. To Rudas for the continuous talks about consciousness and processes. To the project "*Caracterización de la conectividad estructural y funcional del sistema reticular ascendente por medio de resonancia magnética con tractografía y BOLD, para la predicción del estado de conciencia en pacientes posreanimación o con lesión cerebral traumática*" (Code: 5007-744-55796. CT: 702-2016) from programa nacional de ciencia, tecnología e innovación en salud of Colciencias 744. This project provides the images of patients with an acute altered state of consciousness. Finally, to the Universidad Central, and its Programa de Desarrollo Profesoral, for the partial-time and fund which help me to support this journey.

Awards, Publications and Conferences

Awards

- Grant to be part of the 2014 International Brain Research Organization course of Neurobioinformática y Neurociencia Computacional at Universidad Javeriana and Universidad Nacional de Colombia. October - November 2014.
- Fees exemption due to average grades in the VIII Catedra Internacional - Computational Neuroscience. Universidad Nacional de Colombia. January 2015.
- Best paper award in the 10CCC Congreso Colombiano de Computación. September 2015.
- Merit Abstract Travel Stipend in the 23^{rd} Annual Meeting of the Organization of Human Brain Mapping. June 2017.
- Best student paper award, 7^{th} BESC, International Conference on Behavioral and Social Computing. November 2020.

Publications

Journals

- **Martínez D.**, Rudas J., Demertzi A., Charland-Verville V., Soddu A., Laureys S. & Gómez F., "Reconfiguration of large-scale functional connectivity in patients with disorders of consciousness", *Brain and behavior* **10 (1)**, e1476 (2019).
- Parra-Morales A. M., Rudas J., Vargas J. A., Gómez F., Enciso-Olivera C., Trujillo-Rodríguez D., **Martínez D.**, Hernández J., Ordóñez-Rubiano E., & Marín J., "Structural and functional connectivity of ascending reticular activating system in a patient with impaired consciousness after a cardiac arrest: A case report", *Medicine* **98 (19)**, e15620 (2019).
- Rudas J., **Martínez D.**, Castellanos G., Demertzi A., Martial C., Carriére M., Aubinet C., Soddu A., Laureys S. & Gómez F., "Time-Delay Latency of Resting-State Blood

Oxygen Level-Dependent Signal Related to the Level of Consciousness in Patients with Severe Consciousness Impairment", *Brain Connectivity* **10 (2)**, 83–94 (2020).

- Moreno-Ayure M., Páez C., López-Arias M. A., Mendez-Betancurt J. L., Ordóñez-Rubiano E. G., Rudas J., Pulido C., Gómez F., **Martínez D.**, Enciso-Olivera C. O., Rivera-Triana D. P., Casanova-Libreros R., Aguilera N.,& Marín-Muñoz J., "Establishing an Acquisition and Processing Protocol for Resting State Networks with a 1.5 T Scanner: A case series in a middle-income country", *Medicine* **99 (28)**, e21125 (2020).

- Enciso-Olivera, C., Ordóñez-Rubiano, E., Casanova-Libreros, R., Rivera, D., Zarate-Ardila, C., Rudas, J., Pulido, C., Gómez, F., **Martínez-Riaño, D. E.**, Guerrero, N., Hurtado, M., Aguilera-Bustos, N., Hernández-Torres, C., Hernandez, J. & Marín-Muñoz, J., "Structural and Functional Connectivity of the Ascending Arousal Network for Prediction of Outcome in Patients with Acute Disorders of Consciousness", *Scientific Reports* **11**, 22952 (2021).

- **Martínez-Riaño, D. E.**, González, F., Gómez, F., "$\mathcal{H}_1$ persistent features of resting-state connectome in healthy subjects", *Network Neuroscience* , 1-33 (2022).

Proceedings

- **Martínez D.**, Mahalingan J., Soddu A., Franco H., Lepore N., Laureys S. & Gómez F., "Influence of the segmentation on the characterization of cerebral networks of structural damage for patients with disorders of consciousness", *Proc. SPIE 9287 - Symposium International of Processing and Analysis of Medical Images (SIPAIM) 2014* , 1–8 (2015).

- **Martínez D.**, Martínez J., Rudas J., Demertzi A., Heine L., Tshibanda L., Soddu A., Laureys S., & Gómez F., "A graph based characterization of functional resting state networks for patients with disorders of consciousness", *Proc. IEEE - 20^{th} Signal Processing, Images and Computer Vision (STSIVA) 2015* , 1–8 (2015).

- Rudas J., **Martínez D.**, Guaje J., Demertzi A., Heine L., Tshibanda L., Soddu A., Laureys S. & Gómez F., "Reduction of resting state network segregation is linked to disorders of consciousness", *Proc. SPIE - SIPAIM 2015* **9681**, (2015).

- **Martínez D.**, Martínez J., Rudas J., Demertzi A., Heine L., Tshibanda L., Soddu A., Laureys S., & Gómez F., "Functional resting state networks characterization through global network measurements for patients with disorders of consciousness", *Proc. IEEE - 10^{th} CCC Congreso Colombiano de Computación* , 286–293 (2015).

- Rudas J., **Martínez D.**, Demertzi A., Heine L., Tshibanda L., Soddu A., Laureys S. & Gómez F., "Multivariate functional network connectivity for disorders of consciousness", *Lecture Notes in Computer Science - Proc. CIARP 2016* **10125**, 434–442 (2016).

- Rudas J., **Martínez D.**, Demertzi A., Di Perri C., Heine L., Tshibanda L., Castellanos G., Soddu A., Laureys S. & Gómez F., "An extended representation of the brain dynamics based on hypergraph for disorders of consciousness", *Proc. Human Brain Mapping* , (2017).

- **Martínez D.**, Rudas J., Demertzi A., Heine L., Soddu A., Becerra E., Perea J., Laureys S., & Gómez F., "TDA barcodes to identify topological features of resting state fMRI time courses in healthy subjects", *Proc. Human Brain Mapping* , (2017).

- Quiazúa G., Rojas C., Ordoñez J., **Martínez D.**, Enciso-Olivera C. & Gómez F., "Computer Assisted Assignment of ICD Codes for Primary Admission Diagnostic in ICUs", *Proc. Springer - 12^{th} Congreso Colombiano de Computación* **CCIS 735**, 211–223 (2017).

- Parra-Morales, A. M., Ordóñez-Rubiano E.G., Rudas J., Gómez F., **Martínez D.**, Hernández J., Marín Muñoz J. H., Enciso-Olivera C. O. & Trujillo-Rodríguez D., "Tractography and Resting State fMRI Analysis in a Patient with Impaired Consciousness after a Cardiac Arrest: A Case Report", *Proc. Understanding consciousness: A scientific quest for the 21st century* , 235–238 (2018).

- Rudas J., Trujillo D., **Martínez D.**, Salomón C., Vargas J., Ordóñez-Rubiano E., Herández J., Marín J. & Enciso C., "Assessing Multiple Resting State Networks in 1.5 T Functional MRI in Patients with Acute Brain Injury", *Proc. Understanding consciousness: A scientific quest for the 21st century* , 242–244 (2018).

- Rudas J., **Martínez D.**, Trujillo-Rodríguez D., Enciso-Olivera C., Ordóñez-Rubiano E., Marín J. & Gómez F., "Disruption of Functional Connectivity Between Ascending Reticular Activating System and Cortex in Patients with Impaired Consciousness After a Hypoxic Brain Injury", *Proc. Brain Injury Conference* **33**, 277–278 (2019).

- Reyes A. M., Rudas J., Pulido C., Victorino J., **Martínez D.**, Narvaez L. Á. & Gómez F., "Characterization of temporal patterns in the occurrence of aggressive behaviors in Bogotá (Colombia)", *Proc. BESC 2020* , 1–4 (2020).

- Pulido C., Reyes A. M., Rudas J., Victorino J., **Martínez D.**, Narváez L. Á. & Gómez F., "An evolutionary algorithm for reducing fear of crime", *Proc. BESC 2020* , 1–6 (2020).

- Rudas J., Reyes A. M., Pulido C., Chaparro L. F., Victorino J., **Martínez D.**, Narváez L. Á. & Gómez F., "Consistent spatial decomposition of temporal occurrence of aggressive behaviors: A case study in Bogotá, Colombia", *Proc. ASONAM - FAB 2020* , 715–719 (2020).

- Victorino J., Rudas J., Reyes A. M., Pulido C., Chaparro L. F., **Martínez D.**, Narváez L. Á. & Gómez F., "Spatial-temporal patterns of aggressive behaviors. A case study Bogotá, Colombia", *Proc. ASONAM - FAB 2020* , 667–672 (2020).

- Chaparro L. F., Pulido C., Rudas J., Reyes A. M., Victorino J., **Martínez D.**, Narváez L. Á. & Gómez F., "Sentiment Analysis of Social Network Content to Characterize the Perception of Security", *Proc. ASONAM - FAB 2020* , 685–691 (2020).

- Chaparro L. F., Pulido C., Rudas J., Reyes A. M., Victorino J., Narváez L. Á., **Martínez D.** & Gómez F., "Interpretability Of The Perception Of Security Based On Tweets Content", *Proc. ICAPAI 2021* , e0001-e0006 (2021).

- Reyes A. M., Rudas J., Pulido C., Chaparro L. F., Victorino J., Narváez L. Á., **Martínez D.** & Gómez F., "Multimodal prediction of aggressive behavior occurrence using a decision-level approach", *Proc. 11th ICPRS 2021* , 163–169 (2021).

Conferences

- **Martínez D.** & Gómez F., "Influence of the segmentation on the characterization of structural damage for patients with disorders of consciousness", *School of Computational Neurocience, IBRO*, Bogotá, Colombia, November 6 2014.

- **Martínez D.**, Mahalingan J., Soddu A., Franco H., Lepore N., Laureys S. & Gómez F., "Influence of the segmentation on the characterization of cerebral networks of structural damage for patients with disorders of consciousness", *Symposium International of Processing and Analysis of Medical Images (SIPAIM) 2014*, Cartagena de Indias, Colombia, October 15 2014.

- **Martínez D.**, Martínez J., Rudas J., Demertzi A., Heine L., Tshibanda L., Soddu A., Laureys S., & Gómez F., "A graph based characterization of functional resting state networks for patients with disorders of consciousness", 20^{th} *Signal Processing, Images and Computer Vision*, Bogotá, Colombia, September 3 2015.

- **Martínez D.**, Martínez J., Rudas J., Demertzi A., Heine L., Tshibanda L., Soddu A., Laureys S., & Gómez F., "Functional resting state networks characterization through global network measurements for patients with disorders of consciousness", 10^{th} *CCC Congreso Colombiano de Computación*, Bogotá, Colombia, September 24 2015.

- **Martínez D.**, Rudas J., Demertzi A., Heine L., Soddu A., Becerra E., Perea J., Laureys S., & Gómez F., "TDA barcodes to identify topological features of resting state fMRI time courses in healthy subjects", *23rd Annaul meeting of the Organization for Human Brain Mapping*, Vancouver, Canada, June 29 2017.

- **Martínez D.** & Gómez F., "TDA to identify topological features of resting state fMRI time courses in healthy subjects", *Primera Conferencia Colombiana de Matemáticas aplicadas e industriales*, Bogotá, Colombia, August 10 2018.

- **Martínez D.** & Gómez F., "Altered functional connectivity of resting state networks in patients with disorders of consciousness cheracterized by network measurements", *Primera Conferencia Colombiana de Matemáticas aplicadas e industriales*, Bogotá, Colombia, August 10 2018.

- **Martínez D.**, Rudas J. & Gómez F., "Topological description of resting state functional connectome through different parcellations", 7^{mo} *Coloquio doctoral Universidad Nacional*, Bogotá, Colombia, November 18 2018.

- **Martínez D.** Invited speaker at Neuroimágenes en Colombia with a talk "*Análsis de connectomas*", Bogotá, Colombia, June 14 2019.

Abstract

Computational strategies to characterize topological properties of pathologically altered functional brain networks

Consciousness alterations, including disorders of consciousness (DOC), propose a defiant scenario from the prognosis and diagnosis perspectives. Brain resting-state functional imaging mitigates this challenge, offering alternatives to explore brain activity in altered consciousness states. Furthermore, connectivity functional variations in resting have been linked with consciousness alterations. So, considering the evidence of connectivity alterations in altered consciousness states, this thesis inquires new computational approximations to describe topological characteristics associated with the resting-state connectivity in altered states of consciousness.

This work introduces two computational strategies for the characterization of topological features underlying the graph representation model. The first strategy describes graph connectivity properties of the so-called functional connectome, linking its alterations to the patients' level of consciousness. Despite the capacity characterization of this approach, it is limited only to describe pair-wise interactions, which is the base of the graph model. The second strategy characterizes both low and high-order connectivity properties from the topological perspective using Persistent Homology (PH), resulting in a richer representation of the brain functional interactions. These properties include the number of holes (0 and 1 dimensions) emerging in the resting-state dynamic across different scales. This strategy was investigated in healthy control (HC) subjects and later extended to patients with altered states of consciousness.

The first strategy (graph-based) suggests variations in critical properties related to consciousness, such as integration, segregation, and centrality, when comparing HC and patients with DOC. In HC, the second strategy (PH-based) provided evidence of persistent 1-dimensional holes, indicating that resting-state connectivity exhibits high-order interactions. Results also suggest that brain regions associated with the appearance of these 1-holes have a marked symmetry in both cerebral hemispheres. In patients with altered states of consciousness, results related to 0-dimensional holes indicate dissimilarities among the time courses, likely linking to particular integration mechanisms in these conditions. Additionally, 1-dimensional holes were also identified in the pathological population. However, brain regions involved in the appearance of these features differed from the ones observed for HC. In particular, no symmetry was observed.

These results shows topological changes in the functional connectome of patients with altered states of consciousness, suggesting that high-order functional interaction mechanisms may play an important role in the emergence of consciousness in patients with DOC.

Keywords: Altered Consciousness States, Resting-State, Functional Connectivity, Complex Network Analysis, Topological Data Analysis, Persistent Homology, Topological Description

Resumen

Estrategias computacionales para caracterizar las propiedades topologicas de las redes cerebrales funcionales patológicamente alteradas

Las alteraciones de la conciencia, incluyendo los desórdenes de conciencia (DOC), proponen un escenario desafiante desde la perspectiva del pronóstico y el diagnóstico. Las imágenes funcionales del cerebro en estado de reposo reducen este desafío, ofreciendo alternativas para explorar la actividad cerebral en estados alterados de conciencia. Además, variaciones en la conectividad funcional en reposo han sido relacionadas con alteraciones de la conciencia. Entonces, considerando la evidencia de cambios de la conectividad en estados alterados de conciencia, esta tesis indaga en nuevas aproximaciones computacionales para describir características topológicas asociadas con la conectividad en estado de reposo para estados alterados de conciencia.

Este trabajo presenta dos estrategias para la caracterización de rasgos topológicos subyacentes a los modelos de grafos. La primera estrategia mide las propiedades del grafo o conectoma funcional, vinculando sus variaciones con el nivel de conciencia. Sin embargo, este enfoque está limitado por la base de interacción por pares del modelo de grafos. La segunda estrategia describe propiedades de alto orden de una representación de interacciones simultáneas a través del complejo simplicial mediante el uso de la homología persistente (PH). Las propiedades de alto orden son las fronteras de los huecos de dimensión 0 y 1 del estado de reposo. Esta estrategia se implementa para sujetos controles (HC) sanos y se ajusta para pacientes con estados alterados de conciencia.

Los resultados del primer método, basado en medidas de grafos, muestran variaciones en propiedades clave relacionadas con la conciencia, como la integración, la segregación y la centralidad. La segunda estrategia en HC identificaron huecos 1 dimensionales persistentes, indicando que la conectividad en estado de reposo exhibe interacciones de alto orden. Además, hay regiones cerebrales asociadas con la aparición de estos huecos que muestran simetría al ser vistos sobre los hemisferios cerebrales. En pacientes con estados alterados de conciencia, el método incluye la descripción de los huecos 0 dimensionales, denotando la integración entre las señales en estado de reposo. Los resultados de los huecos 0 dimensionales indican distancias mayores entre las señales. Además, en esta población también se identificaron huecos 1 dimensionales. Su persistencia es comparable a la de los sujetos HC, pero las regiones cerebrales involucradas en su ocurrencia son distintas y no se observa simetría. Estos resultados sugieren que efectivamente existen variaciones topológicas de orden bajo y alto asociadas con la alteración de la conciencia. Además, estas variaciones pueden servir para nuevas investigaciones en conciencia.

Palabras clave: Estados alterados de conciencia, Estado de reposo, Conectividad funcional, Análisis de redes complejas, Análisis topológico de datos, Homología persistente, Descripción topológica.

This doctoral thesis was defended on Wednesday, October 26, 2022 at 9:00 am, and it was evaluated by the following jury:

Gabriel Castellanos Castañeda (Phd.)
Profesor Asistente
Pontificia Universidad Javeriana

Norberto Antonio Malpica González (Phd.)
Profesor Titular,
Universidad Rey Juan Carlos

Enrico Amico (Phd.)
SNSF Ambizione Research Leader
EPFL and University of Geneva

Edgar Eduardo Romero Castro (Phd.)
Profesor
Universidad Nacional de Colombia

Contents

Abbreviations and symbols

Abbreviations

Abbreviate	Meaning
BOLD	Blood Oxygen Level-Dependent imaging
BPMN	Business Process Model and Notation
CRS	Coma Recovery Scale
CRS-R	Coma Recovery Scale-Revised
DMN	Default Mode Network
DC	Distance correlation
DOC	Disorders of consciousness
ECN	Executive Control Network
EEG	Electroencephalography
fMRI	Functional Magnetic Resonance Imaging
FNC	Functional Network Connectivity
FOV	Field of View
FSL	FMRIB Software Library
GCS	Glasgow Coma Scale
HC	Healthy controls
IC	Independent Component
ICA	Independent Component Analysis
ICU	Intensive Care Unit
IQR	Inter Quartile Range
ITK	Insight Tool Kit
MCS	Minimally Conscious State
MNI	Montreal Neurological Institute
MRI	Magnetic Resonance Imaging
PCA	Principal Component Analysis
PET	Positron Emission Tomography
PH	Persistent Homology
PSC	Percent Signal Change
R-fMRI	Resting-state Functional Magnetic Resonance Imaging

Abbreviate	Meaning
ROI	Regions Of Interest
RS	Resting State
RSNs	Resting State Networks
SPM	Statistical Parametric Mapping
STG	Superior Temporal Gyrus
TDA	Topological Data Analysis
TE	Time exposition
TR	Time Resolution
UWS	Unresponsive Wakefulness Syndrome
VS	Vegetative State
WM	White Matter

Symbols

Symbol	Term	Meaning
ϵ	filtration value	Distance to compute the simplicial complexes
$\mathcal{H}$	Homology	Homology space
$\mathcal{H}_k$	k dimension homology	Homology group at dimension k
Hz	Hertz	Cycle per second
mm	Millimeters	Meter divided by thousand
ms	Milliseconds	Sencond divided by thousand
T	Tesla	Unit of magnetic B-field
$^\circ$	Degree	Circumference of a circle divided by 360

1. Introduction

The understanding of brain functions represents a highly challenging area. In the last decades, this scientific endeavor has been the main focus of many pieces of research. In particular, the connectome characterization, both functional and structural [126], and the use of the complex network analysis to characterize brain [85], have increased advances in this area. These tools have improved our knowledge about brain alterations in pathological conditions [85]. Remarkably, they allowed associating variations on graph properties from healthy to pathological states. That is the case of altered states of consciousness, which includes pharmacological sedation, and Disorder Of Consciousness (DOC). DOC encompasses a set of brain conditions, including acute comatose state, Minimally Conscious State (MCS), and Unresponsive Wakefulness Syndrome (UWS). Formally, DOC is the name given to a group of related disorders which are linked by disruption to some common underlying system known as consciousness [128]. The patients with altered consciousness do not respond to external stimuli; then, distinct approaches to measuring brain activity are needed to get clues about their brain state.

Advances in functional neuroimaging provide a way to assess brain activity, and resting-state protocols emerge as an alternative to measure brain function in altered states of consciousness without the need of a patient response [18, 17]. The brain's spontaneous activity without stimuli constitutes the base of the resting-state signal, which provides a resting functional connectome [64]. This connectome represents a suitable description of brain function for subjects which not respond to stimuli, as in patients with altered states of consciousness, such as DOC. The study of this connectome on these patients suggests that some graph properties variations are associated with functional brain changes under states of consciousness alterations [12, 49]. These variations can be understood more generally as changes on the topological features of the functional resting connectome [29]. However, these topological descriptions are based on network construction, i.e., the existence of pair-wise relationships between elements. This assumption may oversimplify brain dynamics descriptions by only considering the connection of pairs of elements, putting aside the potential existence of high-order topological structures [35], which may play an important role in the consciousness phenomena emergence. This thesis aims to overcome limitations on the topological characterization imposed by the graph representation of the resting functional connectome for characterizing patients with altered states of consciousness.

1.1. Brain function description and variation in pathological states

Anatomical and functional characterization of the distinct brain injuries, particularly those related to alterations of consciousness, has emerged as an area of high research activity in diverse fields. For instance, in health, because of the clinical implications of diagnosis and prognosis in these patients [129], in ethics, due to the issues of life of patients with consciousness alterations [140], and social, because of the impact in the public health system of care of these patients [13, 63]. Some of the principal research objectives in the area include diagnosis support based on the structural and physiological [49] alterations caused by brain damage [83], prognosis in accordance with the severity of the damage based on functional and biomechanical models of characterization of consciousness states [90], among others.

Recently, studies based on dynamic neuroimaging (functional Magnetic Resonance Imaging - fMRI) have established the existence of functional brain networks activated during resting state [41]. Some of these studies have suggested that in normal conditions, the brain in resting-state is organized in regions of sensory-cognitive relevance, in the so-called resting-state networks (RSNs). These regions are functionally co-activated, i.e., spatially segregated areas show functional activation simultaneously. The resting-state fMRI (R-fMRI) has been employed as an objective alternative to study the alterations of consciousness because it registers brain activity without patient collaboration, and it is not restricted by the availability of sensory channels of stimulation [46]. Alterations in connectivity on these entities have been proposed as biomarkers of different pathological brain conditions [170, 6, 84, 192]. Investigating functional activation dynamics and patterns of these resting-state networks constitutes open research areas [61]. In particular, these connectivity variations have been proposed for the characterization and classification of distinct brain disorders [141]. However, despite advances, the processing, analysis, and understanding of these signals and the extraction of features to build bio-markers linked to specific neuro-pathologies are open problems in the information processing of brain functional data [2, 82].

Graph theory has been employed to characterize resting-state networks, notably functional and structural interactions, variations, and relationships with specific brain development and alterations [192]. Recently, it has been suggested that brain function is organized in specialized and segregated brain areas or hubs of fast processing [158, 89]. Also, functional and anatomical brain networks have been proposed to be organized in small-world and rich-club topologies [28]. Besides, variations of brain network properties have been linked to specific brain diseased conditions, for example, the increment of the hub's efficiency in comatose patients [1].

1.2. Problem statement

fMRI studies have established the existence of functional brain networks which are activated in resting-state [139]. The alterations of connectivity levels in these entities have been proposed as biomarkers for the study of various pathological conditions, including Alzheimer's disease, Autism, Parkinson's disease, Schizophrenia, and DOC, among others [87, 85]. Thus, studies of brain functional connectivity in combination with the so-called complex network analysis have been established as a strategy to get knowledge about brain function in healthy and diseased conditions. It gives many descriptors, including topological, which rely on a unitary element of analysis, the network. Identifying the bio-markers and incorporating the assessment of variations produced by the pathology. It is commonly performed by comparing against healthy brain networks. However, the brain structure and function of patients diagnosed with disorders of consciousness are severely damaged. This deterioration is thought to result in a complete reconfiguration of the functional brain networks [128, 50, 82]. Conditions associated with altered states of consciousness could lead to scenarios where the comparison with healthy control subjects is not suitable, resulting in an unsatisfactory description and posterior examination of its connectivity. The challenge here is the characterization of functional connectivity in severely damaged brains. In particular, the identification of topological variations in functional network connectivity for patients with altered states of consciousness. Therefore, the development of computational strategies that use functional information of severely damaged brains and its emergent properties could improve our current knowledge about brain function, in particular those that include a recent strategy called Topological Data Analysis (TDA) to describe the topology of the resting functional connectome for patients with altered states of consciousness.

1.3. Justification

Severe alterations of brain function in altered states of consciousness could lead to challenging neuroimaging analysis scenarios. Neuroimaging approaches may not differentiate the resulting brain activity patterns in extremely damaged brains. In particular with those which use a global perspective of the functional brain network. Global network properties capture dynamic and topological information through statistical measurements [19]. They are computed over the whole network as a unique entity, leading to analysis conditions that hide local properties which may be relevant in DOC and other altered states of consciousness studies. For instance, scenarios with apparent disconnections represent topological changes probably hidden in the global strategy. Recently, TDA has emerged as an alternative to overcome these limitations. The aim of TDA is to understand the shape of data in order to extract meaningful insights [112]. It includes the classification of loops and higher dimensional voids within the space [33], providing a high-order connectivity-based description.

Then, TDA represents an alternative to study the brain function of severely damaged brains. Even more for those brains with apparent disconnections and other topological variations.

1.4. Contributions

This thesis investigates the topological properties of altered functional brain networks. In particular, brain networks of patients with consciousness alterations. It begins with a pairwise interaction representation of the functional activity at rest, forming a graph. This graph representation allows describing interactions and topological properties from the connection distributions. In a set of segregated areas, the RSNs describe topological connectivity alterations associated with the level of consciousness, allowing to characterize key properties related to consciousness in the R-fMRI, such as integration, segregation, and centrality. However, despite the richness of this characterization, high-order topological features can not be described from the graph perspective. Therefore, later persistent homology (PH) is used as a tool to describe high-order topological features in R-fMRI for healthy people. This approach found by the first time high-order 1-holes features appearing robustly in this population. The brain regions involved in the emergence of these high-order features were also investigated, finding that particular brain regions were more frequently involved in the occurrence of these features. The existence of these topological features, 1-holes or loops, in association with the identification of the involved brain regions in healthy subjects may provide a new perspective for functional connectivity. But, does this approach powerful enough to describe R-fMRI functional connectivity in pathological conditions? To answer this question, we improve classic description coming from PH method to describe key high-order features for patients with an acute altered state of consciousness. The improved description considered the characterization of the rate of integration of 0-holes to examine the functional disruption attributed to the pathological condition. We found that this 0-holes description suggests a displacement due to dissimilarities in R-fMRI patients' time courses. Also, we found 1-holes appearing robustly in patients, but the regions implicated in their occurrence were different from brain regions obtained in healthy subjects. To summarize, we describe high-order features through 0-holes and 1-holes of R-fMRI functional connectivity, which may provide new insights about consciousness alterations in patients with DOC. Figure **1-1** presents an illustration of the properties identified in the different settings.

1.5. Thesis structure

This thesis is organized as follows: Section 1.6 provides the basics about disorders of consciousness, imaging and diagnosis. Next, Chapter 2 provides a first topological description of resting-state alterations through graph measurements, finding differences between populations due to pathological conditions. Chapter 3 addresses the use of TDA as a tool

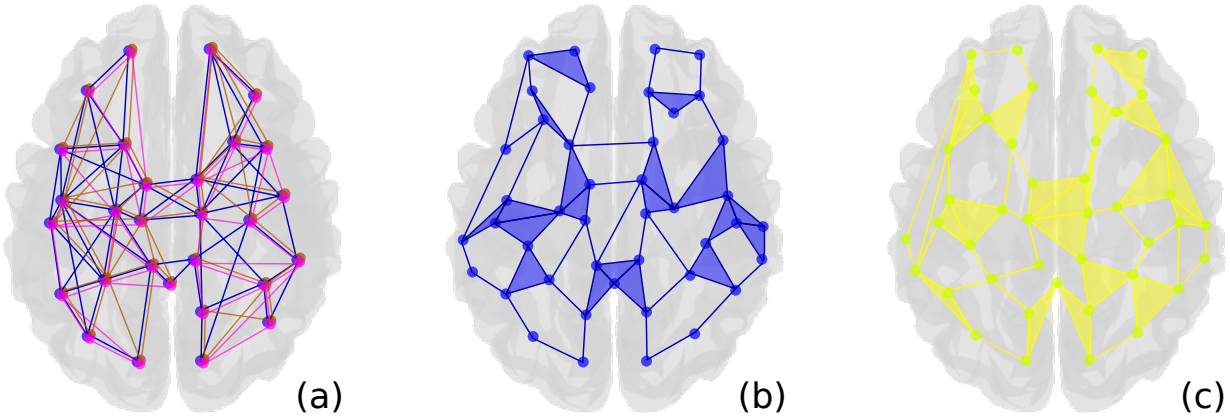

Figure **1-1**.: Illustration of process and contributions of this thesis. (a) Representation of the graph-based approach studied in Chapter 2. Edges describe topological features. The blue network represents healthy people while magenta and orange represent patients with DOC. (b) Representation of the persistent 1-holes description for healthy subjects examined in Chapter 3. Similar loops found in both hemispheres. (c) Representation of the 0-holes and 1-holes in the R-fMRI of patients with an acute altered state of consciousness studied in Chapter 4, no hemisphere similarities were found.

to describe resting topology on HC subjects and reports the regions involved in functional topological structures. Chapter 4 investigates the use of TDA on patients with acute alterations of consciousness and compares these features with the ones identified for HC. Finally, Chapter 5 covers the main conclusions and recommendations.

1.6. Disorders of consciousness, imaging and diagnosis

Consciousness refers to the state of awareness of self and one's relationship with the environment. From a clinical view, it commonly consists of two components, wakefulness or arousal and awareness [24]. Both features seem to link to anatomic structures and their specific functions [115]. DOC encompasses a set of particular conditions occurring after a coma state, affecting these dimensions [153, 24]. Patients with brain injuries can remain in a coma state for several weeks, and the recovery from this state may lead to distinct consciousness levels [153, 24]. These levels include the minimally conscious state (MCS) and the unresponsive wakefulness syndrome (UWS). Patients in MCS exhibit signs of fluctuating yet, reproducible remnants of non-reflex behavior. UWS is related to patients that open their eyes but remain unresponsive to external stimuli [128, 153, 103, 138]. Also, a subcategorization of MCS was recently proposed to classify patients into MCS+ or MCS- based on the level of observed behavioral responses [25]. Figure **1-2** illustrate how these states locate in the two dimensions that define consciousness, awareness, and vigilance. Recent evidence suggests that these DOC conditions link to particular affectations of brain structure and function [74]. For instance, the breakdown of particular circuits like the mesocircuit is related to the loss of neurons from the central thalamus, causing functional affectations in the thalamostriatal and thalamocortical paths.

Diagnosis of DOC conditions is commonly performed by using neurophysiological assessments, such as the Coma Recovery Scale (CRS) [73, 152] or the Rancho Los amigos scale [182], that aim to assess the behavioral response of the patient. Nevertheless, these patients may present substantial motor deficits, sensory losses, language impairments, and vigilance fluctuations resulting in affectations of this response capacity. Therefore, these clinical evaluations may lead to a high rate of misdiagnoses and non-appropriate treatments [153]. Despite this, the knowledge of diagnostic criteria and the use of valid and sensitive standardized scales are necessary and crucial to establish a precise diagnosis of DOC [153]. Recently, approaches for DOC diagnosis incorporate various neuroimaging techniques in addition to the scale-based behavioral assessments, aiming to reduce misclassification rates. The following section presents an introduction to neuroimaging in DOC.

1.6.1. Neuroimaging to support DOC diagnosis

Neuroimaging is the name given to a variety of techniques that directly or indirectly record in an image the structure or function of the nervous system [62]. These techniques include different brain function and structure assessments [40] like Electroencephalography (EEG) [133], magnetic resonance imaging (MRI) [105], fMRI [7, 31], diffusion-weighted magnetic resonance imaging (diffusion MRI) [113, 59], Diffusion Tensor Imaging [8], positron emission

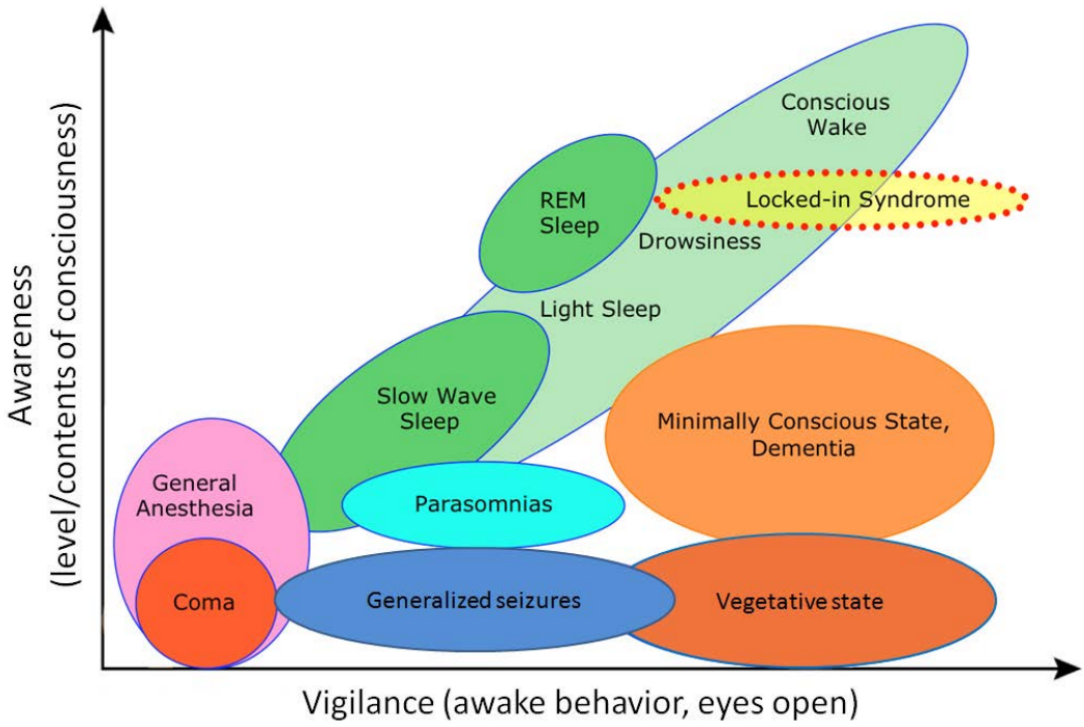

Figure **1-2**.: Level and contents of consciousness. The level of consciousness can be dissociated from behaviors that are traditionally regarded as a sign of vigilance or arousal (such as the opening of eyes, command following, among others). Typically, high conscious levels are associated with an increased range of conscious contents. Whether or not a high level of consciousness without any conscious contents is possible remains unclear [22]

tomography (PET) [91, 104], among others. In general, neuroimaging allows observing the structure and function of the brain of living organisms. Two of the techniques widely used to study brain function are PET and fMRI. PET is an image acquisition technique that captures the metabolism of glucose in the brain [104, 128], and fMRI is a technique that captures the hemodynamic brain activity [31].

Neuroimaging techniques can be used to study conditions of DOC. For instance, the levels of metabolized glucose per minute in DOC are illustrated in figure **1-3**. This image shows how the brain consumes glucose caused by its activity. Particularly, healthy individuals and patients with Lock-in syndrome evidence high metabolic activity compared to patients with DOC. However, the acquisition, analysis, and interpretation of neuroimaging data from patients with severe brain damage are challenging [104]. For example, in quantitative PET studies, the absolute value of cerebral metabolic rates depends on many assumptions, and in cases of cerebral pathology, a consensus for diagnosis using this tool has not been yet established [104, 103]. In fact, for patients with DOC is more extended the use of relative value metabolism [161].

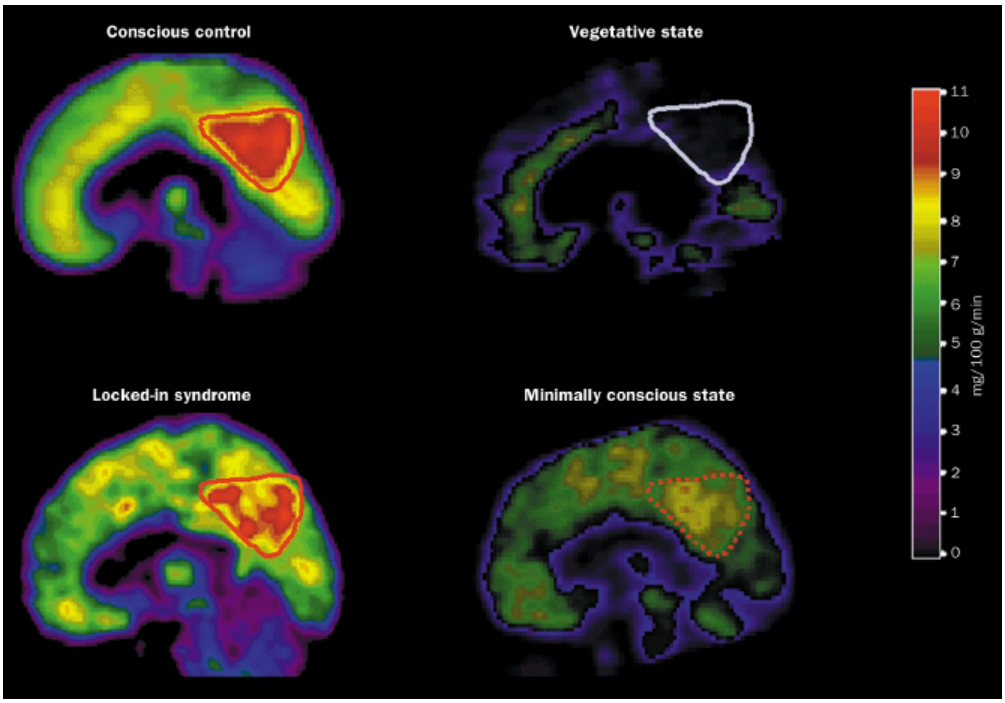

Figure **1-3**.: Resting cerebral metabolism in healthy individuals and patients in unresponsive wakefulness syndrome/vegetative state, locked-in syndrome and minimally conscious state [104].

Brain imaging, acquisition protocols, and posterior analysis and interpretations, of patients with severe brain damage, as in patients diagnosed with a DOC, is challenging because the

protocols are commonly proposed and adjusted to healthy controls subjects. For instance, many fMRI studies require the subjects' active participation in the so-called evoked protocols. They record the activation produced after some form of stimuli. Those evoked protocols are not suitable for DOC patients because their condition implies the unresponsive to external stimuli. As an alternative to overcome this limitation, the resting-state protocols emerge to register brain activity without a requirement of external stimuli.

1.6.2. Resting-State Networks and functional network connectivity of DOC diagnosed patients

During the last two decades, the brain activity registered at rest, i.e., while the brain is not exposed to any stimuli [46], has been studied. The main advantage of the protocol is that it does not require sophisticated experimental setups and overcomes the need for active participation of the subject. Therefore, this protocol has been explored as an objective alternative to characterize brain dynamics further and construct bio-markers for different pathological brain conditions [17]. For instance, research in brain activity in resting conditions suggests that healthy brains organize into large-scale functionally connected RSNs of sensory/cognitive relevance [41, 64, 139]. At least ten of these RSNs are consistently identified in healthy control subjects: default mode network (DMN), sensory/motor, executive control left, executive control right, saliency, auditory, cerebellum, and three visual networks(medial, lateral, and occipital) [41]. Alterations on these networks correlate to DOC, i.e., the dynamic of some of these networks links to DOC condition. For instance, DMN is the principal network activated in an awake state at rest [136, 26] whose alterations have related to the disorder of consciousness [177, 60, 44].

Different analysis methods at resting-state have been explored in consciousness alterations research [45, 196]. Including different imaging modalities, such as EEG and fMRI [88, 66, 148], among others. To identify RSNs and to link them to distinct pathologies, including DOC, it is necessary to talk about the interactions. Both EEG and fMRI provide a set of signals associated with specific brain regions. Then, each brain region has an associated time-course that represents the activity at the region. In fMRI, each voxel has an associated time-course. This way, it is possible to compute the functional interaction between pairs of regions by computing an interaction measure between its corresponding time courses. The interaction between regions is normally computed by correlation. Two kinds of approaches are used to study the brain region interactions, seed-driven and data-driven [82, 130]. In the seed-driven approach, a specific region is chosen and characterized by estimating the correlation between this predefined area, the seed, and all other voxels around the brain. This strategy is used in DOC analysis [44, 22, 49], showing that consciousness in these patients is related to specific regions connection. Consciousness is associated with the emergence of specific circuits into the brain, involving regions inside the DMN [21, 44, 82]. Region selection in this approach

is critical because incorrect choices of seeds may result in wrong characterizations. Furthermore, consciousness does not seem to be a phenomenon of isolated circuits [44, 168], even if some specific circuits have been related to this emergence. It is a phenomenon of underlying global processes [99], which local, seed-based approaches can poorly characterize. Then, a complete connectivity scenario that accounts for the whole brain regions becomes necessary.

An alternative that considers relations between the entire brain regions is the independent component analysis (ICA) [121, 12, 41]. In fMRI, ICA is a data-driven approach to decompose the whole-brain BOLD signals into a number of contributing volumetric spatial maps and their associated time-courses [130], ICA assumes that the time series on each voxel is a mixture of a set of statistically independent hemodynamic sources of activity in the brain [31], considering the signal as a global feature. ICA looks for functional activity of spatially segregated but correlated brain areas by using higher-order statistics to enforce spatial independence between components [193, 170]. Other approaches to analyze RSN signal include seed based methods [102], principal component analysis (PCA) [68], and clustering techniques [86], among others. The use of these methods has improved the understanding of the RSN's dynamic and activation patterns for healthy controls. Functional connectivity alterations within RSNs serve as biomarkers for the study of a variety of pathological conditions [17] including, Alzheimer [170, 23] and Schizophrenia [192], among others. However, in patients with pathological conditions, these phenomena are still poorly understood [84]. The following section illustrates the standard processing of time-courses to create the functional connectivity network.

Functional connectivity network computation

fMRI detects small changes in the MRI signal, which is associated with neuronal activity. MRI signal measures the excitation of hydrogen atoms in the brain the exposure to a magnetic field. Specifically, fMRI detects the variations associated with the depolarization of the neuron. When neurons depolarize, a hemodynamic response is triggered that increases the amount of oxygenated blood relative to deoxygenated blood. In particular, deoxygenated blood is paramagnetic and distorts the MRI signal from hydrogen atoms in the surrounding tissue, while oxygenated blood is diamagnetic. When the ratio of oxygenated over deoxygenated blood increases, the MRI signal also increase, see Figure **1-4**. This phenomenon results in a blood oxygen level-dependent contrast (BOLD) in a region of increased neuronal activity [20]. Furthermore, when the brain is in a resting wakeful state (R-fMRI), regions of correlated low-frequency fluctuations can be detected in the time series of the BOLD signal ($<$0.1 Hz) [18].

Preprocessing of the BOLD signal usually includes a correction for temporal shifts and section-dependent intensity differences. This is followed by regression of head motion and

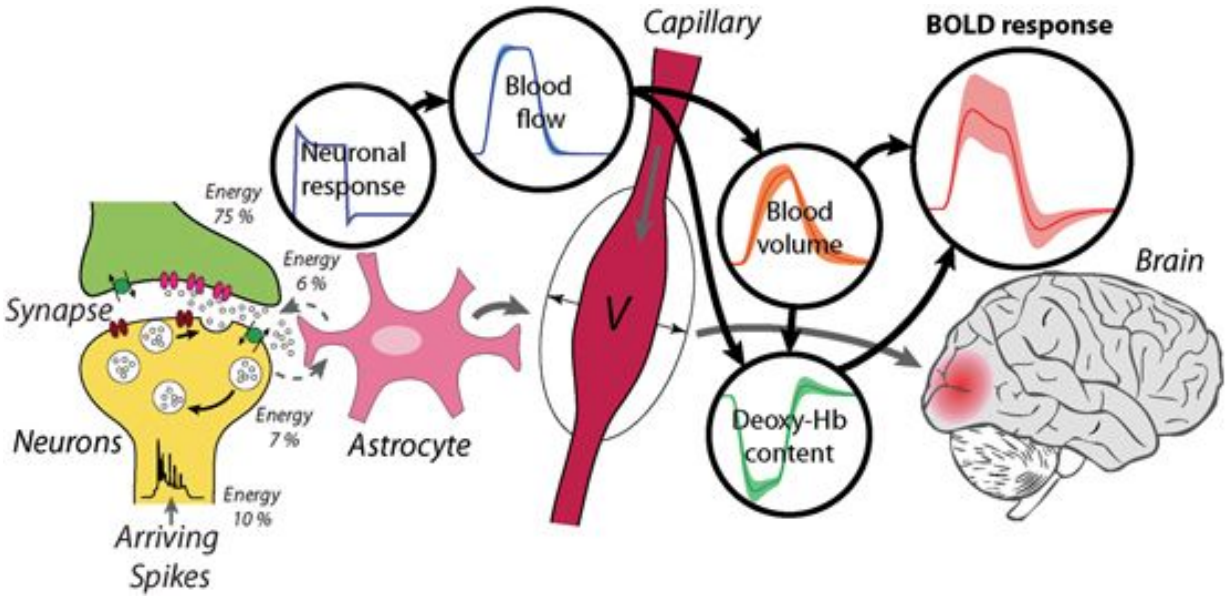

Figure **1-4**.: Physiological and physical processes leading to the measured fMRI signal. fMRI signal depends on both blood oxygenation and volume as a function of physical acquisition parameters, such as magnetic field strength and MRI sequence [175]

other nuisance regressors, including signal time courses for regions of interest located in the ventricles and white matter, which are related to high proportions of noise associated with cardiac and respiratory signals [173]. Spatial smoothing and low-pass filtering to retain frequencies <0.1 Hz let remove the signal from non-neural causes and improve the signal-to-noise ratio. Then images are registered in atlas space to achieve spatial agreement with coordinate systems and between subjects [106]. Some approaches in data preprocessing include whole-brain regression and head motion correction. Whole-brain regression, which regresses the mean time course of the whole brain, has been proposed as a method to improve the specificity of correlations and reduce noise [64]. Both become a subject of debate because whole-brain regression may produce spurious negative correlations that have no physiological significance, and inadequate head motion correction can result in spurious correlations in fMRI analysis [106].

Distinct methods can be used to analyze the data after preprocessing. One method is a seed-based analysis, which involves selecting regions of interest (ROIs) and correlating the average BOLD time course of voxels within these ROIs with each other and with the time courses of all other voxels in the brain. Typically, a threshold is determined to identify voxels significantly correlated with the region of interest. However, this approach requires an a priori selection of ROIs. Another approach is independent component analysis (ICA), a mathematical technique that maximizes statistical independence among its components [41]. ICA can be used to identify spatially distinct RSNs of RS-fMRI data. Compared to seed-

based methods, ICA has the advantage of requiring few a priori assumptions, but requires the manually selection of important components and distinguish noise from physiological signals. Nevertheless, some studies have attempted to automate this process and use ICA as a method to identify noise within the BOLD signal [106]. Despite their differences both approaches exhibits similar results in analysis of healthy subjects groups [139]. Finally, functional network connectivity (FNC) approach considers a collection of ROIs as nodes connected by edges. This connection could be established as the correlation between ROIs [86]. Formally, Functional connectivity refers to temporal correlation between spatially remote neurophysiological events, expressed as deviation from statistical independence across these events in distributed neuronal groups and areas [68, 18]. Distinct correlation measures have used to compute the FNC, for instance, Pearson's correlation [94] and distance correlation [163, 143]. The graph representation of ROIS as nodes and connectivity as edges provides a basis for characterize the connectivity of brain regions [106], see Figure **1-5** for a FNC process summary. This representation and graph measurements reveals a small-world topology of functional connectivity [28]. Small-world is achieved through the existence of hubs. Hubs are critical nodes with large numbers of connections, that allow high levels of local connectivity [28]. This way small-world networks have high clustering coefficients, i.e. high level of local connections, and an overall short distance between any two nodes, or a small average path length [106].

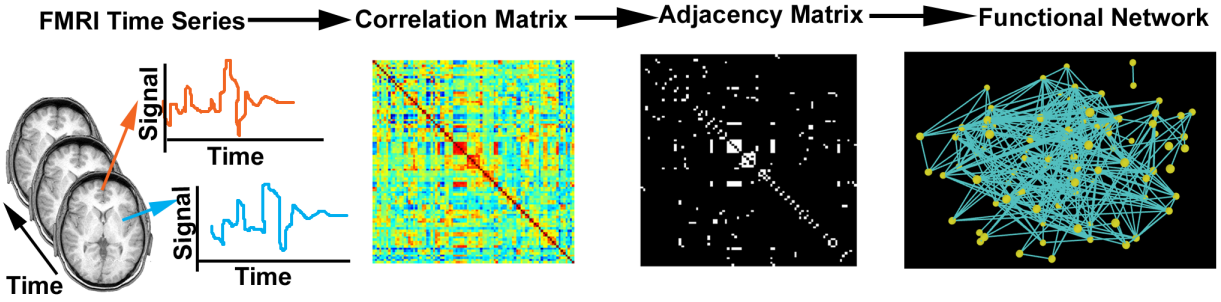

Figure **1-5**.: Resting state fMRI data are collected from a subject. Voxel time series are extracted from the set of images, and a Pearson correlation analysis is performed between all possible pairs of voxels. The correlations are represented in the form of a correlation matrix, which is binarized at a given threshold to yield an adjacency matrix. The functional network is thereby defined, where each ROI is represented by a node and connections are determined by the adjacency matrix [96]

Functional connectivity within RSNs

As previously mentioned, a complementary RSNs analysis strategy that considers the functional relationship among RSNs is explored in FNC [82]. FNC studies focused on the assessment of the level of interaction during spontaneous activity among different RSNs. This dynamic brain representation results from computing pair-wise measurements of connectivity between the RSNs time-courses. Typical measurements of interaction include Pearson's correlation coefficient that aims to capture linear relationships among the time-courses [94], Granger causality that characterizes directional connectivity [185], and temporal slicing window that allows exploring temporal changes in the RSN connectivity [146]. Most of these approaches rely on the underlying assumption that RSN brain dynamics follow linear regimes. However, recent evidence suggests that the neuronal function of cortical ensembles during resting-state may follow non-linear behaviors [186]. Therefore, these interaction measurements may be limited to capture this phenomenon. An alternative approach to characterize these non-linear conditions is the distance correlation that aims to capture non-linear relationships between different RSNs [143, 3, 71, 191]. These no-linearities could suggest high-order interactions. In addition, this FNC has been explored as a possible biomarker of loss of consciousness [44, 74, 82].

To summarize, the FNC provides a framework for the analysis of healthy and pathological conditions. In altered states of consciousness, including DOC, the FNC was created based on the connectivity of specific circuits linked to consciousness emergence. Variations in the connectivity and topology of the nodes in these circuits have been successfully associated with DOC, pharmacological sedation, and other conditions of altered consciousness [84, 44, 52, 79] . Then, many studies are centered on consciousness-related circuits, leaving aside the connectivity with the rest of the brain. Furthermore, a general view of the connectivity changes due to altered states of consciousness stills unexplored. Moreover, brain connectivity from a general perspective could be described by the associations between RSNs, providing a rough characterization of brain function in DOC. The next chapter develops the description of the brain connectivity between RSNs by using network measurements. This approach allows characterizing connectivity properties associated with altered states of consciousness, specifically for DOC.

2. Brain function topological description from networks

This chapter presents a description of the topological features computed over a network structure. First, it introduces the uses of network representations on resting-state signals as an object that encompasses the brain regions and associations between pairs of them. Then, the chapter presents the definition of features used to describe a network. In particular, for a network that represents the interactions between RSN in normal and pathological DOC conditions. Next, it exposes the network properties variations linked to the consciousness levels (healthy subjects, MCS, and UWS patients). The main content of this chapter were published as an article in Brain and Behavior [119].

As described in previous chapter, due to the communication difficulties imposed by the DOC conditions, functional connectivity analyses based on R-fMRI serve as an alternative to overcome the need to record the responses to stimuli [159, 46]. Also, the brain organization in RSNs provides a suitable representation to study the preservation of sensory and cognitive brain functions without any explicit stimulation [139] specifically for DOC studies. First analyses of RSNs in patients with DOC were focused on alterations of the functional connectivity inside the DMN. This functional structure encompasses specific brain regions linked to the consciousness emergence phenomenon [21, 44]. Decreases in functional connectivity within this network links to modifications of the level of consciousness in these patients. Posterior studies showed that DOC conditions might affect functional connectivity within multiple RSNs [84, 80, 44, 49, 52, 130]. In particular, variations in intrinsic connectivity for specific RSNs relate to alterations in sensorial and awareness functions [21, 44, 49]. For instance, in decreased connectivity levels in DMN and frontoparietal networks [122]. Additional evidence indicates changes in the connectivity between RSNs, for instance, reductions of the connectivity strength between RSNs in patients with DOC compared to healthy controls (HC) [143] and alterations in the level of anti-correlation between RSNs associated with the recovery of consciousness [51]. These variations in the RSNs circuits were also observed in patients with induced altered consciousness states, as in propofol sedation [80, 79]. Recently studies which incorporate time-delay models found variations in specific talamo-cortical circuits associated with DOC [32]. Also, Bodien et al. [20] review the degree of the functional and effective connectivity alterations in relation with the severity of impaired consciousness. Additionally, stimulus of specific circuits identified in R-fMRI and correlated with DOC

awareness level have been used to improve diagnosis between acute and chronic DOC [156], and the identification of specific circuits as feasible targets for neuro-modulation [122]. All these analyses converged to alterations within particular RSNs or between specific pairs of RSNs that may have functional relevance for consciousness emergence.

Nevertheless, these approaches may be limited because they lack a more general view of the brain, regarding, for instance, the existence of multiple functional units in the brain interacting among them [87]. They instead focused on specific consciousness-related circuits within the brain. A more general perspective would be important because consciousness preservation in these patients may also require functional units related not only to consciousness processing but also to stimuli and response, and possibly systems to orchestrate them [169]. The understanding of interactions among these units may provide valuable information about these conditions [169]. A model of functional connectivity among RSNs has been proposed in the so-called Functional Network Connectivity (FNC) [94], which considers the functional interaction between these large-scale units. This model provides a network representation in which interactions between high-order functional systems are characterized using network measurements [28, 87]. Lately, connectivity density decreases were associated with consciousness alterations in coma states, providing a general description of FNC alterations [114]. However, the specific reconfiguration of FNC associated with consciousness states remains poorly understood. In other words, how the FNC model may highlight reorganizations of connectivity related to the underlying pathology characterizing the DOC condition. In this section, the FNC interaction patterns were studied by assessing modifications in integration, segregation, and centrality properties, which have been suggested to be highly relevant for consciousness emergence [169].

Functional connectivity alterations within and between some RSNs observed in patients with DOC may be interpreted as variations of the integration, segregation, and centrality properties. For instance, functional connectivity changes within some RSNs could relate to alterations in the integration levels of some particular functional systems known to be involved in the consciousness phenomena, such as DMN [21]. Similarly, the variations of the connectivity between functional systems might associate with variations in brain segregation mechanisms. For example, the changes observed in the thalamocortical connectivity in unconsciousness may result in decreases in their level of segregation [44]. Additionally, reductions in functional connectivity of a central node as the thalamus reported in patients with DOC would generate centrality disruptions [150]. In the network, the topology refers to how the elements are connected and grouped from the pair-wise relation, how some of them are integrated into clusters, and how some nodes become relevant. Thus, variations in the connectivity levels between brain regions, or the role change of a node in the network, are expressions of topological changes in the FNC. This way, FNC topology variations due to the DOC pathology, patients in MCS or UWS, are described by alterations of these three

properties on the specific consciousness circuits when compared against healthy people.
In contrast to previous studies that only focused on a limited set of RSNs, we considered the interactions among the whole set of functional units. To reach this objective, the FNC was computed for each subject obtaining a general brain functional representation with the interactions between RSNs. This approach allows studying integration, segregation, and centrality for the general brain by considering the interactions between high-order functional systems. Next, we used a set of network measurements to assess the mentioned properties. In particular, degree, strength, clustering coefficient, betweenness, and eigenvector centralities [28, 87, 27] were used to understand relevant brain functional properties modifications for different states of consciousness. Degree and strength assess the integration between functional brain regions, i.e., how the brain regions are connected and how strong are connections respectively. The clustering coefficient measures the segregation of brain regions, i.e., how the brain regions are interconnected, creating functional units. Betweenness and eigenvector centralities evaluate the relevance of a region in the functional connectivity model, i.e., how important a brain region is for communication because it belongs to the shortest path, or it is connected to other relevant brain regions respectively.

The main contributions of this chapter are: (i) A graph measurement-based method was developed, characterizing pair-wise interactions between RSNs, and (ii) measured values were associated with the consciousness levels, indicating topological variations in R-fMRI related to the consciousness phenomenon.

2.1. Graph theory approximations used to gain knowledge about brain pathologies

2.1.1. Complex network analysis

Networks are systems composed of many highly interconnected units. Initially, its study was mainly of a branch of discrete mathematics known as graph theory. Nevertheless, during the last two decades, the investigation of networks whose structure is irregular, complex, and dynamically evolving in time became of research interest in the so-called complex networks. Complex networks were firstly motivated for their use as proper representations in real problems, like transportation, Internet, protein chains, among others [19]. Therefore, the research on complex networks was encouraged to define new concepts and measures to characterize relevant network characteristics, such as its topology, i.e., structure and arrangement of the network. Remarkably, these researches unveiled unifying principles and statistical properties, which resulted common to many existing networks [19, 162]. Then, their study, in early stages modelling real phenomena, results in important emerging characteristics which revives the research in graph theory but considering the properties of the real networks. The

real networks are characterized by the same topological properties, as for instance relatively small characteristic path, lengths, high clustering coefficients, fat tailed shapes in the degree distributions, degree correlations, and the presence of motifs and community structures. All these features make real networks radically different from regular lattices and random graphs, the standard models studied in mathematical graph theory [4, 19].

Complex networks investigations mainly focused on the changing from small networks to systems with thousands of millions of nodes, and they were initially modeled as random graphs or generalized random graphs assuming that they were large-scale networks with no apparent design principles [4]. However, two main directions of complex network analysis were emerged to model its structure, small-world, and scale-free networks. Both of them were introduced to model networks that mimic the growth of a network and to reproduce the structural properties observed in real topologies [19].

Random graphs

A random graph is a graph in which the edges are distributed randomly, i.e. the nodes in the graph that have the same number of links have the same probability to be selected [4]. Large-scale networks with no apparent design principles have been described as random graphs. They have been proposed as the simplest and most straightforward realization of a complex network because networks with a complex topology and unknown organizing principles often appear random [19]. Random-graph theory studies the properties of the probability space associated with graphs. In general, properties of such random graphs can be determined using probabilistic arguments where the attributes of graphs are studied as functions of the increasing number of random connections [19]. Then, in a random graph, the probability of select a node with a fixed number of links follows a uniform distribution.

Small-world networks

The small-world concept in simple terms describes the fact that despite their often large size in which most nodes are not neighbors, in most networks there is a relatively short path between any two nodes. The distance between two nodes is defined as the number of edges along the shortest path connecting them. Then, in a small-world network, the distance between two randomly chosen nodes is small, and it grows proportionally to the logarithm of number of nodes in the network [180].

Scale-free networks

Scale-free networks are networks whose their degree distribution follows a power law [19]. The degree of a node is the number of its direct connections to other nodes. The distribution degree $P(k)$ gives the probability that a randomly selected node has exactly k edges.

Scale-free nature of real networks is rooted in two generic mechanisms shared by many real networks The number of nodes increases by the subsequent addition of new nodes. The likelihood of connecting a new node depends of the node's degree [4]. Numerical simulations indicated that a network with these properties evolves into a scale invariant state with the probability that a node has k edges following a power law with an exponent $\gamma = 3$ independent of number of nodes already present in the network [4, 19].

As was mentioned previously, graph theory and more specifically complex network analysis had been used to model, to understand and to get insights about several types of real systems. The complexity arises in the behavior of a system of interacting elements that combines statistical randomness with regularity [28]. During the last decades, brain studies and investigations had also adopted these kind of approaches to model brain structure and function in healthy and pathological conditions.

2.1.2. Complex network analysis in brain imaging

The brain is a network which consists of spatially distributed, but functionally linked regions that continuously share information with each other [89, 43]. As mentioned previously, functional neuroimaging allows to explore and identify functional connections of specific brain regions and local connections. These connections permit to define a brain functional network or functional connectome [160]. By analyzing this connectome important clues about overall organization of functional communication in the brain network have been unveiled [89, 44]. This analysis have been mainly performed by using complex network measurements that allows to capture emerging organizational principles of complex systems [28]. Complex network measurements are supported on graph theory, see anexe table **A-1** for a brief description of some complex network measurements commonly employed to characterize brain networks.

Complex network measurements have been used to understand function affectations and reconfigurations in pathological brain conditions such as, Alzheimer [196, 23, 170], Schizophrenia [141, 192] and Autism [141], among other conditions, see Table **2-1**, for a brief reference of network measurements used in brain pathological conditions studies. Complex network analysis has been also applied to study relationships among resting-state networks, and their topological structure [178]. Brain networks alterations were consistently related with some brain affectations, but for DOC conditions graph properties remain poorly understood [84]. Recently, approaches adopt local [118] and global [117] complex network measurements to characterize the functional network connectivity of patients in DOC. These works link some alterations of network topology with the consciousness variations. They mainly relate local variations of the default mode network, and global variations of the average clustering coefficient and average strength with the alterations of consciousness.

Table **2-1**.: Researches which use network measurements to evaluate brain conditions with specific pathologies

Pathology	**Network Measurement**	**Alteration**
Schizophrenia	Connectivity	Connectivity fluctuations [192, 151]
Alzheimer	Clustering, modularity and path length	Clustering and modularity reductions [23]
	Strength	Strength reduction [65]
Epilepsy	Connectivity	Global connectivity decrease [164]
	Eccentricity and betweenness centrality	Decrease of eccentricity and betweenness centrality [176]
	Strength, clustering coefficient, efficiency and characteristic path	Decrements of strength, clustering coefficient, efficiency and increment of characteristic path [189]
Multiple Sclerosis	Modularity	Increased modularity [69]
Parkinson	Clustering coefficient and modularity	Higher clustering and modularity [6]
Autism	Betweenness centrality	Higher betweenness centrality [137]
DOC	Clustering coefficient, strength, efficiency and characteristic path	Increment of clustering coefficient and strength [118, 117]
	Degree and hubs	High degree, hubs reorganization [1]

Measurements to quantify complex networks topological properties were used to understand brain normal processes like aging and cognition, and pathological states like Schizophrenia, Dementia, Alzheimer among others [94]. Alterations in complex measurements as modularity, hierarchy, centrality and the distribution of network hubs have been also related

with specific behaviors of brain diseases. These properties modifications can be associated with topological changes. Then, the complex network analysis allows to understand some topological variations of the networks induced by brain pathologies.

2.2. Functional connectivity reshape in patients with disorders of consciousness

This section presents the characterization of a functional connectome for Healthy Control (HC) subjects and patients with DOC [31, 87, 27, 159], in particular, a connectome with RSNs as nodes. This connectome corresponds to a large-scale network of functional relationships between functionally related brain regions. Network-based measurements computed on this connectome provide a functional depiction of synchronized, spontaneous and segregated activity [87, 141, 159]. There is an important methodological challenge in the characterization of the functional relationship between large-scale areas (RSNs), mainly related with the severe brain damage of patients in DOC conditions. Particularly, brain-injured patients may present functional and structural affectations that may change the connectome properties. Therefore, a particular processing pipeline that accounts for these alterations was considered, including, severe structural affectations, large head motions, and individual variability, among others. Figure **2-1** summarizes the process used to characterize functional connectivity alterations at the general brain level of interactions between RSNs.

2.2.1. Materials and Methods

Subjects and patients

Participants were healthy volunteers and patients with UWS or MCS following severe brain damage studied at least 5 days after acute brain insult. HC subjects were subjects free of psychiatric or neurological history. Clinical examination was performed using the French version of the Coma Recovery Scale-Revised (CRS-R) [73, 154]. The CRS-R is a standardized measure for characterizing the level of consciousness and monitoring recovery of neurobehavioral function [73]. It consists of 30 hierarchically arranged items that comprise 6 subscales addressing auditory (5 items), visual (6 items), motor (7 items), oromotor/verbal (4 items), communication (4 items), and arousal (4 items) processes. The scoring is based on the presence or absence of specific behavioral responses to sensory stimuli administered in a standardized manner, and the lowest item in each subscale represents reflexive activity while the highest item represents cognitively mediated behaviors [73, 154]. Exclusion criteria were contra-indication for MRI (e.g., presence of ferromagnetic aneurysm clips, pacemakers), MRI acquisition under sedation or anesthesia and large focal brain damage ($> 50\%$ of total brain volume). Structural brain damage was assessed by visual inspection of two experts. Written informed consent to participate in the study was obtained from the healthy subjects and

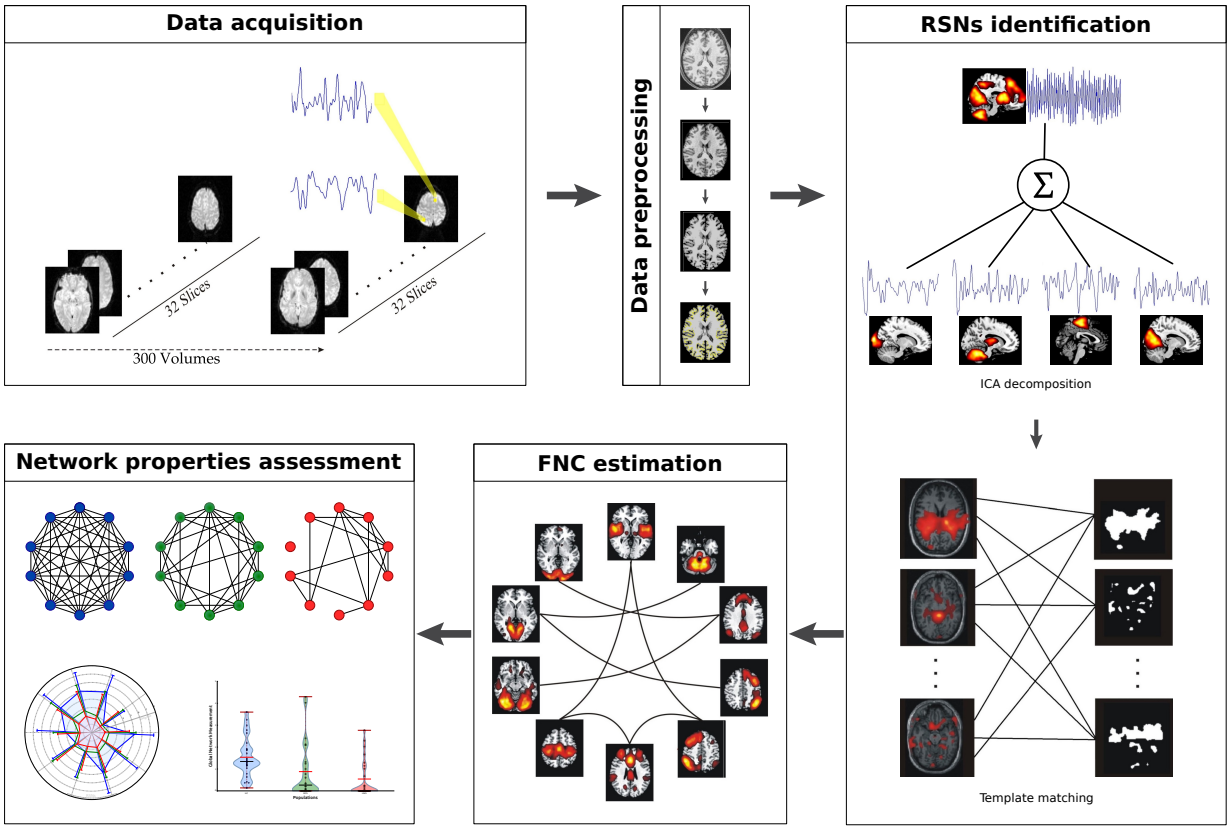

Figure **2-1**.: Illustration of methodological procedure defined as the sequence of the following processes: Data acquisition consist of 300 volumes functional MRI at rest and a structural MRI for each subject. Next, data preprocessing including brain extraction, alignment, registration, Gaussian smoothing, motion correction and normalization. Following by a data driven approach to extract the RSNs using spatial independent component analysis and a template matching strategy. Then, functional network connectivity between RSNs were computed by the lagged distance correlation method. Finally, integration, segregation and centrality measurements were computed to characterize the populations in different states of consciousness

from the legal surrogates of the patients. The study was approved by the Ethics Committee of the Medical School of the University of Liège [46].

Data description

Acquisitions from 75 subjects were used for this study: 27 HC subjects (14 women, mean age 47 ± 16 years), 24 patients with MCS (8 women, mean age 47 ± 16 years; 9 of non-traumatic etiology: 2 anoxic, 3 with cerebrovascular accident, 3 with hemorrhage, 1 with seizure; 14 of traumatic, and 1 of mixed etiology) and 24 with UWS (12 women, mean age 50 ± 18 years; 18 of non-traumatic etiology: 9 anoxic, 6 with cerebrovascular accident, 2 with hemorrhage, 1 metabolic; 5 of traumatic, and 1 of mixed etiology). 31 patients with UWS and MCS were assessed in the chronic setting, i.e., $\geqslant$ 50 days post-insult. For each subject, fMRI data were acquired in a 3T scanner (Siemens medical solution in Erlangen, Germany). Three hundred fMRI volumes multislice T2*-weighted functional images were captured (32 slices; voxel size: $3 \times 3 \times 3\ mm^3$; matrix size $64 \times 64 \times 32$; repetition time = 2000 ms; echo time = 30 ms; flip angle = 78°; field of view = 192×192 mm^2). The three initial volumes were discarded to avoid T1 saturation effects. Additionally, a structural T1-weighted image was acquired for anatomical reference. Patients were scanned in sedation-free condition, and healthy volunteers were instructed to close their eyes, relax without falling asleep and refrain from any structured thinking (e.g. counting, singing, etc.), as commonly performed in resting-state paradigms [12, 80].

Data preprocessing

Data preprocessing was performed using the Statistical Parametric Mapping (SPM8) [67] toolbox for Matlab (The Mathworks, Inc., Sherborn, MA, USA). SPM preprocessing stages included realignment and adjustment for movement-related effects, co-registration of functional onto structural data, segmentation of structural data, normalization into standard stereotactic MNI space, and spatial smoothing with a Gaussian kernel of 8 mm. Motion correction (e.g. small, large and rapid motions, noise spikes and spontaneous deep breaths) was applied by using ArtRepair toolbox for SPM [120, 46]. To evaluate the data acquisition quality, the frame-wise displacement [134] was assessed on each population, figure **2-2** present the computation for each population set, red-line indicates the average displacement per frame in the population. The HC subjects exhibit the lowest values while the UWS patients show the highest.

Resting-State Networks identification

The RSNs were selected for each subject as follows: First, the R-fMRI signal was decomposed into maximally independent spatial maps using spatial ICA [121]. ICA decomposition was performed with 30 components [94] and the infomax algorithm as implemented in GroupICA

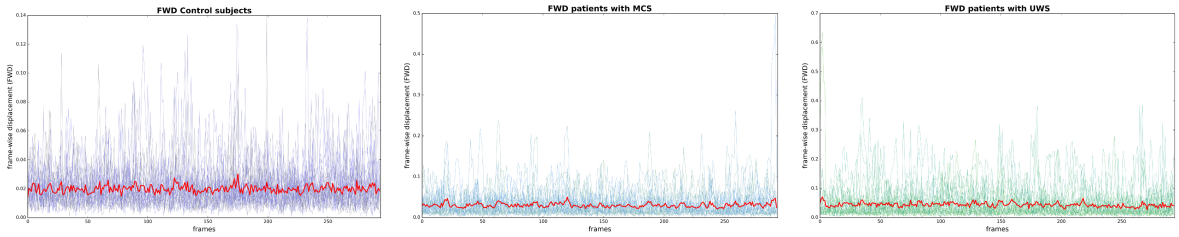

(a) Healthy Controls (b) MCS patients (c) UWS patients

Figure **2-2**.: Frame-wise displacement computed for (a) Healthy control subjects, (b) Minimally Conscious State (MCS) patients, and (c) Unresponsive Wakefulness Syndrome (UWS) patients. Red line indicates the average displacement.

toolbox [31]. Each spatial map (source fMRI signal) has an associated time-course. It corresponds to the common dynamic exhibited by the component. Second, RSNs were identified at individual level [46] by using a two-fold process: template matching and neuronal/artifactual classification. Template Matching is an approach that aims to identify each RSN directly from the single subject spatial ICA decomposition [46]. It is a matching problem with two constraints: (i) a template had to be assigned to one of the 30 ICs and (ii) an IC could be labeled as an RSN or not. These two conditions ensure that all the templates (one for each RSN) have to be assigned and a unique identification of each IC, which deal with the potential concurrent component assignation. The pair between the template and the IC with the highest goodness of fit score was selected [46]. Later, a Neuronal/Artifactual classification of independent components (ICs) was performed by using a machine learning based labeling method [46]. It consists of a binary classification approach by means of support vector machine (SVM) classifier trained on 19 independently assessed healthy subjects. This SVM uses the fingerprints obtained from ICA decomposition (n = 30 components) as the feature vector containing both spatial (i.e. degree of clustering, skewness, kurtosis, spatial entropy) and temporal information (i.e. one-lag autocorrelation, temporal entropy, power of five frequency bands: 0 - 0.008 Hz, 0.008 - 0.02 Hz, 0.02 - 0.05 Hz, 0.05 - 0.1 Hz, and 0.1 - 0.25 Hz). Commonly, components of artifactual origin encompasses (i) high-frequency fluctuations > .1Hz, (ii) spikes, one or more abrupt changes in the normalized time-course, (iii) the presence of sawtooth pattern and (iv) the presence of threshold voxels in the superior sagittal sinus. Finally, neuronal time-courses of the RSNs were extracted at the individual level, and they were subsequently used for the functional connectivity computations.

Functional Network Connectivity estimation

For each subject, a FNC matrix was computed by using a measure of dependency between pairs of representative time-courses, resulting in a matrix with the strengths of interactions between the identified RSNs. The strength for edges pointing to RSNs marked as no-neuronal were set as zero, indicating no interaction. The measures of dependency level were computed

using the distance correlation (DC) between time-courses [163]. DC aims to measure non-linear dependencies between two random variables X and Y with finite moments in arbitrary dimension. In order to account for time delays, a circular shifted lagged version of the DC was used [94, 143]. Once the FNC was computed, it induces a functional connectivity matrix, which was used to characterize alterations of functional connectivity. A 10×10 weighted matrix was computed to model interactions between different RSNs. Each one of them models a brain region associated with specific arousal and awareness regions related to consciousness emergence. An entry c_{ij} in this matrix corresponds to the interaction between the RSN_i and RSN_j assessed by using the lagged DC.

Network characterization

FNC matrix contains a measure of dependency between pairs of RSNs time-courses. To assess functional connectivity alterations, three network properties were computed for each FNC matrix, namely, integration, segregation and centrality of the functional connectivity between RSNs. FNC integration was assessed by degree and strength [28, 27, 142]. FNC segregation was characterized by clustering coefficient [28, 27, 142], and FNC centrality was estimated by betweenness centrality and eigenvector centrality [110], a brief description of the mentioned measurements is in Table **2-2**. These computations were performed using the brain connectivity toolbox [142].

Table **2-2**.: Brief description of networks measurements used to characterize the FNC.

Networks measurements used to estimate the integration, segregation and centrality of resting-state networks (RSNs) in a network built from functional connectivity between them. N is the set of all nodes in the network, n is the number of nodes, L is the set of all links in the network, and l is the number of links. (i, j) is a link between nodes i and j. (i, j) are associated with normalized connection weights $0 \leqslant w_{ij} \leqslant 1$. a_{ij} is the connection status between i and j: $a_{ij} = 1$ when link exist and $a_{ij} = 0$ otherwise.

Name	**Formulation**	**Description**
Integration Measurements		
Degree	$k_i = \sum_{j \in N} a_{ij}$	Number of links connected to the node (Connection weights are ignored in calculations) [28, 142]
Strength	$k_i^w = \sum_{j \in N} w_{ij}$	Sum of weights of links connected to the node [28, 142]
Segregation Measurements		

Continued on next page

Table **2-2** – *Continued from previous page*

Name	**Formulation**	**Description**
Number of triangles	$t_i^w = \frac{1}{2}\sum_{j,h\in N}(w_{ij}w_{ih}w_{jh})^{1/3}$	Geometric mean of the weights of the triangles around the node i [28, 142]
Clustering coefficient	$C^w = \frac{1}{n}\sum_{i\in N}\frac{2t_i^w}{k_i(k_i-1)}$	Quantifies the number of connections that exist between the nearest neighbors of a node as a proportion of maximum number of possible connections [28, 142]
Centrality Measurements		
Betweenness centrality	$b_i = \frac{1}{(n-1)(n-2)}\sum_{h,j\in N}\frac{\rho_{hj}^{(i)}}{\rho_{hj}}$	The fraction of all shortest path that contains a given node [142]. Where ρ_{hj} is the number of shortest paths between j and h, and $\rho_{hj}^{(i)}$ is the number of shortest paths between j and h through node i
Eigenvector centrality	$Ax = \lambda x = \frac{1}{\lambda}Ax,\ x_i = \frac{1}{\lambda}\sum_{j=1}^{n} a_{ij}x_j$	Self-referential measure of centrality: nodes have high eigenvector centrality if they connect to other nodes that have high eigenvector centrality [110]. A denotes an $n \times n$ similarity matrix. x_i is defined as the i^{th} entry in the normalized eigenvector belonging to the largest eigenvalue of A

FNC degree values quantify the number of non-zero correlations of each RSN with other nodes in the network, while strength values indicate not only a correlation between RSNs but also the robustness of this correlation. They also provide a measure of the communication quality expressed in the correlation, i.e., higher values for these two measurements indicate better communication. Similarly, FNC segregation was measured by clustering coefficient. This assessment indicates how well-connected neighbor nodes are in order to become a grouped unit. High clustering coefficient values indicate that a set of nodes are well connected among themselves. Additionally, FNC centrality was assessed by betweenness and eigenvector measurements. Higher betweenness centrality values of a RSN mean that a node belongs to a high number of the shortest paths (path with the minimum distance between two nodes) between pairs of nodes in the network. For example, when a RSN time-course is better related to other time-course in sequence, it presents a better communication path. Furthermore, a higher RSN eigenvector centrality value indicates that this RSN is better connected to other central nodes. This estimates how central a RSN is based on the direct connections to others that have strong links. All measurements herein used were computed

for each node, i.e., for each RSN in the FNC. Average measurements were calculated to quantify communication quality among the network nodes. They describe the global network functional connectivity properties and depict all the network variations associated with FNC alterations.

Statistical analysis

To assess the discrimination power of the network properties, an unpaired-sample t-test [181] (Bonferroni corrected) was computed. For the statistical analysis, the following comparisons were performed: HC versus subjects with MCS, HC versus subjects with UWS, HC versus subjects with DOC (UWS and MCS), and subjects with MCS versus subjects with UWS.

2.3. Results

2.3.1. Loss of Functional Network Connectivity Integration in DOC

Figure **2-3** shows degree and strength values for subjects in different states of consciousness for the 10 different RSNs herein studied. As observed in Figure **2-3**A, degree values were higher for HC compared to subjects with altered states of consciousness (MCS and UWS) in all RSNs, except by the sensorimotor network. Significant differences ($p < 0.005$) were observed for the values of degree when comparing HC with MCS populations in auditory network, DMN, ECN Left and visual medial network. Significant differences ($p < 0.005$) were also found when comparing HC versus subjects with UWS and when comparing HC and subjects with DOC in auditory network, DMN, ECN Left, visual medial network, and ECN Right. Also, degree values for subjects with MCS were greater than the UWS in all RSN but no significant differences were observed.

As observed in Figure **2-3**B, strength values were higher for HC in comparison to subjects with altered states of consciousness in all RSNs except by sensorimotor and cerebellum networks. Significant differences ($p < 0.005$) in strength values were observed for HC compared to subjects with MCS and for HC versus the population of DOC, in auditory network, DMN and visual medial network. HC presented strength values significantly higher than subjects with UWS. No significant differences were observed between strength values of subjects with MCS compared to subjects with UWS.

Figure **2-4** shows the average degree and average strength values. Average values were estimated as a global characteristic of functional connectivity network between RSNs. As observed in Figure **2-4**A, average degree values were higher for HC compared to altered states of consciousness. Significant differences were also found for HC ($M = 3.81$, $SD = 2.10$) when compared with UWS ($M = 1.71$, $SD = 2.59$) ($t = 3.16$, $p = 0.003$). Similarly,

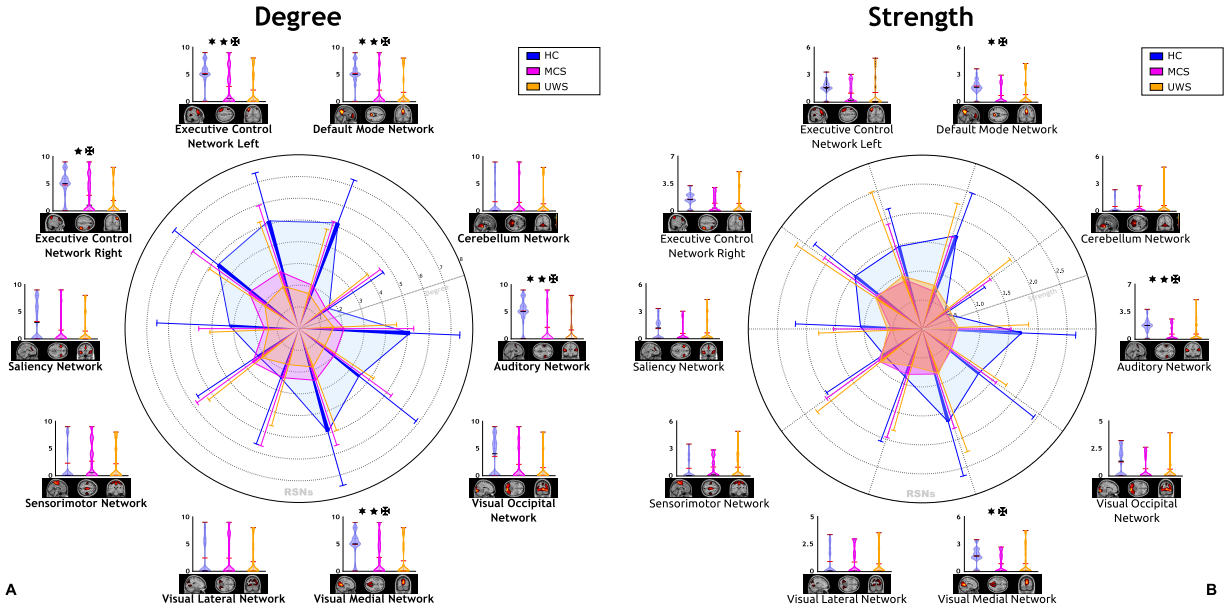

Figure **2-3**.: Integration measurements. (A) Degree and (B) strength show a similar distribution across healthy subjects and patients with Disorders OF Consciousness. Both evidence higher values for Healthy Controls (HC) than subjects with DOC in the same Resting-State Networks (RSNs) (auditory, cerebellum, Default Mode Network (DMN), Executive Control Network (ECN) Left, ECN Right, saliency, sensorimotor, visual lateral, visual media and visual occipital). Significant differences between HC and Minimally Conscious State (MCS) and Unresponsive Wakefulness Syndrome (UWS) patients were assessed in RSNs associated with the phenomenon of consciousness emergence (auditory, DMN, ECN Left, ECN right, Saliency). Fingerprints lines indicate mean values, and thin lines indicate standard deviation values for each RSN. ✭ aims for significant difference between HC and MCS. ★ aims for significant difference between HC and UWS. ✠ aims for significant difference between HC and DOC

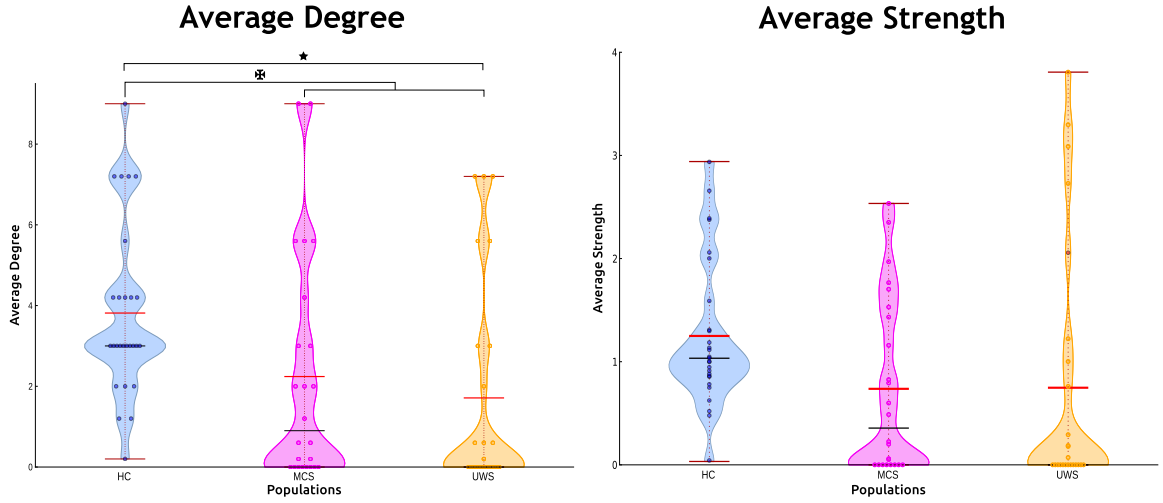

Figure **2-4**.: Distribution of the average integration measurements for the three populations herein studied. (A) Degree and (B) Strength. Red lines indicate the mean, black lines indicate the median and red wine lines indicate the maximum. Each dot in the violin represents the measurement on a single subject. ✯ aims for a significant difference between Healthy Controls (HC) and Minimally Conscious State (MCS) ($p < .05$). ★ aims for a significant difference between HC and Unresponsive Wakefulness Syndrome (UWS) ($p < .05$). ✠ aims for a significant difference between HC and patients with disorders of consciousness $p < .05$).

significant differences in average degree were also found when HC subjects were compared with DOC (M = 1.97, SD = 2.69) (t = 3.03, p = 0.003). Further, the average degree presented a decreasing tendency which corresponds to the increase in DOC severity. As observed in Figure **2-4**B, average strength values were higher for HC compared to altered states of consciousness. No significant differences were observed for these averages when compared among populations, in contrast to the previous observation of decreases in the average degree values. Also, average degree and average strength values exhibit greater spread distributions for subjects with MCS and subjects with UWS than for HC subjects.

Integration measurements suggest that RSNs related to awareness are better connected for conscious subjects [82]. Higher degree values of auditory network, DMN, ECN Left, ECN Right, and visual medial network for HC indicate that, for this population, these RSNs are more connected to other RSNs than in subjects with DOC (Figure **2-3**). This reduction of the degree values in altered states of consciousness could be understood as a reduction of relationships between RSN time-courses, i.e., representative time-courses are less or not correlated, suggesting an alteration of the functional connectivity structure in this patients. This result corroborates the disruption of external and internal awareness networks [44] and the decrease in anti-correlated connectivity previously observed in subjects with DOC [52]. Also, functional connectivity of salience network was reported as diminished in altered states of consciousness [80]. This network is usually associated with the orchestration between internal attention and task-related-states, and its alterations were linked to consciousness disorders [84]. In this experiment degree values for salience network support this observation.

A more detailed analysis of the integration phenomena can be obtained by studying strength values alterations (Figure **2-4**). These values were also reduced in altered states of consciousness indicating that the amount of information that different time-courses share is lower for subjects with DOC. This observation confirms the functional disruption associated with the severity of the pathological condition, as was reported for highly detailed networks in distinct consciousness states [130]. Further, this reduction could result from a deterioration process of the connectivity between RSNs, which can be an effect of the connectivity drops in small regions [82]. Also, averaged integration measurements, both degree and strength, suggest that preserved levels of consciousness seem to be related to narrow distributions for integration values. In particular, patients with UWS seem to exhibit a larger variety of connectivity values including hyperconnectivity (increment of connectivity) and disconnections, when compared to healthy subjects. Subjects with altered states of consciousness not only reduce the number of connections between RSNs, but also degrade the ones that remain, suggesting a reduction of the synchronization level associated with the communication between networks. Importantly, the measures herein proposed were computed in large spatial regions that contain previously studied areas, such as the thalamo-cortical circuit [44]. Therefore, breakdowns in integration seem to appear not only for small brain areas, as reported for

strength reductions in the connectome computed from EEG [29], but also for larger functional systems. Similarly to our results, Cacciola et al. [29] compute integration measurements for subjects with MCS and UWS, but they were also not significant to discriminate between those populations. To conclude, the local integrations measurements corroborates previous findings of connectivity disruptions for patients with DOC, while global integration describes the global integration assessments exhibits a decreasing tendency related to the consciousness level, i.e., the conscious subjects seem to be better integrated than patients with MCS, and patients with MCS seem to better integrated than patients with UWS.

2.3.2. Loss of Functional Network Connectivity Segregation in DOC

Figure **2-5** reports the clustering coefficient values for subjects in different states of consciousness. Higher clustering coefficient values were obtained for HC in comparison to altered states of consciousness except in sensorimotor, cerebellum and visual lateral networks (Figure **2-5**A). Clustering coefficient values for HC present significant differences ($p < 0.005$) compared to subjects with MCS in auditory network and DMN. Significant differences ($p < 0.005$) also were observed when comparing HC and subjects with UWS for auditory and visual medial networks. No significant differences of clustering coefficient values were observed for the RSN when compare subjects with UWS and subjects with MCS. Finally, differences between subjects with DOC and HC subjects were significantly distinct ($p < 0.005$) for auditory network, DMN and visual medial network.

Figure **2-5**B shows the average clustering coefficient values. These values were higher for HC compared to altered states of consciousness. Average clustering coefficient values were significantly higher for HC ($M = 0.20$, $SD = 0.06$) compared to subjects with MCS ($M = 0.12$, $SD = 0.12$) ($t = 2.95$, $p = 0.004$). Similarly, significant differences were also higher when comparing HC and subjects with DOC ($M = 0.12$, $SD = 0.14$) ($t = 2.97$, $p = 0.004$). Further, distributions of the average clustering coefficient were narrower for HC than for subjects with DOC while their means exhibit a slightly decreasing tendency in correspondence with the severity of DOC.

High values in clustering coefficient of the DMN seem to be related to the level of synchronization of this network with other RSNs. This result was previously reported in specific awareness circuits involving the DMN [46]. Segregation measurement assessed by clustering coefficient confirms that consciousness could be a phenomenon involving segregated functional units that work in an integrated manner [167]. RSNs could be understood as segregated regions that execute specific tasks [17] but share information in consciousness phenomena [84]. Sensory and cognitive-related networks appear to be more clustered for HC. In contrast, the segregation increases for sensorimotor in DOC with no significant differences between MCS and UWS. A similar finding was reported in an experiment with altered states

of consciousness and anesthesia [79] where an increment of functional connectivity between thalamus and sensorimotor network was found in altered states of consciousness.

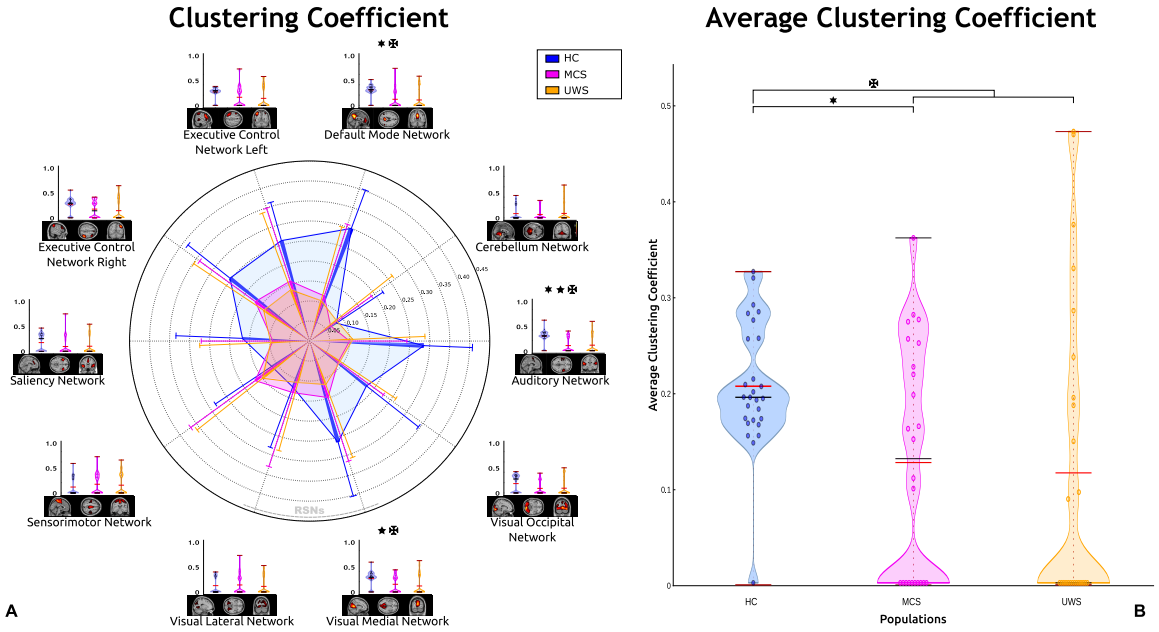

Figure **2-5**.: Segregation measurement between Resting-State Networks by clustering coefficient. (A) fingerprint (B) violin plot. Higher clustering coefficient values were observed for Healthy Controls (HC) than for subjects with Disorders of consciousness (DOC) except by sensorimotor network. ✶ aims for a significant difference between HC and patients with Minimally Conscious State (MCS). ★ aims for a significant difference between HC and Unresponsive Wakefulness Syndrome (UWS). ✠ aims for a significant difference between HC and patients with DOC.

Altered segregation values in the sensorimotor region, jointly with integration changes, are suggesting a variation in the sensorimotor time-course behavior, becoming more synchronized with other high related RSNs; thus, these variations suggest the configuration of a segregated functional unit. This behavior seems to be a consequence of different scenarios out of the scope of the present study that could be analyzed in future explorations. However, this finding is contrary to the reported by Cacciola et al. were they reveal an increment of the clustering coefficient in the patients with UWS when compared against MCS, the mentioned difference could be a result of the computation of the clustering coefficient using a binary matrix [29] instead of a weighted connectivity matrix, as in our case. In brief, variations of the segregation measurements in patients with DOC seems to be caused for a reconfiguration of the functional synchronized groups.

2.3.3. Alterations of Functional Network Connectivity Centrality in DOC

Betweenness centrality and eigenvector centrality values are reported in Figure **2-6**. Betweenness centrality values were higher for HC in contrast to subjects with altered states of consciousness for DMN, ECN Left, ECN Right, salience network and cerebellum network, as observed in Figure **2-6**A. These centrality values of subjects with UWS were higher when comparing to subjects with MCS and when comparing to HC subjects, for auditory, sensorimotor, visual lateral, visual medial and visual occipital networks. Also, ECN Right and salience network has values of zero of betweenness centrality for UWS patients, indicating that these nodes were not part of any shortest path in the network.

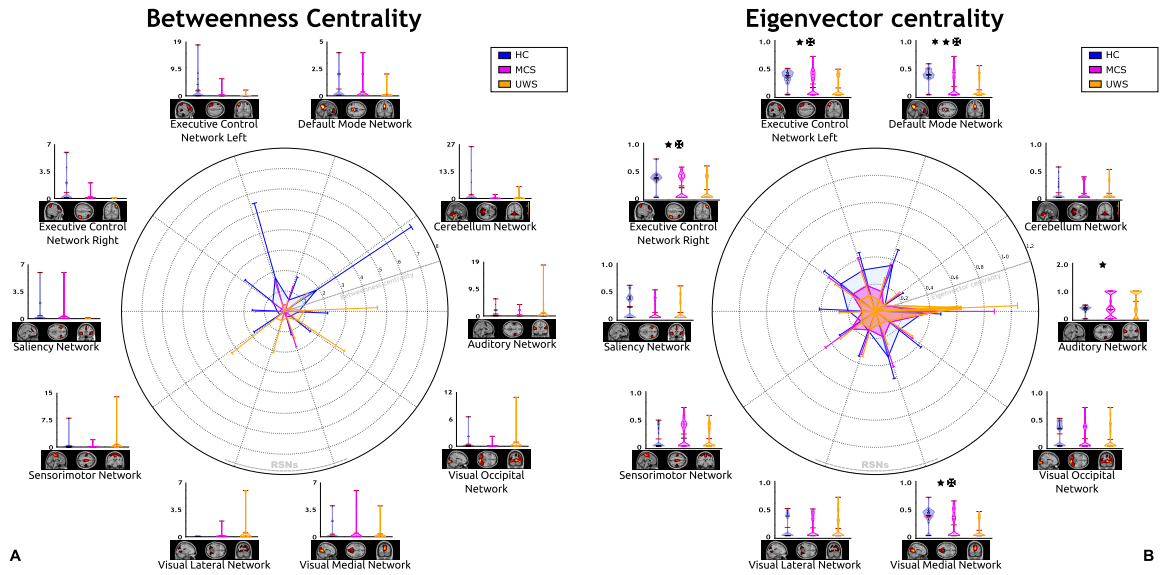

Figure **2-6**.: Centrality measurements. (A) Betweenness centrality exhibits a central role changing in auditory, sensorimotor, visual lateral and visual occipital networks for subjects with Disorders of Consciousness (DOC). Similarly, (B) eigenvector centrality presents a role alteration for auditory and sensorimotor networks in subjects with DOC. ✭ aims for a significant difference between Healthy Controls (HC) and patients with Minimally Conscious State (MCS). ★ aims for a significant difference between HC and patients with Unresponsive Wakefulness Syndrome (UWS). ✠ aims for significant difference between HC and patients with DOC.

As observed in Figure **2-6**B, eigenvector centrality values were higher for HC compared to subjects with DOC except by auditory and sensorimotor networks. Higher values of eigenvector centrality for HC with significant differences ($p < 0.005$), were observed for DMN, ECN Left, ECN Right, and visual medial network compared with subjects with DOC. Similarly, when contrasting HC and subjects with MCS, significant differences ($p < 0.005$) were obtained for DMN. Eigenvector centrality values were significantly different ($p < 0.005$) for DMN, ECN Left, ECN Right and visual medial network in comparison with HC and subjects with UWS. Further, eigenvector centrality values were higher for subjects with MCS compared to HC, and for subjects with MCS versus UWS for the sensorimotor network. Finally, auditory network eigenvector centrality values were higher for subjects with UWS compared to subjects with MCS, which were also higher than HC. This observation in the auditory network indicates an increasing tendency in centrality, which corresponds with the severity of the pathology. For this network, significant differences ($p < 0.005$) were found between subjects with UWS and HC.

Figure **2-7** illustrates average betweenness centrality and average eigenvector centrality. Average betweenness centrality values were higher for HC in contrast to subjects with altered states of consciousness. Also, the distribution of these values is narrower for MCS compared to HC and subjects with UWS (Figure **2-7**A). Similarly, higher values of average eigenvector centrality were observed for HC when comparing to subjects with DOC (Figure **2-7**B). Significant differences were observed when compare the populations, between HC ($M = 0.25$ $SD = 0.06$) and subjects with MCS ($M = 0.19$ $SD = 0.08$) ($t = 3.61$ $p = 0.00071$), between HC and subjects with UWS ($M = 0.16$ $SD = 0.08$) ($t = 5.04$ $p= 0.00001$), and between HC and subjects with DOC ($M = 0.18$ $SD = 0.08$) ($t = 4.54$ $p = 0.00002$). Further, average eigenvector centrality values exhibit a decreasing tendency as the severity of the pathology increases. They also showed a narrower distribution for HC in comparison to subjects with DOC.

Centrality measurements indicate how central a node is in the network. High centrality scores in auditory and sensorimotor networks suggest that these functional units play a central role in patients with altered states of consciousness, revealing a behavior alteration phenomenon even if these regions exhibit a functional connectivity reduction in patients with altered states of consciousness, as was previously reported [44, 98]. This observation could be further explored to understand the kind of variation induced by DOC that reveals a centrality increment. Similarly, higher scores in sensorimotor network suggest that this network also change its nature, becoming more important in subjects with altered states of consciousness. Interestingly, even if the sensorimotor input-output loops were reported as not required for consciousness [168], the circuits involving these RSN were altered by the pathology [49]. A surprising finding is the increment of centrality values for this external awareness network in subjects with DOC, which is not expected due to its associated behavior to sensory stimuli

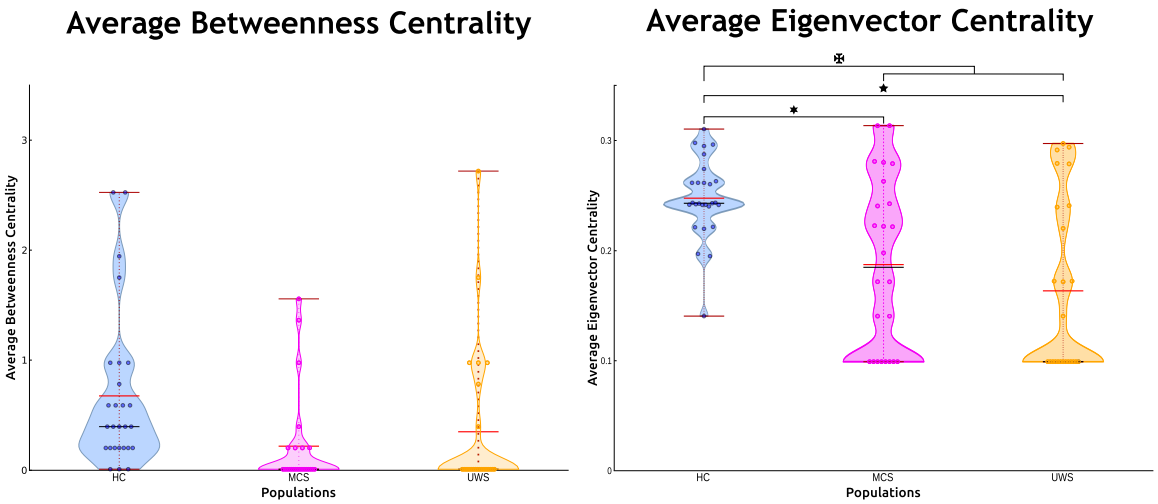

Figure **2-7**.: Average centrality distribution measurements (A) Betweenness Centrality, (B) Eigenvector Centrality. Red lines are the mean, black lines are the median, red wine lines are the maximum. Average eigenvector centrality shows narrower distributions for Healthy Controls (HC) than subjects with Disorders of Consciousness (DOC). Also, a decreasing tendency is observed in correspondence with the consciousness content. ✶ significant difference between HC and patients with Minimally Conscious State (MCS). ⋆ significant difference between HC and patients with Unresponsive Wakefulness Syndrome (UWS). ✠ significant difference between HC and patients with DOC.

and motor reaction. A similar finding was reported by Cacciola et al, where an increment of the betweenness centrality in posterior cingulate and visual areas were stated for patients with UWS [29]. However, this finding at RSN level can be a result of a brain reconfiguration in response to not-conscious stimuli response [169]. Increases of centrality values of functional connectivity between RSN in altered states of consciousness suggest a modification of their time-courses nature, becoming more relevant in subjects with DOC. Nevertheless, this new central role of some RSNs would be not suitable for consciousness phenomena, where a sort of equilibrium between segregation and integration is required [167, 168, 169, 29]. Summarizing, centrality alterations describe a reconfiguration of the relevant functional units in altered consciousness states that seem to be not suitable for the emergence of consciousness.

2.4. Discussion

Complex network analysis have been proposed to capture topological variations of real networks derived from pathologies (see Table **2-1**), this approach is strongly supported on the assumption that the complex network represents a single object [19], i.e., the complex network measurements describe the properties of nodes and relationships of a single network. Some of their measurements can be related with topological features in the sense that they describe particular connection patterns, those patterns can be accounted and evaluated making possible to identify variations associated to different phenomena. That is the case of the measurements used to characterize integration, segregation, centrality and other specific network properties.

Integration measurements allow to identify connectivity disruptions. Decreases in the degree and strength average values account for these events. They capture the loss of a connection as well as the quality of the connection reduction. A lost connection directly alters the topology of the element, in particular if with that loss some nodes of the network cannot be reached. In patients with DOC, the integration values measured on the FNC computed from RSN evidence a decreasing tendency linked with the consciousness level, i.e., high integration values mean more consciousness content.

On another hand, segregation measurements may indicate a sort of topology variation by the identification of the groups appearance. It might be understood as a second analysis level, it is based on the integration measurements, but it describe not only the connections, they also describe the way as the connection co-occurs indicating collections of connected components. These collections and their conformation have been used to describe specific network topologies, like small-world, rich-club among others. The segregation measurements on RSN based connectivity for patients with DOC exhibits variations that seems to be caused for a reconfiguration of the functional synchronized groups.

Finally, centrality measurements describe the relevance of network elements, e.g., nodes, edges, paths, among others. Centrality variations describe reconfiguration of the network accounting for changes in the role of the units in the network. The centrality alterations in DOC points to regions with change its role, in particular signaling which become more relevant in association with the consciousness level, as in the sensorimotor and auditory networks, or indicating which reduce its relevance as the DMN, visual media and executive control networks.

To conclude, complex network measurements provide a set of tools to describe, evaluate and characterize a network. Even in a global scale as the FNC built from RSN, they capture some variations that can be linked with a specific pathological condition, and in some cases they can be associated with the severity level of the pathology. However, their measurements partially describe the topological properties focused on the existence of links between nodes. Other interesting topological features, like loops or voids are left a side by this complex network approach. Also, they were limited by the existence of a single structure, one network, and this assumption could be not suitable in scenarios where are multiple objects of interest, like disconnected nodes or regions in the networks.

3. Topological Data Analysis on functional network connectivity for healthy control subjects

As previously mentioned, the functional connectome of brain activity acquired on resting-state emerged as an alternative to provide measurements of brain function at multiple scales [17, 85]. Analyses on these connectomes encompass various graph theory methods to identify central nodes, critical paths, and communities, among other essential functional brain components [85]. These functional descriptions characterize various Functional Network Connectivity (FNC) properties associated with brain dynamics in healthy subjects and provide biomarkers for several pharmacological and pathological conditions [183, 179]. Notably, most of these analyses operate on the graph abstraction with nodes representing the brain regions, and edges the values of measures of interaction or synchronization between pairs of regions [142, 159, 85]. In FNC, this measure commonly links to the correlation value between two time-courses, which describe commonalities in the activation of both areas. This approach provides a powerful representation to model a variety of phenomena related to connectivity [85]. However, the pairwise interaction assumption underlying the functional graph model over-simplifies brain dynamics by considering at the very base only co-fluctuations on the activity of two brain regions [9]. This could underestimate how brain function may exhibit high-order interactions among multiple brain regions, i.e., interactions among more than two areas [9]. This paper investigates the existence of robust high-order functional components on the resting state dynamic in healthy subjects at an individual level by using Persistent Homology (PH), a data analysis strategy based on topology to characterize high-order connectivity features robustly.

Description of high-order interactions in resting state has been previously explored, mainly through graph measurements based on triangles. In contrast to an edge, a triangle represents the co-existence of interactions for ensembles of three nodes [159, 132]. This high-order interaction representation is the base for different connectome characterizations, like the clustering coefficient, transitivity, and small-worldness [142]. These approaches aim to describe the resting state as a network of distributed modules likely performing segregated tasks [159]. However, despite the success of these strategies for the resting state connectome characterization, other high-order interactions mechanisms are still poorly studied [9]. More recently,

alternative methods for exploring these interactions in the fMRI brain functional connectome have emerged, such as Topological Data Analysis (TDA) [135, 111, 75, 35]. TDA encompasses methods aimed to characterize datasets using techniques from topology. In contrast to graph-based methods, TDA allows the description of high-order interactions [72]. For instance, Saggar et al. [145] proposed a TDA description of brain function, identifying the topology of fMRI acquired in related evoked stimuli by using a combination of dimensionality reduction, clustering, and graph networks techniques [155]. They found cohesive high modularity across different tasks, where each module reflects similarities in task responses. Salch et al. illustrated the use of TDA for characterizing loops in fMRI acquired during an associative learning paradigm [147]. Similarly, Ellis et al. showed that TDA could discover cycles in simulated event-related fMRI data [56], and Billings et al. used TDA to segment brain states that differ across a time series of experimental conditions [16]. These approaches confirm the capacity of TDA to identify high-order structures of interaction over functional datasets [56, 16, 147]. However, in these cases, the emergence of the functional structures was conditioned by an experimental stimulus, absent during resting-state protocols. On the other hand, Cassidy et al. used TDA to examine the Spatio-temporal consistency of resting-state at different temporal and spatial scales. However, they focused on a description of low-order topological features [35]. Petri et al. also used TDA on resting-state fMRI to investigate the emergence of loops in R-fMRI dynamic, showing that the distribution of the complete set of loops observed for the whole population may help distinguish between two conditions, namely, placebo and psilocybin [132]. This evidence points to the existence of loops underlying the resting state. However, these works do not indicate whether these cycles emerge individually or if they are persistent enough to be considered as functional components.

This work investigates the existence of robust cycles at the individual level in the R-fMRI dynamic. For this, we devised a strategy for characterizing loops on the R-fMRI dynamic using PH. We evaluated this strategy at the individual level on healthy controls population. Finally, we characterize the brain regions involved in the emergence of these loops. Our main contributions are the description through high-order topological features in R-fMRI applying PH at an individual level, and the identification of brain regions involved in the emergence of these features. In contrast, previous studies aimed to characterize loops in the fMRI induced by stimuli or focused on the whole set of loops at the population level on R-fMRI.

This chapter first provides a motivation to use TDA to describe (R-fMRI) time-courses. Second, it presents some relevant TDA concepts and their use in the brain function description. Third, it describes the TDA method employed to characterize R-fMRI time-courses for healthy control (HC) subjects. Finally, it reports the high-order features of the HC subjects and the brain regions implicated in its emergence.

The main contributions of this chapter are: (i) A high-order topological features description in R-fMRI of Healthy Subjects through persistent homology, (ii) these high-order R-fMRI features robustly appear across the healthy population, and (iii) brain regions involved in the appearance of these high-order features were identified, providing a new analysis perspective. Besides, this chapter was submitted to Network Neuroscience, and it is under review.

3.1. From resting-state connectivity to topology description through boundaries

Topology provides a straightforward alternative to encode high-order interactions by describing them as groups of nodes or simplices. Simplices represent the simultaneous interactions of multiple elements. Moreover, simplices can be collected on a simplicial complex, just like graphs are collections of edges and vertices. Then, the simplicial complex represents the connectivity among elements from a general perspective not limited by the number of interacting components. To characterize the properties of the simplicial complex, TDA, or specifically algebraic topology, provides tools like PH [54]. PH is a method to describe topological features at various resolutions [14, 54, 72]. For this, PH first represents the data, a set of points, as a simplicial complex, and then computes robust descriptors related to boundaries of the holes across different scales [54]. These descriptors correspond to the number of loops, voids, and in general, cavities [33, 55], summarizing the topological properties of data. These topological features may provide meaningful data insights because they describe robust data organization structures.

Figure **3-1** illustrates some simplicies and a particular simplicial complex, the figure shows the first four simplices that describe simultaneous interactions among elements. A simplex of degree k or k-simplex indicates the structure with $k+1$ elements connected simultaneously, i.e., a 0-simplex refers to points, a 1-simplex refers to an object with two points with a connection (a line), a 2-simplex represents an object with three points with a simultaneous connection among them (a triangle whis is also called a face), a 3-simplex a tetrahedron, and so on for higher-dimensional simplices [72, 111], Figure **3-1**a. Figure **3-1**b displays a simplicial complex. As observed, a simplicial complex is formed by simplices of different degrees in configurations that may also include holes. For instance, a graph is a simplicial complex with 0-simplices (nodes) and 1-simplices (edges). The simplicial complex object (simplices and holes) constitutes a base to describe high-order features in terms of cavities. Figure exemplifies three distinct types of cavities: a) 0-holes, which are cavities in the space that emerge by the existence of clusters, i.e., a set of points conected by simplices of degree 1 or more. Figure **3-1**b shows three different clusters, and the corresponding three 0-holes, each indicated by the shaded areas, b) 1-holes, cavities completely bounded by at least three 1-simplex, i.e., are empty spaces surrounded by lines, the illustration shows two of these

1-holes, and c) 2-holes, voids enclosed by at least four 2-simplex, i.e., holes surrounded by triangles. Figure illustrates one 2-hole, i.e., a cavity completely contained by eight 2-simplex.

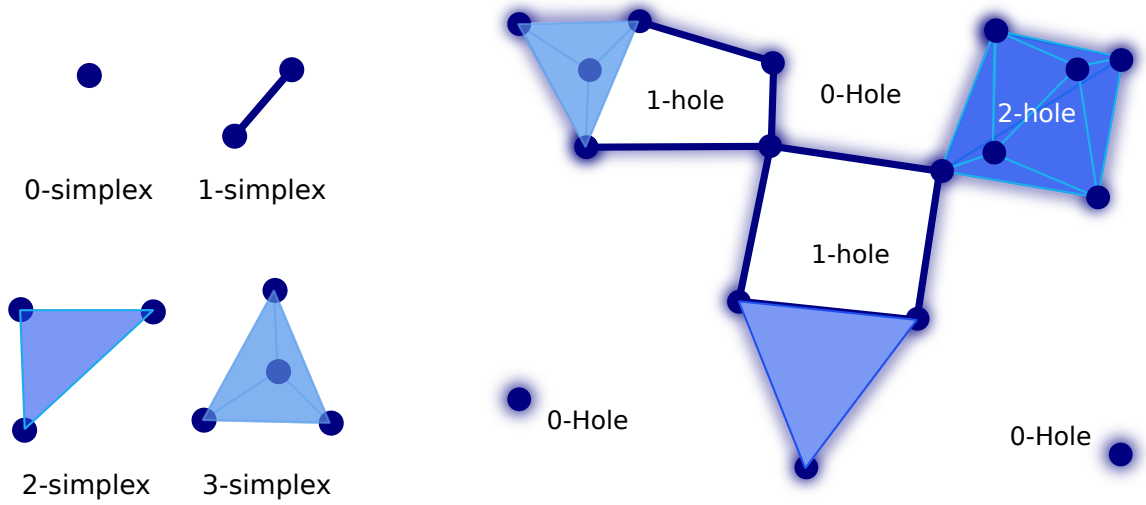

(a) Simplices (b) Simplicial complex

Figure **3-1**.: Illustration of simplices and simplicial complex. (a) Simplices from 0 to 4 simultaneusly interacting elements. (b) A simplicial complex with three connected components, two 0-simplex and a complex composed by simplices of different dimensions, and a set of holes defined by these simplices. The 0-hole appears at the boundaries of a set of connected simplices (shaded area). Similarly, the 1-hole is a cavity completely bounded by at least 1-simplices. The 2-hole is completely bounded by at least 2-simplices, and so on.

This differentiation in holes of different dimensions extends the notion of interaction, providing a complementary perspective beyond the pairwise interactions used on graph theory. Importantly, holes in dimensions greater than one represent an alternative mechanism of integration between points because the presence of one of these holes indicates the existence of a surrounding high-order particular structure of interactions.

To compute this structure PH starts with a point cloud expressed in some adequate representation space, commonly a metric space. From this point cloud, the first step is the construction of a connectivity structure representing the neighborhood associations between these points, codifying high-order relationships. According to Ghrist [72], "the more obvious way to convert a collection of points $\{x_\alpha\}$ in a metric space into a global object is to use the point cloud as vertices of a combinatorial graph whose edges are determined by proximity (the vertices within some specified distance ϵ)". This construction results in a high-dimensional object, a simplicial complex, which is a space built from simple pieces (simplices) identified combinatorially by faces that codify a proximity representation between points [72].

Figure **3-2** illustrates the simplicial-complex computation via the Vietoris-Rips algorithm (further details in Ghrist [72]). In this approach, the simplicial complex contains k-simplices, each corresponding to unordered $(k+1)$-tuples of points that are pairwise within a distance ϵ. This ϵ is called the filtration value, and it represents the extent of a neighborhood considered around each point. The term filtration is also used to designate the process of adding simplices to form a simplicial complex when changing the filtration value up to ϵ. In this particular example, the filtration starts with a set of twenty-one disconnected nodes, $\epsilon = 0$. Then while the filtration value increases, the intersections of the balls with radius ϵ centered around points result in neighborhood relationships (see the green area around points), involving more than two points, as illustrated with triangles in the Figure. These neighborhood relationships are codified as simplices that together conform the simplicial complex. As observed in Figure 2 for an increasing sequence of ϵ values, namely, 0, a, b, c, d, and e, each filtration value results in a corresponding simplicial complex modeling a particular extent of the neighborhood relationship. So, the filtration and the filtration value are comparable to the network and threshold in the traditional connectome approach, where the threshold codifies the structure of the network, as the filtration value codifies the filtration [9].

Once the neighborhood relationships between points, corresponding to particular ϵ values, have been defined and codified as a simplicial complex. It is possible to compute the topological invariants that describe high-order interactions [72]. These invariants are features associated with a topological space that do not change under continuous space deformations, such as the number of holes [76]. Then, the notion of topological invariant is related to those features that survive across successive deformations, and a hole can be understood as a structure that prevents an object from being continuously shrunk to a point. Thus, the existence of a hole is an indicator of a particular connectivity structure around it, i.e., the connectivity configuration that prevents that the space represented by the simplicial complex collapses under continuous deformations, acting as a connectivity boundary.

Remarkably, well-known facts about R-fMRI signal can be interpreted in the PH context. For instance, from the PH perspective, the resting-state connectome can be understood as the complement of the 0-holes, i.e., the connected components at a given threshold. This connected components are simplicial-complex of degree 1 or more (see Figure **3-1**). Thus, it is possible to macth the graph in the connectome approach with the connected components that produce the 0-holes described by PH. Nevertheless, it is worthy to recall that the PH approach accounts for the "holes" that emerge from the data rather than for the connection itself. This way, it provides a view of the interaction among elements complementary to the view commonly used in R-fMRI brain analysis. Furthermore, the PH could be understood as a generalization of the graph approaches where a graph is a fixed instance with degree 1.

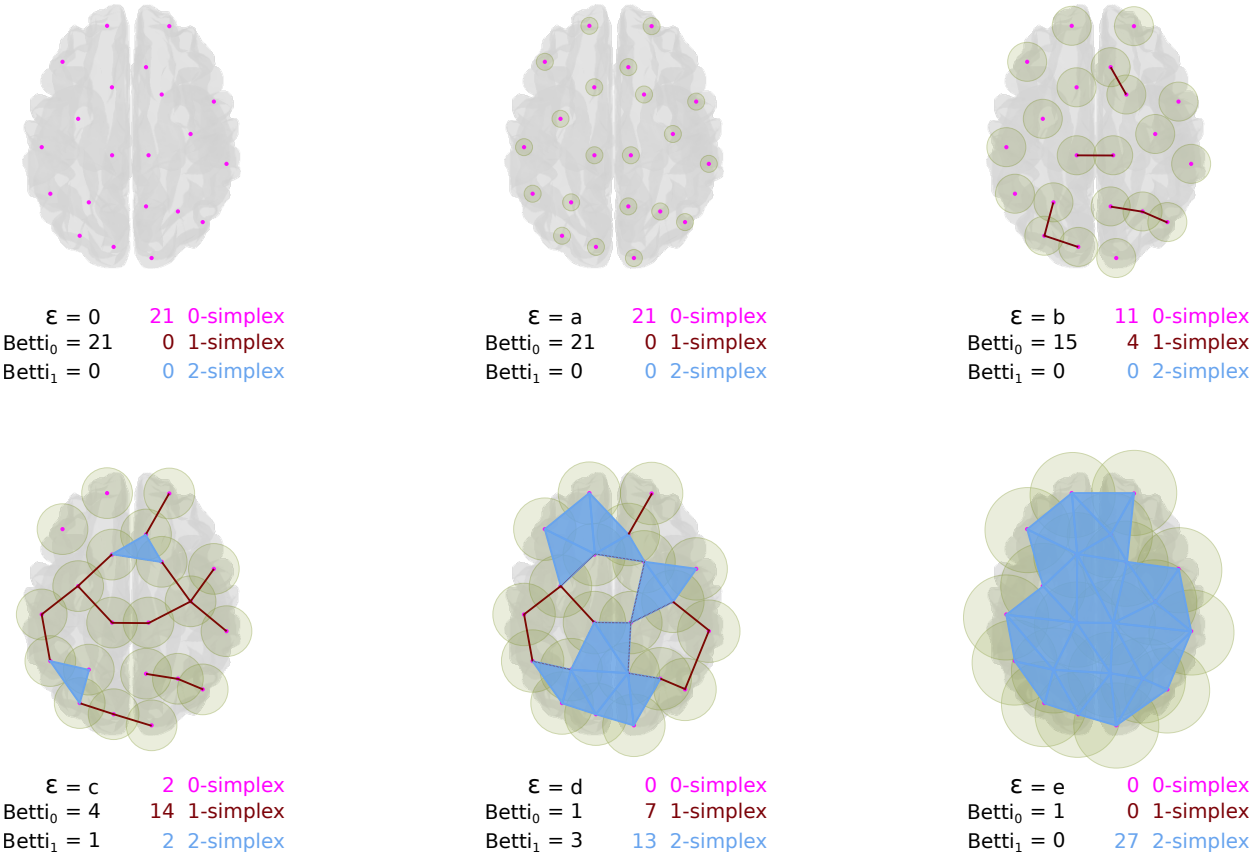

Figure **3-2**.: Illustration of the simplicial constructions from a cloud point set. The pictures shows the simplices for an increasing value ϵ. Thus, as the ϵ value grows, different simplices configurations appears, and with them the corresponding topological features counted by Betti numbers.

PH or specifically algebraic topology provides tools for counting these holes. In particular, PH relies on the notion of homology, which allows counting the number of holes of finite simplicial complexes. The homology or homology group ($\mathcal{H}$) of a simplicial complex is the collection of k-holes formed by k-simplices (further details in [72, 75]). PH counts the boundaries surrounding the holes that are persistent for a sequence of filtrations, i.e., the number of simplicial complex holes of filtrations at different filtration values. Then, PH counts the persistent k-holes, i.e., holes in the homology at dimension k ($\mathcal{H}_k$). In this context, another tool for homology description is the Betti numbers, they are the rank of features of a particular k-dimension for a complex at a fixed ϵ value. Betti numbers count the occurrence of k-holes (a k-hole is a hole bounded by k-simplices); Betti 0 counts the 0-holes, Betti 1 counts 1-holes, i.e., the appearance of a hole surrounded by 1-simplex, an empty area surrounded by pairs of connected objects; Betti 2 counts voids, the emergence of a 2-dimensional hole, i.e., a void enclosed by 2-simplices (triangles), and so on, see Figure **3-2**.

Two distinct approaches are commonly used to represent the emergence and disappear of the topological features, namely, the TDA barcodes [72], and the persistence diagrams [14], see Figure **3-3**. A barcode is a representation of the homology groups resulting from different filtration values as a collection of bars (intervals) representing the birth and death times of the k-dimensional holes [5, 72]. It allows studying the evolution of these holes along a nested sequence of a simplicial complex [5]. This nested sequence of a simplicial complex results from using increased values of filtration. A significant attribute of this representation is that long barcodes are associated with robust features, i.e., long barcodes link to features that persist along different filtration values [93]. In contrast, short barcodes are commonly related to noisy topological features, such as holes that appear during small intervals of filtration values.

Persistence diagrams provide an alternative way to summarize the topological structure of data. As in the barcodes, persistence diagrams summarize the topological features for the sequence of filtration values. Formally, the persistence diagram is a collection of triplets <homology degree, birth time, death time> of the filtration sequence [14]. The set of triplets can be represented as points in a two-dimensional plot, with x the birth time and y the death time. The triplets with short distances between birth and death time corresponds to short barcodes, which can be associated with noise and are represented as points close to the diagonal line. In contrast, the triplets with long distances correspond to persistent or highly robust features, i.e., the points far from the diagonal line, see Figure **3-3**.

Therefore, Betti numbers, barcodes and persistent diagrams allows to identify persistent features, in R-fMRI context, it provides a description of high-order structures that could be associated to connectivity phenomena from a complementary perspective focus on “holes”.

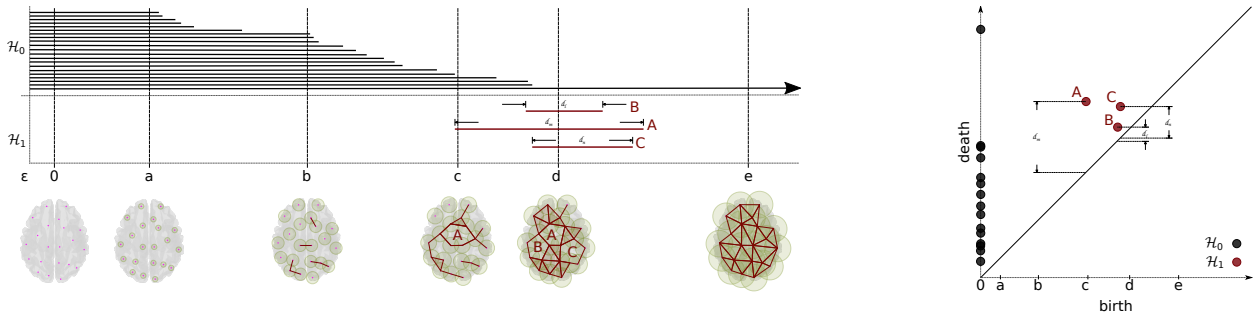

Figure **3-3**.: Illustration of the barcodes (left) and persistence diagrams (right). Both barcodes and persistence diagrams show the features birth and death for the homology $\mathcal{H}_0$ and $\mathcal{H}_1$. Persistent $\mathcal{H}_1$ features are labeled with capital letters, in appearance order, (A, B and C respectively) in both diagrams. In the barcodes, the length of the horizontal line indicates persistence of a feature, while the number of lines crossed by a vertical line is the Betti number at a specific ϵ value. Similarly, in the persistence diagram, the distance d_i between each point and the diagonal indicates persistence, but it is hard to see the Betti number for a given ϵ.

3.2. Materials and methods

Figure **3-4** shows the proposed strategy to characterize the topological features for the resting-state functional brain activity. The first stage (blue rectangles) encompasses the computations made on each individual in the dataset. This phase extracts a representative time-course per cortical region using Independent Component Analysis (ICA) followed by the computation of topological features, which includes (i) estimation of the distance matrix summarizing the neighborhoods relations among representative time-courses, (ii) description of $\mathcal{H}_0$ and $\mathcal{H}_1$ features on the filtrations resulting from the Vietoris-Rips algorithm, (iii) identification of the most persistent $\mathcal{H}_1$ feature at the individual level. The second stage (orange rectangle) characterizes $\mathcal{H}_1$ features emerging at an individual level for the whole population and consists of two main sub-processes. The first one summarizes the topological features found at an individual level for the whole population through a 1-hole distribution. The second one identifies the brain regions most involved in the emergence of the longest $\mathcal{H}_1$ feature. This last process estimates the number of times that a region appears associated with the persistent $\mathcal{H}_1$, the depiction of frequency of occurrence of these regions onto a brain map representation.

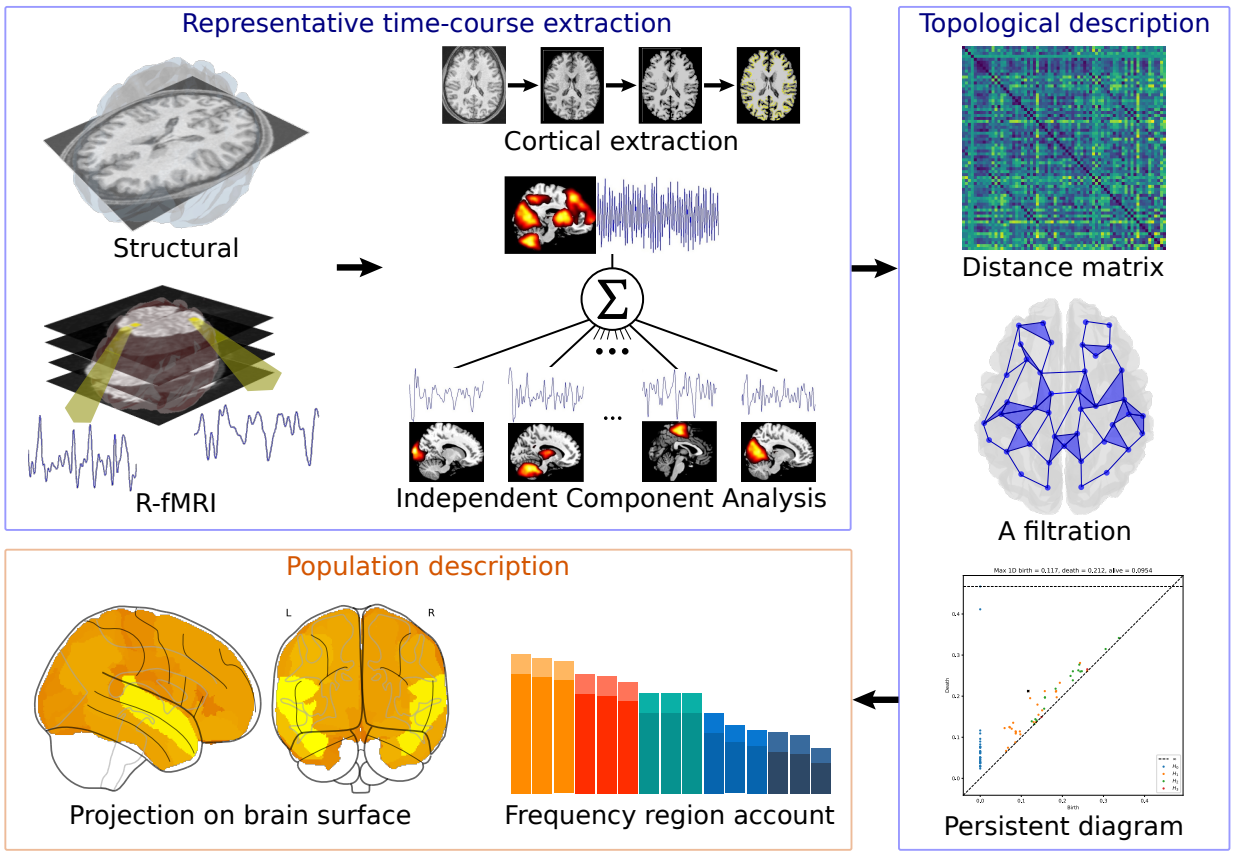

Figure **3-4**.: Method to compute the topological features for R-fMRI, starting with the images acquisition, followed by the data preprocessing, continuing with the topological description, and ending with the summarization of properties on the population. Blue boxes indicate the process done per individual.

3.2.1. Dataset

The Beijing-Zang center dataset from the 1000 functional connectome project, consisting of resting-state functional MRI (R-fMRI) acquisitions and a T1 MRI for anatomical reference, was used to investigate loops in synchronization. It is composed by 198 subjects (122 Females) in ages between 18 to 26 years. The R-fMRI acquisition properties are: time resolution of 2.0 seconds, 33 slices and 255 time points. All datasets in the project are anonymous, and the demographic information is limited to gender, age, and handedness.

3.2.2. Data preprocessing

The structural T1 image was segmented into cortical and subcortical regions by the FreeSurfer standard stream. This segmentation process offers two atlas-based region sets (Desikan-Killiany and Destrieux). The segmentation is based on a probabilistic information model. The model was estimated from manually labeled images and uses geometric information from the cortical model plus the naming convention for the final segmentation [47]. In this approach, the Desikan-Killiany parcellation was selected, which provides a set of sixty-four (64) cortical regions and fifteen (15) subcortical regions, but only the cortical were considered for the functional analysis. The R-fMRI process provides signals linked to neuronal activity. It entails two stages made by using SPM and AirRepair toolboxes [120]. The first stage includes realignment and adjustments for movement effects for functional images; also, the co-registration onto structural data, normalized into standard stereotactic MNI space, and spatially smoothed with a gaussian kernel of 8mm. These were motion-corrected (small, large, and rapid motions, noise spikes, and spontaneous deep breaths), as described previously [46]. Second, the R-fMRI signal was decomposed into maximally independent spatial maps using spatial ICA. This decomposition used a fixed point algorithm implemented in the GroupICA toolbox. The signal was described by thirty (30) independent components classified by their origin into neuronal or artifactual. The classification employed a machine learning labeling method, a support vector machine trained on nineteen healthy subjects independently assessed. Then, the signals were reconstructed by combining the independent components exhibiting neuronal behavior [46]. The preprocess ends with the computation of the representative signal of each cortical region estimated by averaging the reconstructed signals that belong to a specific area.

3.2.3. Functional Connectome TDA description

The topological description was made based on the assembly of simplicial complex per subject. It was built from the dataset of reconstructed functional signals. These signals constitute a set of points in an n-dimensional Euclidean space, one point per signal, and one

representative signal per brain region, see Figure **3-5**. The ensemble of points turns into a global object via simplicial complex computation. Here, proximity is defined as a joint distance, i.e., a distance from a similarity measurement. In this case, Pearson's correlation (r) is used to compute the distance matrix [58], which is the input of TDA, see equation 3-1:

$$d(X,Y) = \sqrt{1-\frac{1}{2}r} = \sqrt{1-\frac{1}{2}\cdot\frac{\frac{1}{n}\sum_{i=1}^{n}x_i y_i - \bar{x}\bar{y}}{\sqrt{\sum_{i=1}^{n}(x_i-\bar{x})^2}\sqrt{\sum_{i=1}^{n}(y_i-\bar{y})^2}}} \tag{3-1}$$

where $X = (X_1, X_2, \cdots, X_n)$ and $Y = (Y_1, Y_2, \cdots, Y_n)$ are two R-fMRI time courses, and $\overline{x}$ and $\overline{y}$ are the mean of the time-course X and Y respectively.

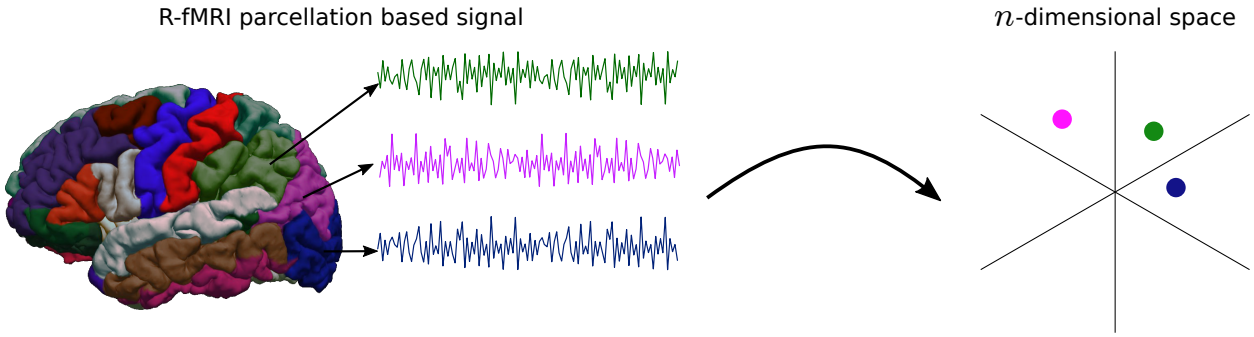

Figure **3-5**.: Cloud point representation from n-dimensional signals. For each brain region a representative signal is considered as a point in a n-dimensional space

Persistent homology computations

Barcodes computation was performed on the distance matrix by using Ripser [10], through its python wrapper (PyRipser) [171]. This tool provides a simple set of settings to compute homology features. PH Computations were based on the Vietoris-Rips approach, establishing the criteria to compute a simplex based on the distances. (Py)Ripser allows specifying the homology group and the max number of dimensions to consider in the computation of TDA features. Informally, 0-degree homology groups (0-hole topological feature) capture the connected components, and 1-degree homology groups capture regions forming a loop structure [54]. The Ripser process on a distance matrix results in a set of birth and death values per bar at the respective degree or dimension. It also provides a corresponding set with the list of elements associated with the feature emergence. The process supplies two lists with corresponding components, one with the bar description and the other with the elements involved in the appearance of a topological feature. Once the topological features are computed, the process continues with the association of the longitude to each $\mathcal{H}_1$ bar. Then, all bars in $\mathcal{H}_1$ have the birth, death, and longitude. The set of $\mathcal{H}_1$ bars are sorted by the longitude value. The persistent feature is the 1-hole with the largest longitude, the first

in the sorted bars. Finally, the selection of regions related to the persistent 1-hole consists of (i) sorting the list of associated elements based on the longitude criteria and (ii) choosing the first list.

3.2.4. Topological features population description

The description of the topological features, in this case for $\mathcal{H}_1$, was performed from two perspectives. The first one summarizes the computed features for the population. The second one estimates the frequency of the brain region appearance in the persistent 1-holes.

Summary of the $\mathcal{H}_1$ topological features

The $\mathcal{H}_1$ persistent features at the group level were summarized using the length of the most persistent $\mathcal{H}_1$ feature per subject. In particular, the longest bar linked to $\mathcal{H}_1$ was selected per subject, and the distribution of these features was calculated. Following this, the probability of observing particular longitudes for these features was computed, indicating the distribution of these persistent features in the population. Similarly, the birth values of these features could be different through the group. An enhanced persistent diagram illustrates the summary of the 1-holes. It depicts the distribution of 1-holes, one point per subject in the group, and the frequency of longitudes as a histogram at left.

Brain regions in persistent 1-hole

Brain regions associated with the emergence of $\mathcal{H}_1$ were also characterized. In principle, any brain region can belong to a $\mathcal{H}_1$ feature; the 1-holes could be related to distinct elements. Therefore, the number of times a brain region appears to be related to the largest $\mathcal{H}_1$ emergence was quantified. This quantification results from searching all the regions in the element list of nodes conforming the $\mathcal{H}_1$ nodes of each subject. The frequency of brain regions in the emergence of 1-hole in the population is two-fold, presented as a sorted bar diagram and projected into a brain representation.

3.3. Results

3.3.1. Loops in the fMRI resting-state connectivity dynamic

Figure **3-6** shows the topological features exhibited by the fMRI resting-state dynamic summarized as barcodes and the persistent diagrams for a subject. Figure **3-6** also shows the

corresponding distance matrix (Figure **3-6**a), computed from the Pearson's correlation between the regional time-courses, used for the PH calculations. This distance matrix induces an implicit data space to describe the brain's time-courses fMRI dynamic on the subject. This space contains the connectivity relationships or neighborhoods linked to regional R-fMRI regional time-course synchronizations.

Topological holes characterize the connectivity relationships in this fMRI data space, 1-dimensional holes ($\mathcal{H}_1$), which refers to loops in the R-fMRI data space, i.e., sets of time-courses weakly synchronized in pairs that together conform cycles. Each line in the barcode (Figure **3-6**b) represents a particular hole. Large lines refer to persistent holes, i.e., holes that consistently appear across different filtration values. The persistent diagram (Figure **3-6**c) also shows these persistent topological features as two-dimensional points appearing far from the diagonal, with different colors representing the dimension of the topological feature. As observed, the fMRI resting-state time-courses in this subject show high levels of connectivity, as evidenced by the 0-holes found in the persistent analysis (blue dots in Figure **3-6**c). Remarkably, the time-courses are organized around 1-dimensional holes (see Figure **3-6**b), indicating that resting-state may also exhibit high order interactions. Importantly, these high-order interactions seem to be highly robust across different extends of filtration values or scales, as illustrated for instance by the topological 1-hole feature marked as an orange line in H_1 and also showed in the persistent diagram with a black cross (see Figure **3-6**c).

Figure **3-7** shows the distribution of the most persistent $\mathcal{H}_1$ feature at the group level. This figure includes a histogram summarizing the length of the largest $\mathcal{H}_1$ bars. These lengths indicate the persistence of the 1-holes in the population under study. Importantly, this figure shows that a large percentage of subjects showed persistent 1-holes, with lengths between 0.05 and 0.24 for most of them (183 of 198). However, the complete range of distances was between 0.02 and 0.51, showing that there are also subjects for which the R-fMRI dynamic exhibited both highly persistent and noisy loops in connectivity. The higher frequencies ranged between 0.05 to 0.17, indicating that 1-holes consistently emerge for at least 10% of filtration values range, normalized between 0 and 1. Additionally, the distribution of points exhibits a wide range of birth values for the persistent 1-holes, ranging from 0.02 to 0.34, mainly concentrated between 0.05 and 0.25. The distribution presents no apparent relation between the birth and death times of the largest loop for the population. Also, the radius of the circle representing the $\mathcal{H}_1$ feature is an indicator of the number of regions involved in the emergence of the feature. The figure presents small and big radius at different birth values and lengths, indicating no apparent relation between the number of regions with the length of the features, neither the birth of it. In fact, the most of the $\mathcal{H}_1$ features shows less than fifteen brain regions implicated in their emergence.

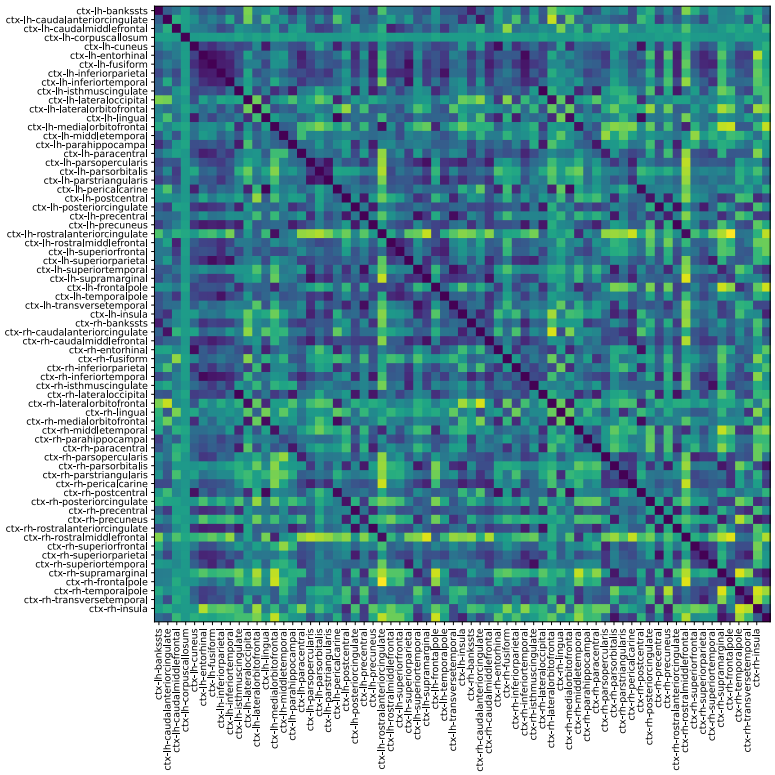

(a) Distance matrix

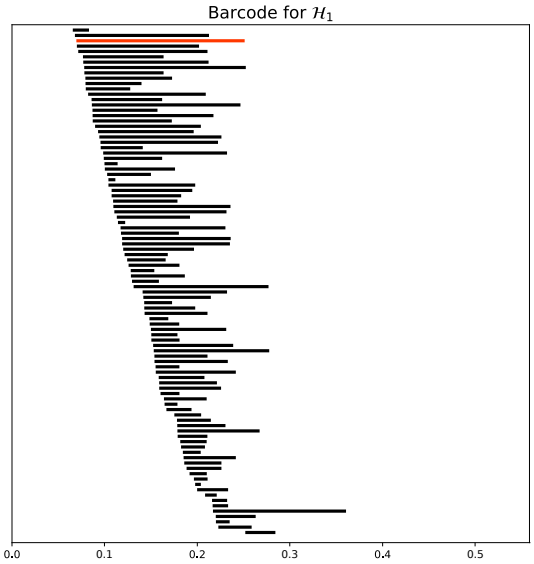

(b) $\mathcal{H}_1$ Barcodes

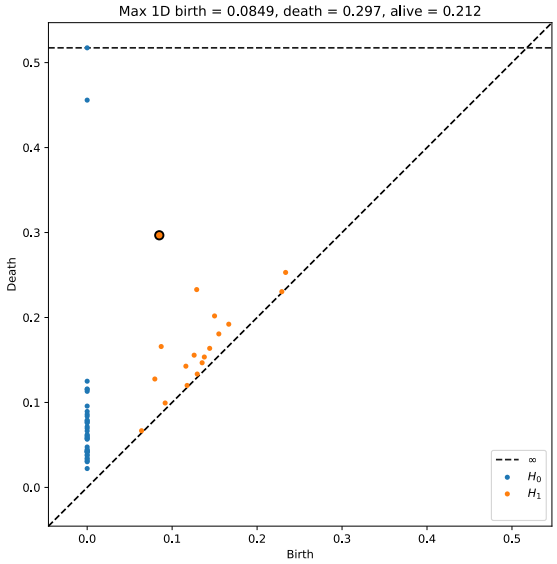

(c) Persistence diagram.

Figure **3-6**.: Topological features computed for a single subject. (a) shows the distance matrix computed from the Pearson's correlation between R-fMRI time-courses, dark blue indicates lower distances while yellow indicates larger distances. (b) shows $\mathcal{H}_1$ barcodes, orange line, highlight the most persistent $\mathcal{H}_1$ loop. (c) persistent diagram summarizing $\mathcal{H}_0$ and $\mathcal{H}_1$ measurements, black contour dot indicates the most persistent $\mathcal{H}_1$ loop.

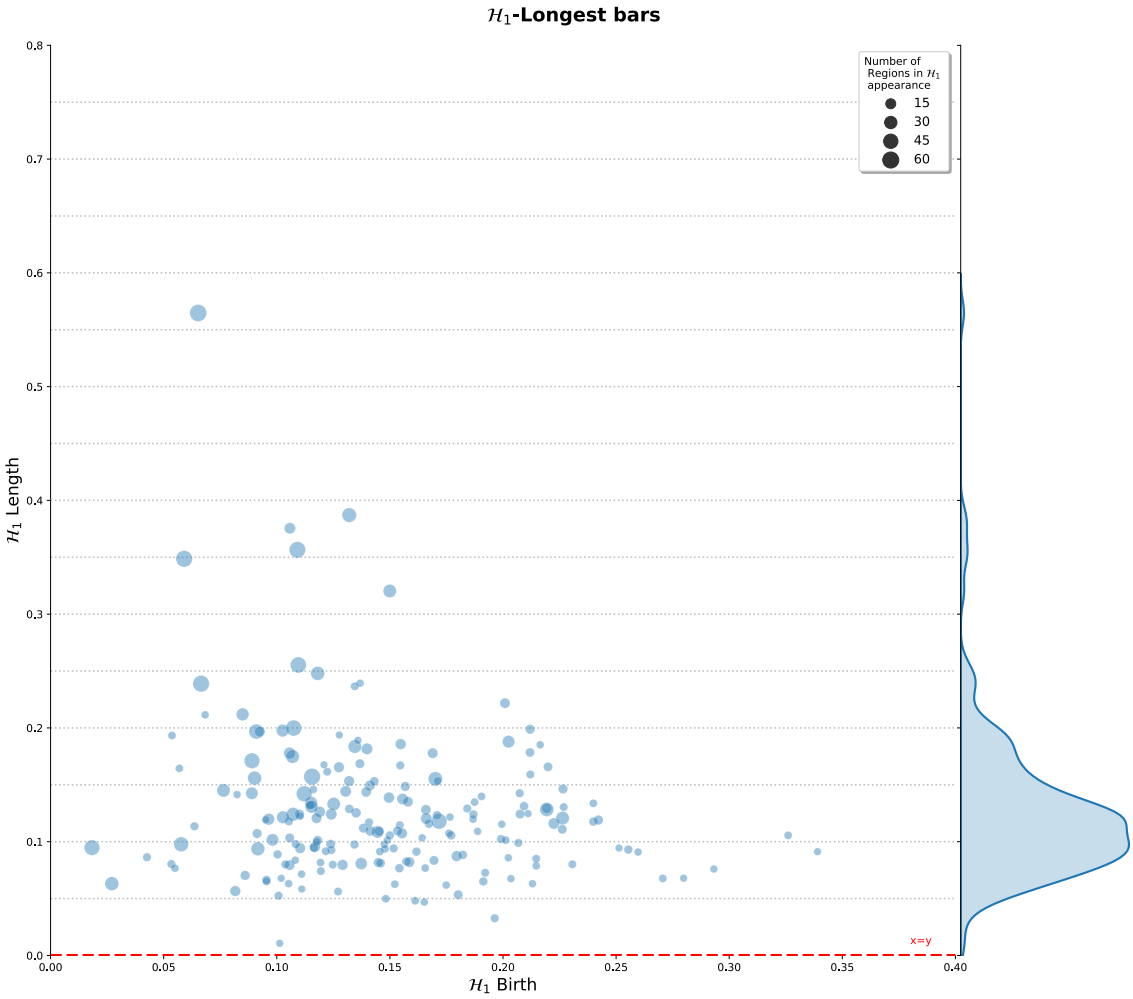

Figure **3-7**.: $\mathcal{H}_1$ persistent summary of the topological features computed over all subjects set. Distribution of the $\mathcal{H}_1$ largest loops at left. Right, length frequency of the persistent 1-holes. Gray dashed lines are only for reference of distances from the $x = y$ line at bottom. Also, the circle radius indicates the number of regions involved in the appearance of the longest $\mathcal{H}_1$ feature in the corresponding subject.

3.3.2. Brain regions involved in $\mathcal{H}_1$ topological persistent structures

Once the existence of robust $\mathcal{H}_1$ topological features in healthy controls at the individual level was established. The next section investigates how these features emerge in the brain regions. But, first, it is worthy to recall that a boundary, or a sequence of nodes, defines a 1-hole. In our case, these nodes refer to the brain regions, which compose the boundary of synchronization loops. These nodes can be recovered from the PH analysis [10, 171]. Figure **3-8**a shows the number of subjects in which each brain region was involved in the composition of the most persistent $\mathcal{H}_1$ loop, i.e., the number of times a region was involved in highly persistent synchronization loops. These regions are sorted in increasing order. The region with the highest occurrence in the large synchronization loops corresponded to the superior-temporal cortical areas in both hemispheres, appearing in most than 30% of the population. The following regions were the left middle-temporal, left inferior-parietal, the right temporal-pole, and the left bankssts involved in more than 22% of the subjects.

Figure **3-8**b shows region occurrences in the most persistent synchronization loops represented onto the brain. Dark orange values represent a low level of occurrences, while yellow areas correspond to high occurrence levels. This projection reveals symmetries in the involvement of the regions in the emergence of the loops, which is more notorious in the temporal lobe, particularly in the superior, middle, and bankssts cortical regions of both hemispheres.

3.4. Discussion

In this study, we used TDA to describe the persistence loops in R-fMRI time-courses on healthy subjects. Remarkably, these topological features emerge robustly across different scales, i.e., while filtration values change. These features are formed by 1-simplexes surrounding a space, indicating at least two directions to reach any other element in the simplex structure. These cycles in the network suggest that information can be delivered using two different redundant paths and interpreted as redundant connections [145]. Importantly, even if cycles can be computed directly from network approaches, their persistence is not considered in the analysis due to the threshold selection in the connectome analysis. These topological features (cycles or loops) constitute evidence of R-fMRI high order arrangements hidden on classical pairwise models. In addition, we identified the brain regions most involved in the emergence of these topological structures. We found that some brain regions frequently appear in these persistence loops, suggesting a particular anatomical substrate of these regions in the emergence of these interactions. Together this evidence supports the existence of high order structures in functional connectivity in R-fMRI. Nevertheless, their meaning and the specific roles of the brain regions involved are still unknown.

Initial studies in R-fMRI discovered the existence of low-level synchronous fluctuations (<0.1

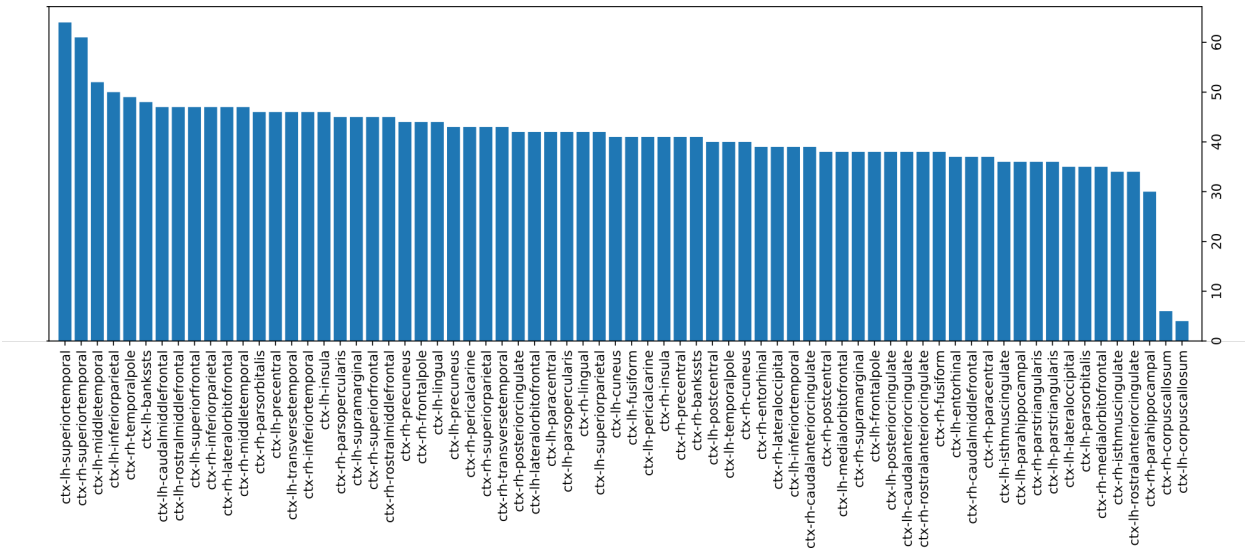

(a) Regions involved in $\mathcal{H}_1$ greatest cycle.

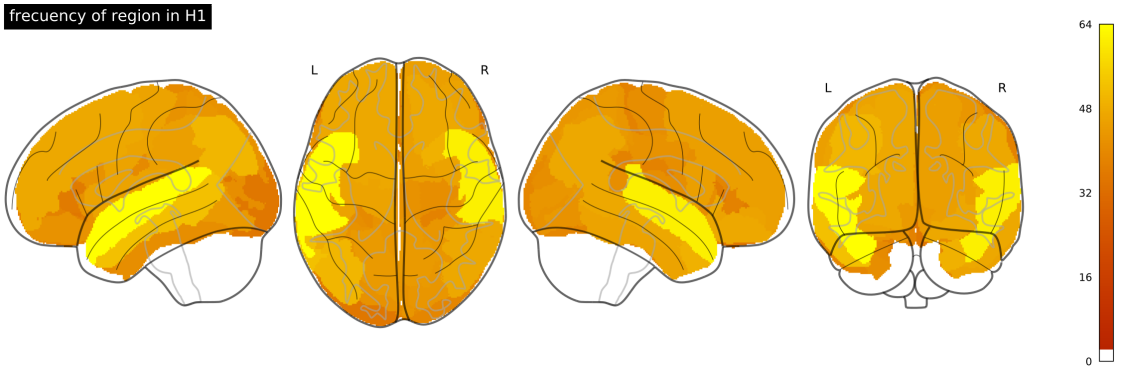

(b) Regions involved in greatest cycles plotted on the brain.

Figure **3-8**.: Regions involved in the most persistent loops. (a) Frequency of appearance of the cortical region in the emergence of a greatest cycle. (b) Projection of the frequency onto the brain.

Hz) in blood oxygen level-dependent (BOLD) signal occurred independently of task stimulation [18, 17]. This evidence pointed for the first time to a non-trivial organization of the resting-state dynamic. Posterior studies robustly identified regions with coherent spatiotemporal fluctuations grouped under the so-called resting-state networks (RSNs) [41]. This evidence suggests that the brain function in the resting state organizes in patterns of coordinated activity related to synchronization mechanisms among brain regions. However, the true extent and the nature of these patterns of coordination remains poorly understood. Notably, the characterization of most coordination patterns described for R-fMRI relies on pairwise synchronicity descriptions between time-courses, neglecting that alternative synchronization mechanisms may also emerge from multi-regional interactions [35, 9]. More recently, some studies in small populations aimed to overcome this limitation by directly studying high-order interactions by looking for high-dimensional topological holes, which indicate surrounding high-order interactions. The proposed analysis confirmed the existence of $\mathcal{H}_1$ topological loops in healthy controls R-fMRI, as in [132], but in a large population. Moreover, our results (Figure **3-7**) suggest that the appearance of these 1-holes across the people is not spurious, i.e., these holes robustly emerged across multiple scales in most subjects for the large population herein studied. Thus, the occurrence of these 1-holes' points to the existence of multi-regional synchronization mechanisms of high-order nature underlying the RS dynamic in healthy controls.

Description of high-dimensional data through algebraic methods as PH is beginning to be widely used by the community. For fMRI (resting and evocated) in particular, these methods avoid the arbitrary collapsing of data in space or time [145, 35]. An interesting approach was developed by Saggar et al. [145]. In their, approach they use Mapper to understand the shape of the fMRI dynamic among different activation processes related to instructions, working memory, video, and math tasks. They found that activation is similar in the related cognitive tasks. Although they describe the resting-state periods between activation tasks as peripheric shapes, it is not the focus of the work. Another approach that tackles the resting-state fMRI was the work introduced by Cassidy et al. [35]. They use TDA to overcome the drawbacks related to the scale and threshold selection in connectome analysis of healthy subjects. They study the first Betti number B_0, which models the topology of connections, and found that the topology properties are robust across different scales; however, they do not use the information of high topological dimensions. Here, we use the second Betti number B_1 to understand the topological structures (loops) of R-fMRI. The TDA loops studies are not new, and asking for the emergence of these structures seems to have a sense in biology and other fields. Topological studies have been introduced to describe different phenomena in various domains, biological, medical, physical, and other specialties. In biology, Bhaskar et al. [15] incorporate the TDA connected loops descriptors to summarize the cell proliferation architectures; also, they use those descriptions to classify particle configurations. Additionally, persistent cycles of gene network information shown to

be robust features appear in the study of different datasets of glioblastoma [116]. In physics, topological voids ($\mathcal{H}_2$ structures) were found in the study of the baryon acoustic oscillation related to the galaxy distribution [100]. Finally, in medicine, Carpio et al. use the topological descriptors for the two first dimensions, i.e., $\mathcal{H}_0$ and $\mathcal{H}_1$. They found that different cancer cells have distinct topological values at these dimensions, indicating the descriptiors usefulness as biomarker.

Our approach in R-fMRI analysis allows identifying the most persistent $\mathcal{H}_1$ loop structures for each subject. Also, it determines the brain regions involved in the emergence of the topological features. Bhaskar et al. [15] identify the largest loop in the multicellular architecture of epithelial cells, but they do not inquire about the elements in the cycle. In our approach, we found that middle temporal gyri, both hemispheres, are the regions that appear more frequently in the most persistent $\mathcal{H}_1$ loops in the population considered for this study. These brain regions are involved in the auditory association, multisensory integration, speech processing, language comprehension [172, 124], and social cognition [127]. From the functional perspective, these regions are in the cognition pathway, associated with the amygdala and the prefrontal cortex [127]. They are involved in spatial working memory tasks with the occipital region [53]. Also, they have been suggested as part of a separate ventral attention system that acts as a circuit breaker to reorient attention [38]. With this in mind, the appearance of the Superior Temporal Gyrus (STG) in the persistent cycle might be associated with the alert systems, i.e., the process of achieving and maintaining a state of high sensitivity to incoming stimuli. In particular, the participants are ordered to keep their eyes closed during the acquisition process, but due to the acquisition condition, they are continuously prepared to follow instructions. These have been described as an interface between language comprehension and the attention network [101]. Then, in this specific acquisition process, the STG appearance in the persistent cycle might be related to the reorientation of the attention.

The approach developed in this study presents some drawbacks. Beginning with the TDA process, the selection of the distance to compute the topological properties influence the appearance of the topological structures [54]. In this case, we use a "distance" built from Pearson's correlation [36] which limits the range of possible distances, as well as affects the Betti numbers and all other topological features. Another TDA consideration is the selection of the coefficients group used. The presented approach uses $\mathbb{Z}/2\mathbb{Z}$ as the coefficient group, which is a 2-order cyclic group [75]. Although it is suitable for loops description, richer structures related to high-order coefficient groups are out of its scope. Another concern is the focus on only the most persistent loop. Figure **3-7** shows the existence of an interesting number of features that are not spurious, so extending the analysis of loops to a percentage of the most persistent could provide a new perspective for the analysis because with more cycles, it is possible to (i) enrich the R-fMRI topological description of each subject which can be used in other developments like classification [15, 34] (ii) identify the nodes

that are involved in more than one persistent loops because they could be relevant in the study of brain high-order processes. Here we highlight that this new perspective not only found the nodes and associations that are important by their connections, as in connectome analysis, but that are important because there are some emerging limits, and the properties of these boundaries in brain functions are unknown. An interesting perspective is to use the approach proposed here in the topological description of the R-fMRI in pathological conditions where the STG are involved. Then, the topological features ($\mathcal{H}_1$) could be used in research with clinical application, mainly focusing on those where functional connectivity alterations have been reported, in particular, for the study of bipolar and unipolar depression [107], corneal ulcer [197], deafness [53], depression in Alzheimer disease [109], Alzheimer disease [81], Comatose patients [92], Tinnitus [188, 30], anxiety disorders [187], attention deficit hyperactivity disease [194], post-stroke memory [108] and internet gaming disorder [195] among others. But not only pathological conditions alter the functional connectivity of the superior temporal gyri so that this topological approach could be used for studies of brain function related to chess practice [157], meditation [95] and second language learning [37].

3.5. Conclusion

The presented PH strategy characterizes the resting-state connectome for healthy control subjects. Persistent $\mathcal{H}_1$-holes were robustly found in healthy people, providing a new set of features to consider in resting-state studies. These $\mathcal{H}_1$-holes indicate the existence of boundaries surrounded by 1-simplex (lines), conforming to a loop, i.e., a structure providing two directions of connections for the boundary elements. Additionally, specific brain regions were linked to the occurrence of these properties, pointing to a functional boundary. Moreover, these brain regions frequently appear across populations, expressing a sort of symmetry in the resting-state connectome topology and providing biological insight.

4. Topological Data Analysis for R-fMRI of patients with altered states of consciousness

Characterization of consciousness alterations, including DOC, is a highly challenging task from the diagnosis and prognosis perspectives. Advances in neuroimaging, specifically, resting-state imaging aims to mitigate this challenge, offering an alternative viewpoint to explore brain activity in altered states of consciousness. In recent years, several investigations link the variations in the connectivity of specific consciousness-related circuits to affectations of consciousness [84, 44, 79, 80]. From a global network perspective, evidence herein reported suggest that DOC patients exhibit functional connectivity alterations. As reported in Chapter 2, these patients show network connectivity alterations between RSNs, which are associated with modifications in properties likely required for consciousness emergence such as integration, segregation, and centrality.

On the other side, TDA provides a specialized tool, the PH, to study high-order features of data connectivity emerging from R-fMRI (see Chapter 3). Therefore, if DOC condition alters R-fMRI connectivity, and in consequence, its topological properties, then it is reasonable asking about changes in other topological features during altered states of consciousness, for instance, in $\mathcal{H}_0$ and $\mathcal{H}_1$. Therefore, connectivity alterations due to DOC might result in changes on the segregation and integration which can be associated with topological features variation. Remarkably, our analysis showed that high-order connectivity features characterize the R-fMRI of healthy subjects. In particular, persistent loops, or $\mathcal{H}_1$-holes (chapter 3), which link to high-order interaction mechanisms. Then, considering the evidence of graph connectivity alterations in patients with DOC related to topological changes and accounting for persistent high-order features in healthy subjects, the following questions arise: *are there high-order features that describe the resting-state topology of patients with altered states of consciousness?* and if these features exist, *do they variate in these patients?*.

This chapter aims to investigate these research questions by introducing a TDA analysis approach to characterize high-order topological features in altered states of consciousness. The proposed approach was used to describe a population of fifty patients in the intensive care unit, all in an acute coma caused by severe brain injuries. Unlike the population with

permanent DOC condition (Chapter 2.2.1), these patients present less gray matter damage due to the permanent condition, improving the quality of acquired image mainly for the automatic parcellation step. In permanent condition the gray matter is to thick resulting in corrupted parcellations. Topological features obtained for these patients were then compared to the ones obtained for healthy controls. Results show that R-fMRI of patients with altered states of consciousness exhibits topological variations in $\mathcal{H}_0$ and $\mathcal{H}_1$ linked to integration. In addition, the regions involved in the appearance of the persistent $\mathcal{H}_1$ feature differ in both populations. This evidence supports the role of high-order interaction features on the alteration of consciousness in acute states. Also, it shows the role that topological analysis may have in the characterization of these conditions.

The main contributions of this chapter are: (i) a method based on persistent homology to describe topological properties of functional connectivity for patients with an acute altered state of consciousness, (ii) a new description of R-fMRI time-courses integration through the 0-holes, (iii) a characterization of high-order features for altered functional connectivity for acute state patients, and (iv) the identification of brain regions involved in the appearance of these high-order features, which are different from the brain regions identified in healthy people setting.

This chapter is organized as follows. First, it introduces the TDA-based analysis aimed to describe pathological conditions. Second, it describes the population with severely altered consciousness here studied. Following, it presents the method used to measure the TDA properties. Finally, it reports and discusses the main findings of TDA features resulting from the acute unconsciousness condition studied compared to healthy people.

4.1. Materials and Methods

The approach used here improves the one presented in Section 3.2 to consider the variations associated with DOC. Thus, some additional methodological adjustments were introduced in the experimental setting for accounting the patients with disorders of consciousness. The adjusted processes in the first stage (individual tasks) were: (i) the data acquisition, (ii) the preprocessing of images, and (iii) the topological description including $\mathcal{H}_0$ description. In the second stage, other summaries were added to the process, consolidating the $\mathcal{H}_0$ and $\mathcal{H}_1$ population features, see Figure **4-1**. This chapter focuses on describing the adjusted or added processes.

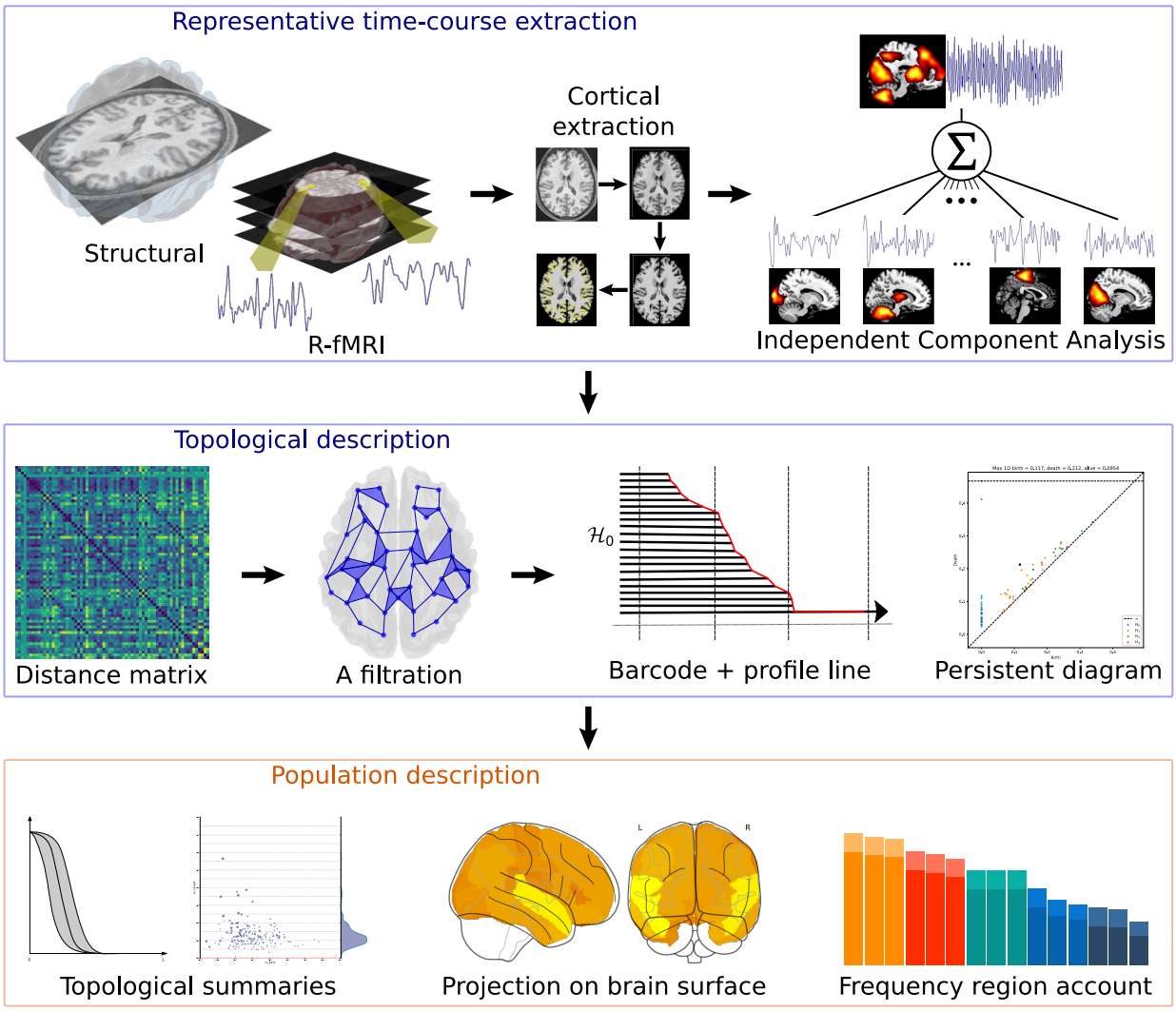

Figure **4-1**.: A general method to compute the high-order features in patients with an acute altered state of consciousness. Top section represents the image acquisition and processing to extract the functional representative time-courses. Middle section illustrates the topological measures per individual, and finally the bottom section shows the procedures to summarize the population features, including $\mathcal{H}_0$.

4.1.1. Subjects demography and data description

Fifty patients with severe brain damage admitted to the intensive Care Unit (ICU) were studied[1]. Admitted patients were in an acute coma after any of these three causes, stroke, hypoxic-ischemic brain injury after cardiac arrest, or severe traumatic brain injury [57]. An acute comatose state refers to a deep state of prolonged unconsciousness. Also, patients in an acute coma state may evolve to MCS, UWS after some weeks [103]. The project examined the admission of 293 candidates. The exclusion criteria included psychiatric or neurological disease antecedents, impossibility to be transferred to the MRI scanner due to medical condition, death in the 48 hours after ICU admission, familiar interdiction, and Glasgow Coma Scale (GCS) score equal or greater to eight (8) [57]. The GCS is a standard measure for assessing the depth and duration of impaired consciousness and coma [165, 166]. It is composed of fifteen (15) hierarchically arranged items that contain three (3) subscales addressing eye-opening response (4 items), verbal response (5 items), and motor response (6 items). The scoring is based on the presence or absence of specific responses to stimuli, and the highest score item represents cognitively mediated behaviors. Written informed consent to participate in the study was obtained from the legal surrogates of the patients. The study was approved by the Ethics Committee of the Medical School of the Fundación Universitaria de las Ciencias de la Salud.

A total of fifty (50) patients (27 women (54%)) were included in this study. Their median age was 64 years (IQR 49-74), nineteen patients (38%) were admitted with stroke, 18 (36%) with hypoxic-ischemic brain injury after cardiac arrest, and 13 (26%) with severe traumatic brain injury. From the consciousness perspective, 23 patients were in coma (44%), 11 in MCS (20%), and 16 in UWS (32%). Table **4-1** reports further details of the patients. The evaluation and classification of patients in a consciousness state were performed weeks after the image acquisition.

Feature	**Coma**	**MCS**	**UWS**	**Total**	**p-value**
	(n=23)	(n=11)	(n=16)	(n=50)	
Age median (IQR)	50 (72-86)	48 (73-90)	47 (76-92)	49 (74-88)	0.42
Sex					0.56
Female (%)	13 (56.5)	7 (63.6)	7 (43.8)	27 (54)	
Male (%)	10 (43.5)	4 (36.4)	9 (56.2)	23 (46)	

Continue on next page

[1]These patients were the focus of the project "*Caracterización de la conectividad estructural y funcional del sistema reticular ascendente por medio de resonancia magnética con tractografía y BOLD, para la predicción del estado de conciencia en pacientes posreanimación o con lesión cerebral traumática*" which look for the prognosis of the neurological outcome of the patients from structural and functional images

Continued from previous page

Feature	Coma	MCS	UWS	Total	p-value
Education					0.16
Illiterate (%)	0 (0)	0 (0)	1 (6.3)	0 (0)	
High School (%)	9 (39.1)	2 (18.2)	5 (31.2)	16 (32)	
Primary School (%)	10 (43.5)	5 (45.5)	2 (12.5)	17 (34)	
Technical (%)	0 (0)	2 (18.2)	2 (12.5)	4 (8)	
Graduate School (%)	4 (17.4)	2 (18.2)	6 (37.5)	12 (24)	
Comorbidities					0.82
Hypertension (%)	7 (30.4)	7 (63.6)	8 (50)	22 (44)	
Diabetes Mellitus (%)	(26.1)	3 (27.3)	3 (18.8)	12 (24)	
Hypothyroidism (%)	2 (8.7)	2 (18.2)	3 (18.8)	7 (14)	
Dyslipidemia (%)	1 (4.3)	1 (9.1)	0 (0)	2 (4)	
Acute myocardial infarction (%)	0 (0)	1 (9.1)	1 (6.3)	2 (4)	
Other (%)	5 (21.7)	5 (45.5)	11 (68.8)	21 (42)	
ICU admission GCS score median (IQR)	6 (3-7)	5 (4-8)	8 (4-8)	6 (3-8)	0.08
Intracranial Pressure					
ICP monitoring (%)	2 (8.7)	1 (9.1)	1 (6.25)	4 (8)	0.95
Intracranial hypertension (%)	2 (8.7)	2 (18.2)	1 (6.25)	5 (10)	0.57
Mechanical ventilation (%)	22 (95.7)	10 (90.9)	14 (87.5)	46 (92)	0.65
Sepsis (%)	8 (34.8)	3 (27.3)	8 (50)	19 (38)	0.45
Vital status					
Alive (%)	12 (52.2)	4 (36.4)	12 (75)	28 (56)	0.17
Deceased (%)	10 (43.5)	5 (45.5)	2 (12.5)	17 (43)	
Transferred to a different institution (%)	0 (0)	1 (9.1)	2 (12.5)	3 (6)	
GCS score at discharge median (IQR)	6 (3-11)	3 (3-14)	11 (9-12)	9 (3-12)	0.15

Table **4-1**.: Clinical and demographic features according to state of consciousness after ICU admission. P values correspond to comparative measures among the three patient groups [57]

4.1.2. Data acquisition

The images acquisition was made in a 1.5T General Electric scanner. For each patient, the obtained images cover the whole brain. One hundred and eighty multi-slice T2*-weighted functional images were acquired (axial orientation, slice thickness = 4.5 mm without free space, matrix = 64 × 64 mm, TR = 3000 ms, TE = 60 ms, flip angle = 90°, and FOV = 288 × 288 mm). The three initial volumes were discarded to avoid the saturation effects. Resting-State images acquisitions follow the T2 echo-planar imaging process. Also, an axial

structural T1 image was acquired (slice thickness = 1 mm, inter-slice gap = 1 mm, matrix = 256 × 256 mm, TR = 670 ms, TE = 22 ms, flip angle = 20° and FOV = 250 × 250 mm) and axial T2 (slice thickness = 6 mm, gap = 1 mm, matrix = 320 × 320 mm, TR × 6.000 ms, TE × 96 ms, flip angle = 90° and FOV = 220 × 220 mm) for anatomical reference, further details in [123].

4.1.3. Data preprocessing

The T1 and R-fMRI data were preprocessed using the approach suggested in [97]. T1 preprocessing includes manual removal of the neck, brain extraction using FSL [184], correction of low-frequency intensity non-uniformity based on the N4 bias field correction algorithm from SimpleITK [11], image denoising based on the nonlocal means algorithm from Dipy [11, 70], and spatial normalization to standard stereotactic Montreal Neurological Institute (MNI) space using the SPM12 normalization algorithm [11, 70, 131]. R-fMRI preprocessing includes remotion of the six initial volumes to avoid T1 saturation effects, head motion and slice timing corrections were performed on the fMRI data using FSL, followed by artifact correction using RapidArt [125]. Subsequently, the fMRI data were coregistered to a T1 image using SPM12 and spatially normalized to the MNI space using the SPM12 normalization algorithm. Finally, spatial smoothing of the fMRI data was performed with a Gaussian kernel of 8 mm full width at half maximum, as implemented in SPM12. The spurious variance was reduced by regression of nuisance waveforms derived from time series extracted from regions of noninterest (WM and cerebrospinal fluid). Additional nuisance regressors included the blood oxygen level-dependent imaging (BOLD) time series averaged over the whole brain. Regions of interest (ROIs) for topological analysis of consciousness altered brain signals were located based on the Destrieux atlas parcellation computed on the structural image [48]. This parcellation consists of seventy-four (74) cortical regions per hemisphere and specifies gyri and sulci regions. A region representative signal was obtained as the average of the time-courses that belong to the brain region, resulting in 148 representative time-courses, which express the brain function. The main difference with the previously described approach (see Chapter 3.2) is in the parcellation. The Destrieux parcellation has more resolution, and it differentiate between sulcus and gyrus of the cortical regions. This variation obey to the difficulty reached trying to get the Desikan-Killiany parcellation on the new dataset.

4.1.4. Topological Data Analysis process for patients with altered states of consciousness

The TDA analysis process computes the description of $\mathcal{H}_0$ and $\mathcal{H}_1$ features, presented in chapter 3. The TDA analysis per patient starts with the computation of the distance matrix. This matrix synthesizes the differences between representative time-courses of the brain.

The process follows with the calculation of the TDA features on the time-courses from this matrix representation. The persistent features are computed from the simplicial complex obtained for a sequence of filtration values. Each simplicial complex represents a chain of simplices created with the Vietoris-Rips method. Then, PH results in a topological description of boundaries that remain across successive filtrations. Keep in mind that the dimension of boundary elements characterizes the topological features. An $\mathcal{H}_n$ feature is completely bounded for a group of n-simplex, i.e., elements with n simultaneous connections integrating $n+1$ data objects. Then, an $\mathcal{H}_1$ feature emerges as a boundary composed by a group of 1-simplices, which corresponds to lines. In this case, the topological process includes the computations of $\mathcal{H}_0$ and $\mathcal{H}_1$, the estimation of $\mathcal{H}_0$ profile line, explained in the next section, and the identification of the largest $\mathcal{H}_1$, following the process previously introduced in 3.2.3.

4.1.5. Summary of TDA features on patients with an altered state of consciousness

As earlier, the topological features description is performed from two perspectives. The first one summarizes the PH descriptions, in this case, the $\mathcal{H}_0$ and $\mathcal{H}_1$ features for the two populations under study. $\mathcal{H}_0$ is linked to the integration of R-fMRI indicating how similar the time-courses can be, while the $\mathcal{H}_1$ exhibits the appearance of boundaries. The second one estimates the frequency of appearance of the brain regions in the most persistent $\mathcal{H}_1$. This section only introduces the summary of $\mathcal{H}_0$ features. The other remains as described before, see section 3.2.4.

$\mathcal{H}_0$ ribbon and $\mathcal{H}_0$ mean line

Lets remark that a barcode is a collection of horizontal lines representing the PH. It allows to study the topological features in a nested sequence resulting of the increment of the filtration values ϵ. Each line represents the birth and death of a topological feature. For $\mathcal{H}_0$ all lines birth at zero, and they death at some ϵ), indicates when they collapse in a connected component, see chapter 3.1. In fact, the $\mathcal{H}_0$ barcode deaths represents when the components merge with another one to form a larger connected component.

To introduce the $\mathcal{H}_0$ ribbon is necessary to present the $\mathcal{H}_0$ profile line. Each bar in $\mathcal{H}_0$ corresponds to a connected component, indicating the birth and death of the component. For $\mathcal{H}_0$, at the beginning there are as many components as data points, when two connected components merge, one of them dies. Thus, a bar death denotes the moment when a component is integrated to other connected component. At the end all data points are integrated into a single connected component. In consequence, the profile line shows how fast (or slow) the components merge into at single simplicial complex. This line is constructed by considering the increasing sequence of death values computed for the bars in $\mathcal{H}_0$. It is worthy

to recall that in $\mathcal{H}_0$ all bars birth at zero, so the profile line focused only on death values. These profile lines were computed for each subject in the population. Each profile line has a characteristic slope that may reveal how fast the data turn into a connected structure while the filtration value increases. For instance, note that a set of uniformly data elements in the space, i.e., all elements are equidistant among them, should have a completely vertical profile line at a given distance. Figure **4-2** depicts profile lines for two data points sets to illustrate integration, one of them with equidistant points. Therefore, this feature may help to characterize integration properties.

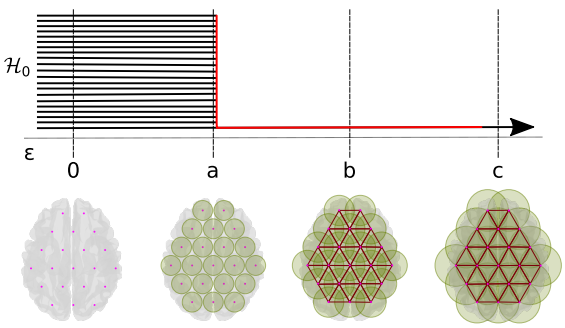

(a) $\mathcal{H}_0$ Barcode and profile line for equidistant (uniform distributed) points.

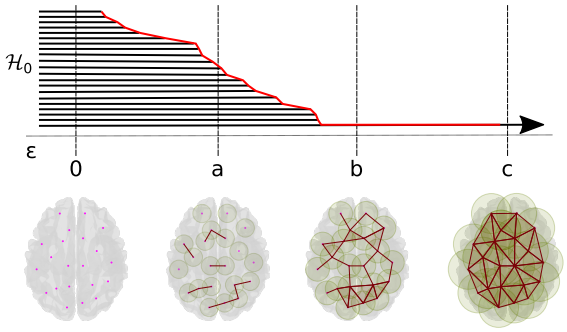

(b) $\mathcal{H}_0$ Barcode and profile line for non equidistant points merged before $\epsilon = b$.

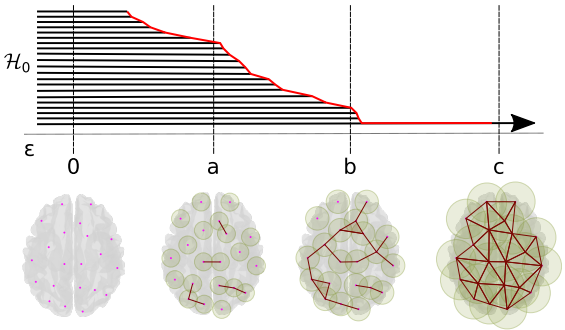

(c) $\mathcal{H}_0$ Barcode and profile line for non equidistant points merged after $\epsilon = b$.

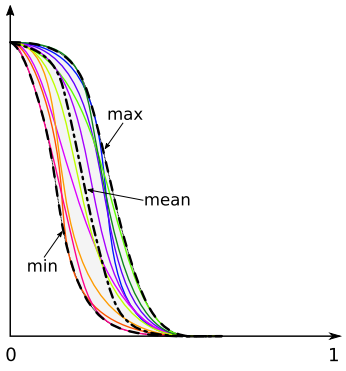

(d) Illustration of a ribbon computation, minimum, maximum and mean of profile lines.

Figure **4-2**.: Profile lines for equidistant (a) and non equidistant (b and c) points. Profile line in (b) shows the merge which starts early and collapse in a single connected component before $\epsilon = b$ when compared with profile line in (c) indicating a fast integration. Late start of integration depicted in (c) shows a displacement in the start of the profile line, which is associated with large dissimilarities in (c) than in (b). Summary of population $\mathcal{H}_0$ profile lines as a ribbon (d) described by the minimum, mean and maximum.

The $\mathcal{H}_0$ ribbon corresponds to a summary of the $\mathcal{H}_0$ profile lines in a particular population. Each profile line describes the integration into one connected component for each subject in a population. The ribbon represents all the profiles obtained in the subjects by using the area in the barcode space where all R-fMRI signals are considered *connected*, see figure **4-2**d. The $\mathcal{H}_0$ ribbon is defined by the minimum and maximum of the profile lines. Then, minimum and maximum profile lines are computed for x axis, which is associated with the integration, as described previously. They indicate the fast and slow integration respectively. Note that the ribbon's width indicates the variation in the profile lines in the population. For instance, a narrow ribbon may indicate similar profiles. The ribbon's area also serves as an indicator of the variability of the $\mathcal{H}_0$ profiles. In order to complement the ribbon area feature, the mean of the profile lines was also computed. $\mathcal{H}_0$ mean represent the mean behavior of connectivity. This feature provides a global tendency view of the integration into a single connected component.

4.2. Results

This section reports the results of the PH analysis in patients with altered states of consciousness and topological variations when compared to the HC population. First, it exemplifies the TDA computations performed for a single patient. Then, it presents the topological features summary, beginning with the $\mathcal{H}_0$ ribbons for the HC and the patients with altered states of consciousness. Following, it reports the persistent $\mathcal{H}_1$ summary for both populations. Finally, the regions more involved in the $\mathcal{H}_1$ appearance are reported.

4.2.1. Persistent homology features on a single patient

For each subject, a distance matrix consolidates the measures between regions. This measure uses a distance based on Pearson's correlation, see section 3.2.3. Once the matrix was computed, the process follows by calculating the topological features. The features calculation was made for $\mathcal{H}_0$ and $\mathcal{H}_1$. Figure **4-3**b shows the persistent diagram for a subject. This diagram shows dots indicating the birth and death of the topological features. $\mathcal{H}_0$ features are shown in blue, and $\mathcal{H}_1$ features in orange.

For this subject, almost all $\mathcal{H}_0$ features fall in a range between 0.05 to 0.3 for the death values. Then, at the 0.3 death value for this patient, most points belong to the simplicial complex object. As in the previous stage with healthy people, the majority of orange dots are near the dashed line, indicating that as soon as a $\mathcal{H}_1$-hole births, it deaths. However, there are some far orange dots, signaling some persistent features. The orange dot with black contour marks the most persistent $\mathcal{H}_1$ -hole. Figure **4-3**a presents the $\mathcal{H}_0$ connectivity characterization in R-fMRI data space through barcodes. $\mathcal{H}_0$-holes, which correspond to the boundaries of groups of highly correlated regional time-courses, i.e., integrated components.

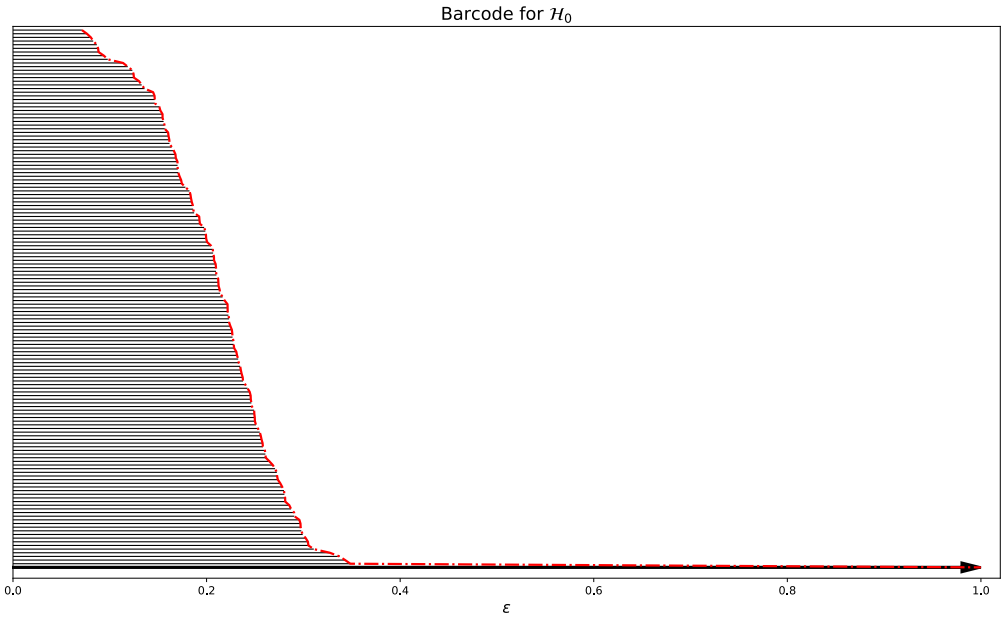

(a) $\mathcal{H}_0$ Barcode for a patient. Red line indicates the $\mathcal{H}_0$ profile line.

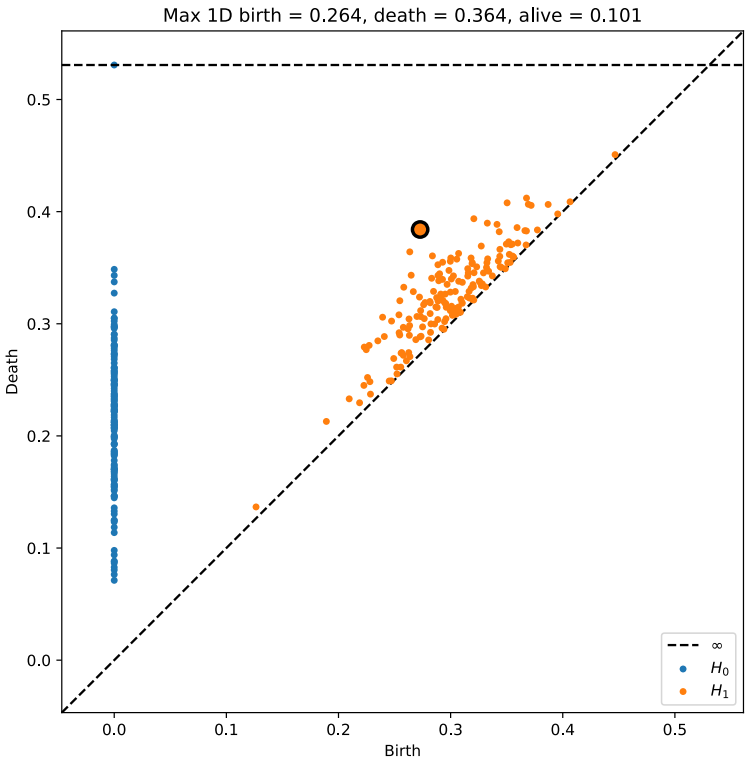

(b) Persistence diagram for a subject, cross indicate the greatest $\mathcal{H}_1$-hole. Black contour dot indicates the most persistent $\mathcal{H}_1$-hole

Figure **4-3**.: $\mathcal{H}_0$ and $\mathcal{H}_1$ diagrams for a patient with DOC.

Each line in the barcode represents a particular hole. The $\mathcal{H}_0$ profile line (red line in the figure) describes the integration of components into a single simplicial complex. The R-fMRI time-courses for this subject show connectivity levels in a wide range. Furthermore, the $\mathcal{H}_0$ integration into a single complex starts at 0.068 and ends at 0.35, in a range of 0.28. It is worthy to recall that in this representation, R-fMRI distances restrict between 0 and 1. Therefore, the late integration start and the long range (28%) indicate dissimilarities across time-courses. However, the R-fMRI time-courses in this subject show levels of connectivity, as evidenced by the $\mathcal{H}_0$-holes found in the persistent analysis.

Finally, the $\mathcal{H}_0$ profile lines were also computed for the healthy control subjects set described in the previous chapter. These profile lines will be used in the ribbon computations to describe integration in healthy subjects, and to establish a comparison base for the $\mathcal{H}_0$ features.

4.2.2. Persistent homology reveals integration features across $\mathcal{H}_0$

The following Figure (**4-4**) shows the summary of the topological $\mathcal{H}_0$ features computed for two datasets, for healthy subjects and the whole set of patients with acute altered states of consciousness. Figure **4-4**a shows the mean and ribbon of the profile line built for $\mathcal{H}_0$ for the healthy population. The mean line starts in a filtration value close to zero for HC. This start denotes that regions exhibit similar time-courses, i.e., a short distance between them. However, the ribbon limit at the right points to subjects that present a different behavior. Particularly, the connections start late, indicating that time-courses are not too similar among them. Additionally, the slope of the profile line is an indicator of the homogeneity of the distances between data elements, in this case, between the R-fMRI signal. Ribbon limit lines and the mean line slopes are similar, indicating a sort of regularity in the $\mathcal{H}_0$ profiles.

Figure **4-4**b reports the $\mathcal{H}_0$ ribbon and the $\mathcal{H}_0$ mean line of the acute altered states of consciousness patients. The ribbon left limit starts near zero while the right ends close to 0.4. Although this difference seems to be high, the mean width is about 0.2, indicating that the maximum difference of the filtration values to reach a full integration is the same.

Compared to $\mathcal{H}_0$ healthy subjects profile ribbon. The $\mathcal{H}_0$ ribbon of the acute unconscious patients looks displaced to the right, i.e., the distance between the brain region's time-courses is greater. Then, the signals are distant in acute unconscious patients than in healthy people. Also, the width of the ribbon indicates homogeneity of the profiles across the populations. The width of the HC ribbon is narrower than the acute unconscious patients' ribbon, indicating that there are more variations in the patients' profiles, i.e., the range of the values resulting in a full integration is greater. Another attribute to consider is the shape of the ribbon limits. This value seems more similar in the acute unconscious patient's ribbon than

in the HC ribbon, indicating that profile lines have different behavior. However, the slope of the mean lines in both settings, acute unconscious patients and healthy people, is similar, indicating that the rate to reach full integration is the same.

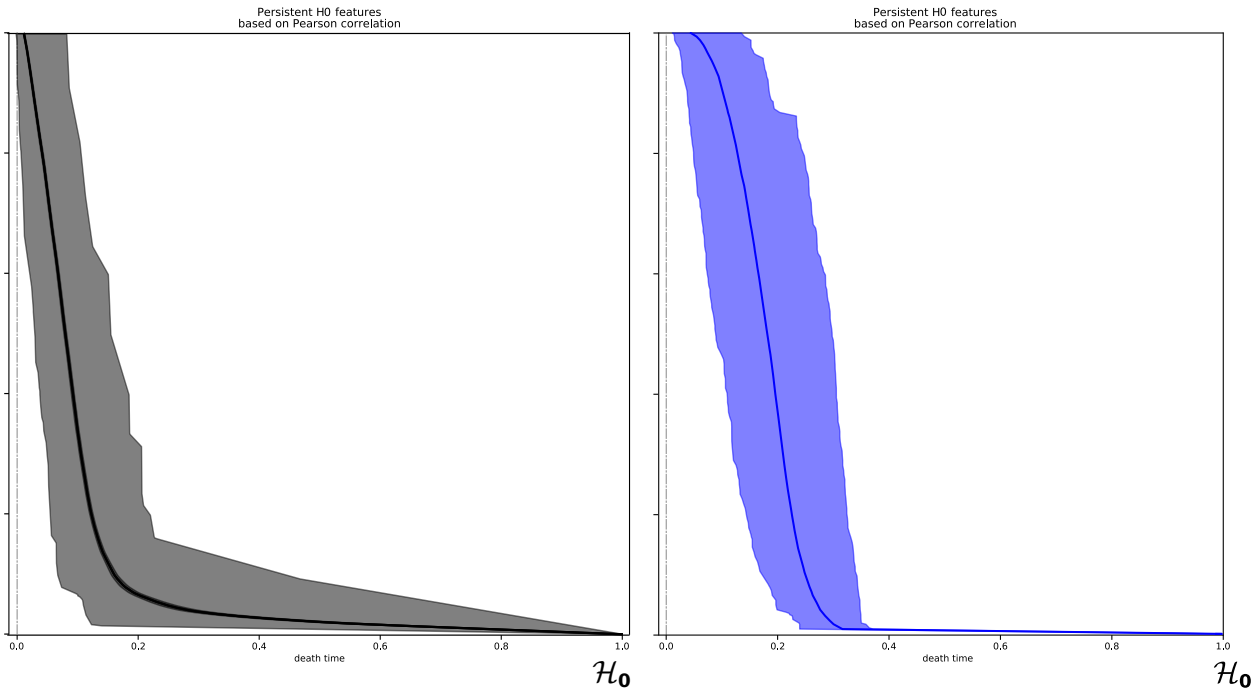

(a) $\mathcal{H}_0$ summary for HC subjects.

(b) $\mathcal{H}_0$ summary for acute state patients.

Figure **4-4**.: Summary of the $\mathcal{H}_0$ topological features computed on the two settings, Healthy Control (HC) subjects and patients with acute altered consciousness state. (a) Ribbon and average $\mathcal{H}_0$ for the HC. (b) Ribbon and average $\mathcal{H}_0$ for the acute patients. Ribbon shows the range of distance values where the signals are integrated into a single structure. Formally, the ribbon indicates the area where $\mathcal{H}_0$-holes disappear. Mean line shows the global behavior, indicating that 0-holes vanish near to distance 0.28 in HC, and to distance 0.34 for patients.

4.2.3. $\mathcal{H}_1$ features in patients with altered states of consciousness

Figure **4-5**b shows the summary of the $\mathcal{H}_1$ most persistent features comparing both populations, HC subjects, and patients in an acute altered state of consciousness. In blue, it displays the frequency diagram and the points distribution for HC previously reported in Figure **3-7**. This figure also shows in green the diagrams for the patients, and at right, the distribution of points characterizing the persistent $\mathcal{H}_1$ features. Each green square represents the persistent feature of an acute unconscious patient. The left picture displays a histogram based on the distance of the point to the diagonal, i.e., the length from the birth

time. Then, as distant is the point from the diagonal, as the persistent is the feature. The points distribution here appears for birth values greater than 0.1 and lesser than 0.3, with a higher concentration for values greater than 0.16. Complementary, the death values are between 0.26 and 0.41. Additionally, the histogram (green area) shows a concentration of the persistent $\mathcal{H}_1$ feature-length in a range between 0.09 and 0.19 for all subjects. As in the healthy people faction, the $\mathcal{H}_1$ features are far from the diagonal, denoting no spurious occurrence. In contrast, the acute state patients distribution seems to be more concentrated.

In HC, birth and death values are in long ranges compared with the values for acute state patients. Also, patients distribution seems to be displaced, yet the appearance of the $\mathcal{H}_1$-features in acute state patients are in the range of birth values reported previously for HC, i.e., the birth range of HC includes the span of patients. The apparent displacement is an expected result due to the late connection expressed in the $\mathcal{H}_0$. Even if this displacement seems to be anticipated and caused by the pathology. The apparent disconnection argued in the functional connectome analysis turns into a weak constraint, and it could be the result of an inappropriate threshold selection.

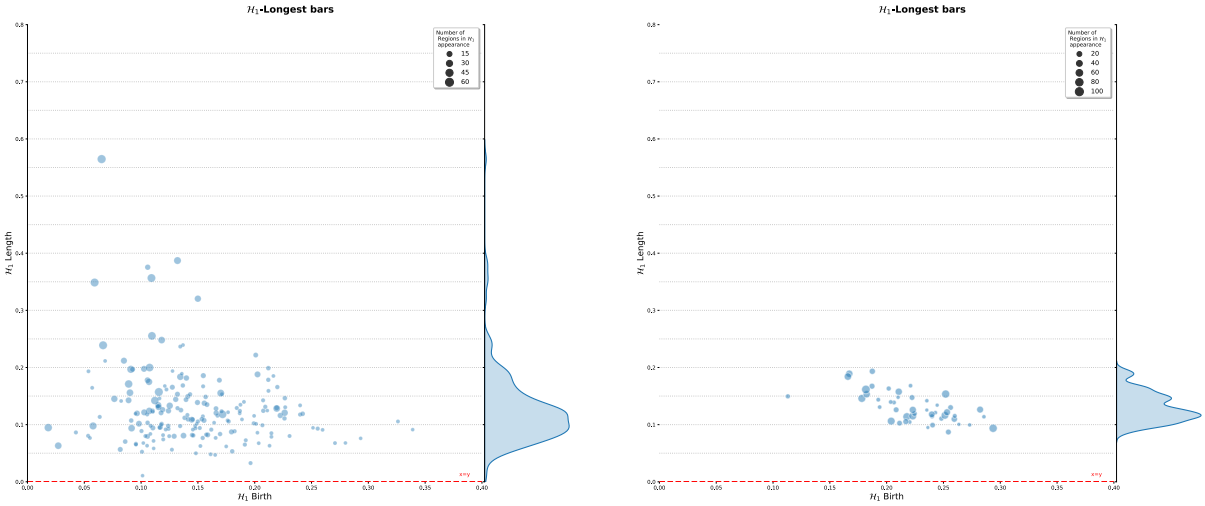

(a) $\mathcal{H}_1$ persistent summary of the topological features computed over healthy subjects.

(b) Summary of the $\mathcal{H}_1$ topological features computed on patients with DOC.

Figure **4-5**.: $\mathcal{H}_1$ persistent summaries of the topological features for two populations. (a) healthy controls (b) patients with DOC. For each one, the distribution of the $\mathcal{H}_1$ largest holes are at left while the histogram of lengths of the persistent hole is at right. Gray dashed lines are only for reference of distances from the $x = y$ line at bottom. Also, the circle radius indicates the number of regions involved in the appearance of the longest $\mathcal{H}_1$ feature in the corresponding subject.

Returning to the distribution ranges, HC exhibits long ranges for both birth and death values. Acute altered state of consciousness patients exhibits short-range values covered by HC ones. Patients $\mathcal{H}_1$ frequency intersects with the HC frequency. The highest frequencies appear for the same feature persistence values. Then, the persistence of the features seems to be not altered by the pathology, only the condensed ranges. In summary, the TDA approach on acute altered states of consciousness patients shows the integration in a single simplicial complex in $\mathcal{H}_0$, and the emergence of no artificial $\mathcal{H}_1$ features.

4.2.4. Brain regions in topological persistent structures for patients with acute altered state of consciousness

Continuing with the TDA analysis for R-fMRI in acute altered states of consciousness, figure **4-6** presents the brain regions that are part of the most persistent $\mathcal{H}_1$-hole, as the regions involved in its birth, i.e. when this regions is integrated into the simplicial complex the persistent $\mathcal{H}_1$-hole emerge. In addition, this figure reports the frequency of the appearance of a brain region in the emergence of the largest loop across the acute altered state of consciousness population. Regions were sorted by the times that a brain region is present in the greatest $\mathcal{H}_1$ loop, considering the whole acute altered states of consciousness population. As observed, the highest frequency of occurrence values was obtained for the left gyrus temporal superior plan temporal (21 times), followed by the left sulcus circular insula inferior (20 times), next to the right gyrus temporal inferior (19 times). Particularly, these regions appear in almost 40% of the patient's large loop. Also, most of the brain regions are present in at least ten of the greatest loops.

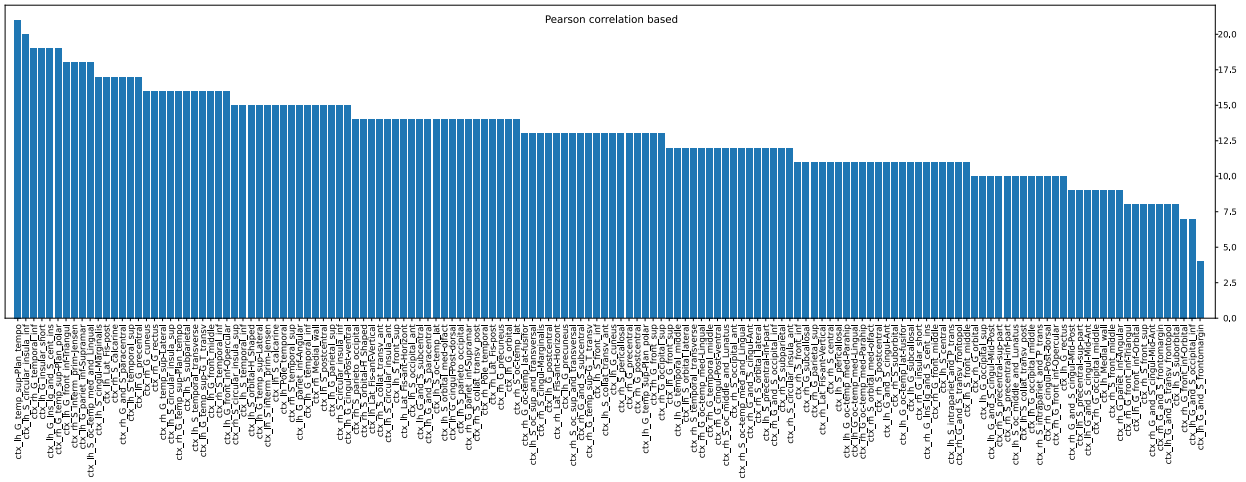

Figure **4-6**.: Frequent brain regions in the most persistent H_1 for patients with acute altered states of consciousness

Figure **4-7** shows a projection frequent brain regions on a glass representation. Brain regions in glass allow identifying the anatomical localization of the frequent region in the $\mathcal{H}_1$-holes. Yellow regions correspond to the most frequently regions involved in $\mathcal{H}_1$ holes.

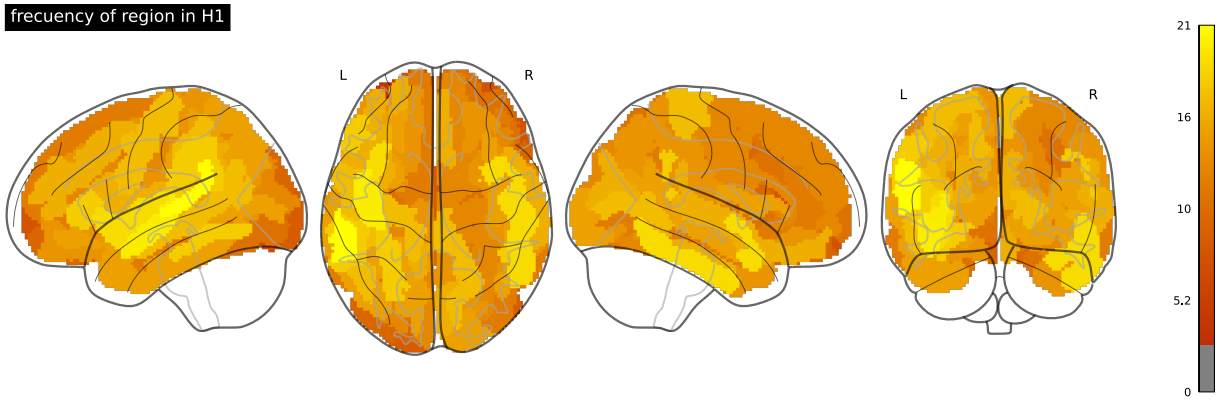

Figure **4-7**.: Frequency of regions involved in $\mathcal{H}_1$ projected on the brain glass representation.

As observed, in contrast with the healthy, here, the regions do not evidence any hemispherical symmetry, indicating alterations in the emergence of the functional connectivity boundary expressed by the $\mathcal{H}_1$. This condition is explicit in figure **4-7**. This figure shows that the projections of the regions that are at least in fifteen (15) of the persistent loop for the set of patients. As observed, the left hemisphere seems to participate in the appearance of topological structures than the right hemisphere more. Also, it exhibits the variation of the regions involved in the mentioned phenomenon. In healthy people, its occurrence is mainly in the superior temporal gyri for both hemispheres, as in their nearest brain regions, i.e., middle temporal and bankssts gyri, both on the temporal lobe. While in patients with acute altered states of consciousness, the referred behavior is not present. The first regions involved in $\mathcal{H}_1$ loops were: (i) left temporal superior plan temporal gyrus, (ii) left circular insula inferior sulcus, and (iii) right temporal inferior gyrus.

4.3. Discussion

This chapter presents the topological description of R-fMRI time-courses of patients with acute altered states of consciousness. As in HC analysis, highly robust $\mathcal{H}_1$ loops emerge from the integration of R-fMRI signals. These topological features persist in a range of longitudes between 10% the 20% of the full range of distances. These features in acute state patients constitute the first evidence about high-order structures of connectivity in these pathological conditions. In addition, this chapter introduces a $\mathcal{H}_0$ analysis perspective. It includes the profile lines to characterize the integration into a single simplicial complex and the population summaries of the profile lines. $\mathcal{H}_0$ ribbon and the population' mean summarize. Acute state patients $\mathcal{H}_0$ ribbon indicates a late integration in contrast to HC $\mathcal{H}_0$ ribbon. Also,

$\mathcal{H}_0$ ribbon exhibits a wide range, suggesting more dissimilarities across fMRI resting-state time-courses in patients than in the HC. Acute state patients $\mathcal{H}_0$ mean descriptor shows a late start of the integration when compared with HC. Furthermore, this delayed beginning is also an indication of the time-courses dissimilarities due to pathological conditions. However, the slope of the two $\mathcal{H}_0$ means descriptors, for acute state patients and HC seems to be similar, indicating that once the integration process starts, the size of the filtration values interval that results in a single unit is the same. In other words, regardless of the start displacement, the values of the differences among resting-state time-courses, which lead to the integrated unit, are similar for both populations. For instance, the difference values among some time-courses in healthy controls are $\alpha < \beta < \gamma$ when measured the differences among some time-courses in an acute altered state of consciousness patients the difference values are the same, i.e., $\alpha < \beta < \gamma$. Complementary, TDA on patients with an acute altered state of consciousness exhibits $\mathcal{H}_1$ features. These $\mathcal{H}_1$ loops seem to be different from those reported in HC subjects. The main variations are (i) the reduction of birth and death ranges, (ii) the increment of birth values (late integration start), and (iii) the brain regions involved in the emergence of the loop. Also, the regions implicated in the occurrence of these $\mathcal{H}_1$ features in patients are different. This finding points that the feature might be involved in a variation of high-order mental processes due to pathological conditions. In particular, the non-symmetry of the regions presented in section 4.2.4. Also, the left circular insula inferior sulcus and left superior plan temporal gyrus to claim the principal roles in the appearance of $\mathcal{H}_1$ features, showing another difference when compared with HC subjects. However, their meaning and function in the high-order description introduced here are still unknown. To conclude, these findings in $\mathcal{H}_0$ and $\mathcal{H}_1$ evidence alterations in high-order interaction mechanisms associated with loss of consciousness.

Topological description through persistent homology begins to be more relevant for the research community. In R-fMRI, some authors used PH to describe the robustness across distinct data scales [35]. Indeed they only use $\mathcal{H}_0$ to overcome threshold selection while evidence robustness. Lord et al. [111] present the use of persistent homological scaffolds to summarize topological properties. Also, they compare persistent homological scaffolds to local graph metrics, showing their robustness. Homological scaffolds, introduced by Petri et al. [132], describe the topological features. The description is made in terms of persistence and (ii) appearance frequency in $\mathcal{H}_1$ cycles, providing two measurements of the importance of edges. This chapter uses the $\mathcal{H}_0$ to characterize the integration into one single simplicial complex for healthy and pathological conditions. Introducing a summarization of $\mathcal{H}_0$ for populations, complementary to the reported by Cassidy et al. [35]. Also, this chapter focuses on the relevance of $\mathcal{H}_1$, in particular for alterations in an acute altered state of consciousness patients. In contrast to the PH scaffolds approximation [132, 111], here the relevance is obtained directly from the PH identifying the largest feature, and the relevant objects, the brain regions in the $\mathcal{H}_1$, with the exploration of the associated lists. However, it is important

to remark that the PH scaffold is centered in the characterization of relevance by counting the appearance frequency of an edge element in the $\mathcal{H}_1$ features emergence. Both approaches use high-order features beyond the graph description.

In consciousness studies, graph or complex network approximations provide measurements to relate consciousness with brain properties. A recent taxonomy of these approximations considering distinct acquisition modalities and processing methodologies provides a consolidated base for consciousness studies [149]. It conciliates the complexity measures to examine consciousness at distinct levels, including DOC. In particular, measures to assess properties related to the coexistence of functional integration and differentiation in the brain [168, 99, 149]. The taxonomy classifies the complexity measures into three groups 1. topological differentiation, 2. temporal differentiation, and 3. mixed strategy All they rely on a pair-wise representation of the interactions, which can be stationary (topological) or dynamic (temporal). This representation limits the topological description to dyadic interactions [111]. Furthermore, graph properties alterations associated with DOC have been related to disconnections in local [84, 80, 39], and global [119] approaches. However, these alterations might be the result of a misconception of weak interaction between nodes as disconnections. This apparent disconnection biases the unconscious states' topological description with this graph representation centered in the edges. The proposed approach describes the integration through $\mathcal{H}_0$-cycles, denoting a delay integration into a single simplicial complex for patients with DOC. This delay is an increment in the distance between time-courses, i.e., a reduction of the interaction strength. Some alternatives from hypergraphs [144, 9] and TDA [35, 111] tackle the graph limitations, providing distinct frames which considers simultaneous interactions. Even more, Petri et al. [132] report topological $\mathcal{H}_1$ features in altered states of consciousness. They describe fMRI $\mathcal{H}_1$ features by the PH scaffolds. The PH scaffold measures the relevance of the elements involved in $\mathcal{H}_1$ appearance. With this measurement, they robustly show $\mathcal{H}_1$ differences in pharmacological induced states of consciousness. On the other side, the approach presented here allows identifying the persistent $\mathcal{H}_1$ loop structures, one per patient, while recognizes the brain regions involved in its emergence. It proposes a different approach to note the relevance of $\mathcal{H}_1$. Furthermore, it associates the relevance and the occurrence frequency in subjects with acute altered states of consciousness, showing differences compared to HC subjects. However, the exact role of the regions in the emergence of $\mathcal{H}_1$ is out of scope. Finally, these findings provide new analysis dimensions in the consciousness study.

Our results suggest some regional differences linked to states of consciousness alterations. For example, the brain regions near to the insula and the regions in the Wernicke's area near to the left temporal superior temporal gyrus seem to be more involved in the $\mathcal{H}_1$ occurrence. At the same time, there are two no contiguous regions in the right hemisphere, the main, the inferior temporal gyrus, and the superior temporal gyrus. The temporal gyrus is related

to the auditory association, multisensory integration, speech processing, language comprehension. The insula function is primarily related to sensorimotor processing, regulation of autonomic function, interoception, pain perception, auditory processing, chemosensory functions (processing of intensity, quality, and affective value of taste stimuli) [174]. Also, it appears related to modulating the intensity of olfactory stimuli. Then, the insula is involved in many different kinds of processing. The arising of the insula as a frequent region in the $\mathcal{H}_1$ persistent feature is one of the main differences when compared with the healthy approach. It could be due to not awareness to follow instructions during the acquisition stage neither to the reorientation of attention described previously for healthy subjects. Then, its emergence as an element in the boundary of TDA functional description might be associated with the reductions in its stimuli response and process.

The presented approach has some limitations. The main drawbacks of the TDA process were already addressed in section 3.4. Here, the discussion is about the limitations due to the pathological condition of the population. In severely damaged brain tissues, as a patient in DOC conditions, this approach cannot be used because the parcellation process fails, making it impossible to assign the representative time-course to a specific brain region. This severe damage is caused by the prolonged time in pathological conditions. Thus, the presented approach considers a set of patients in an acute altered state of consciousness. The PH analysis of acute altered states of consciousness highlights the left superior plan temporal gyrus and the left circular insula inferior sulcus as the more frequent regions in the largest $\mathcal{H}_1$ boundary. So, identifying brain processes in which those regions are or are not active may result in scenarios in which establishing some conditions to understand the emergence of the acute state's boundary could lead to new branches of analysis.

5. Conclusions and Recommendations

5.1. Conclusions

Graph measurements provide a set of tools to describe, evaluate and characterize the resting-state connectome. Even on a global scale, as the FNC is built from large regions, i.e., the RSNs, they capture variations that can be linked with a specific pathological condition. In the DOC case presented here, they can be associated with the severity level of the pathology. Alterations in integration, segregation, and centrality confirm topological variations related to the connectivity level among RSNs for DOC patients. Regardless of these variations through the graph model, underlying topological properties can not be described from this approach.

The strategy considering persistent homology characterizes resting-state connectome for healthy control subjects. Persistent $\mathcal{H}_1$-holes were found in healthy people, providing a new set of features to consider in resting-state studies. These $\mathcal{H}_1$-holes indicate the existence of boundaries surrounded by 1-simplex (lines), conforming to a loop. A persistent loop provides two directions of connections for the elements in the boundary. Additionally, the occurrence of these properties is linked to specific brain regions. The regions in the $\mathcal{H}_1$-features frequently appear across populations, expressing a sort of symmetry in the resting-state connectome topology and providing biological insight.

Persistent homology also describes topological properties in pathological conditions, i.e., patients in acute altered states of consciousness. The displacements $\mathcal{H}_0$-profile lines and consistent appearance of $\mathcal{H}_1$-holes, with lengths comparable to healthy scenarios, provides a set of characteristics for topological-based study. However, the brain regions involved in the appearance of these high-order features, $\mathcal{H}_1$-holes, are distinct and not exhibits a hemisphere symmetry, suggesting an alteration of the boundary in the resting-state activity. These differences could be associated with the pathological condition, particularly with the no response to stimuli.

The PH strategies describe the topology of the resting-state functional connectome. Subjacent high-order features were robustly found for healthy and pathological conditions, suggesting the existence of resting-state processes that go beyond the connectivity itself. These $\mathcal{H}_1$-holes arise as a new element of interest that represents a limited connection among a set of data objects, resting time-courses. The objects in the loop are connected, exhibiting at least two directions to reach all the others in the set. But, the connection is limited because it is not direct. Then, $\mathcal{H}_1$-hole and the elements implicated in its emergence propose a new direction for the resting-state analyses, asking for the functional processes which generate these structures, which imply integration and segregation at the same time.

5.2. Recommendations

The proposed strategy for topological data analysis takes as a basis the distance based on Pearson's correlation. However, the topological description only requires a distance. Then, the use of other distances apart from linearities could lead to distinct topological features. For instance, distances correlation or Granger causality that measures non-linearities and directional connectivity respectively. Using any of these in the topological description may result in a distinct set of persistent homology features. If there are different features, how it impacts the topological description?

Topological characterization was made on a space of modules $\mathbb{Z}/2\mathbb{Z}$. This selection of modules limits the dimension of topological features up to 2, i.e., cavities surrounded by 2-simplex (faces). Then, a high-order description requires superior modules. Thus, computation of topological features in R-fMRI analysis considering different modules lead to high-order cavities descriptions, which might be suitable for resting-state studies.

The R-fMRI topological description through persistent homology in healthy subjects and patients reveals the existence of many $\mathcal{H}_1$-holes that are far from the diagonal. However, this work only considers the most persistent $\mathcal{H}_1$-hole, one feature per individual, leaving aside other persistent features. This way, the inclusion of more relevant $\mathcal{H}_1$ features, not just the most persistent, could provide a rich scenario that giving more clues about integration and segregation phenomena linked to consciousness emergence. Moreover, the selection of the set of relevant $\mathcal{H}_1$-holes could regard the scaffolds approach to improve the meaningfulness of the persistent features to consider.

Study the $\mathcal{H}_0$-profile line provides a first picture about the integration phenomena in R-fMRI, pointing to the interval length where all simplex converges into a single simplicial complex. More formal properties, better than the visual slope introduced here, could lead to a more detailed description of the integration of the data. In this case, the slope indicates how fast the integration is, and slopes variations point to the distances differences regularity in the data. Other properties, computed for a continuous increasing function as the profile, could provide more information about integration.

The computed set of topological features, i.e., $\mathcal{H}_0$-holes and $\mathcal{H}_1$-holes might be used as characteristics in a supervised classification machine learning process. For this, the sequence of $\mathcal{H}_0$-holes and $\mathcal{H}_1$-holes can compose a features vector while the consciousness level is the target vector. Thus, it is reasonable to use the persistent features as characteristics in a machine learning classification algorithm, which can boost the use of persistent homology features in other processes.

A. Annex: Complex Networks Measurements

The table **A-1** provides a short description of some of the complex networks measurements, it does not represent a complete set of the graph measurements.

Table **A-1**.: network measurements employed to characterize brain networks [28]

N is the set of all nodes in the network, and n is the number of nodes. L is the set of all links in the network, and l is the number of links. (i, j) is a link between nodes i and j, $(i, j \in N)$. a_{ij} is the connection status between i and j: $a_{ij} = 1$ when the link (i, j) exists (when i and j are neighbors); $a_{ij} = 0$ otherwise ($a_{ii} = 0$ for all i). We compute the number of links as $l = \sum_{i,j \in N} a_{ij}$ (to avoid ambiguity with directed links we count each undirected link twice, as a_{ij} and as a_{ji}). Links (i, j) are associated with connection weights w_{ij}. Henceforth, we assume that weights are normalized, such that $0 \leqslant w_{ij} \leqslant 1$ for all i and j. l^w is the sum of all weights in the network, computed as $l^w = \sum i, j \in N w_{ij}$.

Measurement	**Formulation**
Degree	$k_i = \sum_{j \in N} a_{ij}$
Number of connections that link a node to the rest of the network	
Strength	$k_i^w = \sum_{j \in N} w_{ij}$
Quality of the connections that link a node to the rest of the network	
Shortest path length	$d_{ij}^w = \sum_{a_{uv} \in g_{i \leftrightarrow j}^w} f(w_{uv})$
Shortest weighted path between i and j, where f is a map from weight to length and $g_{i \leftrightarrow j}^w$ is the shortest weighted path between i and j	
Number of triangles	$t_i^w = \frac{1}{2} \sum_{j,h \in N} (w_{ij} w_{ih} w_{jh})^{1/3}$
Geometric mean of the weights of the triangles around the node i	

Continued on next page

Table **A-1** – *Continued from previous page*

Measurement	**Formulation**
Characteristic path length	$L^w = \frac{1}{n}\sum_{i\in N}\frac{\sum_{j\in N, j\neq i} d_{ij}^w}{n-1}$
Average distance between node i and all other nodes	
Global efficiency	$E_w = \frac{1}{n}\sum_{i\in N}\frac{\sum_{j\in N, j\neq i}\left(d_{ij}^w\right)^{-1}}{n-1}$
The average inverse shortest path length. The global efficiency may be meaningfully computed on disconnected networks, as paths between disconnected nodes are defined to have infinite length, and correspondingly zero efficiency	
Clustering coefficient	$C^w = \frac{1}{n}\sum_{i\in N}\frac{2t_i^w}{k_i(k_i-1)}$
Quantifies the number of connections that exist between the nearest neighbors of a node as a proportion of maximum number of possible connections	
Modularity	$Q^w = \frac{1}{l^w}\sum_{i,j\in N}\left[w_{ij} - \frac{k_i^w k_j^w}{l^w}\right]\delta_{m_i,m_j}$
A network module contains several densely interconnected nodes, and there are relatively few connections between nodes in different modules. Where m_i is the module containing node i, and $\delta_{m_i,m_j} = 1$ if $m_i = m_j$, and 0 otherwise	
small-worldness	$S = \frac{C/C_{rand}}{L/L_{rand}}$
The small-world measures the combination of segregated modules with a robust number of intermodular links. Where C and C_{rand} are clustering coefficients, and L and L_{rand} are characteristics path lengths of the respective tested network and a random network. Small-world networks often have $S \gg 1$	
Betweenness centrality	$b_i = \frac{1}{(n-1)(n-2)}\sum_{h,j\in N}\frac{\rho_{hj}^{(i)}}{\rho_{hj}}$
The centrality of a node measures how many of the shortest paths between all other node pairs in the network pass through it. Where ρ_{hj} is the number of shortest paths between j and h, and $\rho_{hj}^{(i)}$ is the number of shortest paths between j and h through node i	

B. Annex: Resting State Networks Identification

The following RSNs extraction was explained in [46]. First, single-subject ICA with 30 components was performed [190] using the infomax algorithm as implemented in the Group-ICA of fMRI toolbox (GIFT: http://icatb.sourceforge.net/). The component images (spatial maps) were calibrated to the raw data so the intensity values were in units of percent signal change (PSC) from the mean [31]. This fit was used to scale the component images into units, which reflect the deviation of the data from the mean, enabling a second level random effects analysis to be performed [31]. The ICs were then matched to the templates representative of the RSNs by means of a goodness-of-fit procedure. This method extends the single-template goodness-of-fit approach [77] by quantifying the absolute PSC average of voxels falling in the template minus the PSC average of voxels outside the template. The templates for each RSN were selected by an expert after visual inspection from a set of spatial maps resulting from Group ICA decomposition (30 components running GIFT) performed on 12 independently assessed controls (4 women, mean age = 21 years $\pm$ 3, scanned on a 3T MR scanner using a gradient echo-planar sequence of axial slice orientation: 32 slices, voxel-size = 3.4 $\times$ 3.4 $\times$ 3.0 mm^3, repetition time = 2,460 msec, echo time = 40 msec, flip angle = 90, field of view = 220 $\times$ 220 mm^2). These templates were checked by another expert for accuracy of structural labeling. Second, the multiple-template assignation procedure was performed. In order to overcome potentially concurrent IC assignations to the same template, we introduced two physiologic constraints: (i) a template had to be assigned to one of the 30 ICs and (ii) an IC could be labeled as an RSN or not. The first constraint ensured that all templates would be assigned, given that the number of ICs was larger than the number of the templates. The second restriction forced a unique identification of each IC, which overcame the potentially concurrent component assignations. The multiple components labeling with assignation restrictions was formulated as a matching problem:

$$\max_{x} \sum_{i=1}^{N}\sum_{j=1}^{M} x_{i,j} g_{i,j}$$

$$\text{s. t. } \sum_{i=1}^{N} X_{i,j} = 1, 1 \leqslant j \leqslant M \ , \qquad \sum_{j=1}^{M} X_{i,j} \leqslant 1 \quad , 1 \leqslant i \leqslant N$$

with $M = 10$ the number of different templates, $N = 30$ the number of ICs, $g_{i,j}$ the goodness

of fit between the component i and the template j and $x_{i,j} \in \{0, 1\}$, an assignation binary variable indicating the match between the template j and the IC i. Hence, the couple between the template and IC with the highest global goodness of fit (taking into account all templates simultaneously) was eventually selected. The proposed optimization problem was solved by using binary integer programming [78]. Third, for the discrimination between "neuronal" and "non-neuronal", the approach used a binary classification approach by means of support vector machine (SVM) classifier trained on 19 independently assessed healthy subjects. The feature, which was used for the training of the classifier was the fingerprints obtained from ICA decomposition (n = 30 components). The fingerprint is a feature vector which contains both spatial (i.e., degree of clustering, skewness, kurtosis, spatial entropy) and temporal information (i.e., one-lag autocorrelation, temporal entropy, power of five frequency bands: 0 - .008 Hz, .008 - .02 Hz, .02 - .05 Hz, .05 - .1 Hz, and .1 - .25 Hz) and has been shown to discriminate neuronal from artifactual components [42].

Bibliography

[1] Achard, Sophie ; Delon-Martin, Chantal ; Vértes, Petra E. ; Renard, Félix ; Schenck, Maleka ; Schneider, Francis ; Heinrich, Christian ; Kremer, Stéphane ; Bullmore, Edward T.: Hubs of brain functional networks are radically reorganized in comatose patients. In: *Proceedings of the National Academy of Sciences* 109 (2012), Nr. 50, S. 20608–20613

[2] Adolphs, Ralph: The unsolved problems of neuroscience. In: *Trends in Cognitive Sciences* 19 (2015), Nr. 4, S. 173–175. – ISSN 1364–6613

[3] Ahmad, F ; Hussain, A ; Chaudhary, S U. ; Ahmad, I ; Ramay, S M.: A novel method for detection of voxels for decision making: An fMRI study. In: *International Journal of Imaging Systems and Technology* 26 (2016), Nr. 2, S. 163–167

[4] Albert, Réka ; Barabási, Albert-László: Statistical mechanics of complex networks. In: *Rev. Mod. Phys.* 74 (2002), Jan, S. 47–97

[5] Atienza, Nieves ; Gonzalez-Diaz, Rocio ; Rucco, Matteo: Persistent Entropy for Separating Topological Features from Noise in Vietoris-Rips Complexes. In: *arXiv e-prints* (2017), Jan, S. arXiv:1701.07857

[6] Baggio, H.-C. ; Sala-Llonch, R. ; Segura, B. ; Marti, M.-J. ; Valldeoriola, F. ; Compta, Y. ; Tolosa, E. ; Junqué, C.: Functional brain networks and cognitive deficits in Parkinson's disease. In: *Human Brain Mapping* 35 (2014), Nr. 9, S. 4620–4634

[7] Bandettini, P.A. ; Jesmanowicz, A. ; Wong, E.C. ; Hyde, J.S.: Processing strategies for time-course data sets in functional MRI of the human brain. In: *Magnetic Resonance in Medicine* 30 (1993), Nr. 2, S. 161–173

[8] Basser, P.J.: Inferring microstructural features and the physiological state of tissues from diffusion-weighted images. In: *NMR in biomedicine* 8 (1995), Nr. 7-8, S. 333–344

[9] Battiston, Federico ; Cencetti, Giulia ; Iacopini, Iacopo ; Latora, Vito ; Lucas, Maxime ; Patania, Alice ; Young, Jean G. ; Petri, Giovanni. *Networks beyond pairwise interactions: Structure and dynamics.* aug 2020

[10] Bauer, Ulrich. *Ripser: A Lean C++ Code for the Computation of Vietoris-Rips Persistence Barcodes*. 2018

[11] Beare, Richard ; Lowekamp, Bradley ; Yaniv, Ziv: Image Segmentation, Registration and Characterization in R with SimpleITK. In: *Journal of statistical software* 86 (2018), aug. – ISSN 1548–7660 (Print)

[12] Beckmann, Christian F. ; DeLuca, Marilena ; Devlin, Joseph T. ; Smith, Stephen M.: Investigations into resting-state connectivity using independent component analysis. In: *Philosophical Transactions of the Royal Society B: Biological Sciences* 360 (2005), Nr. 1457, S. 1001–1013. – ISSN 0962–8436

[13] Bernat, James L.: Ethical issues in the management of patients with impaired consciousness. In: Young (Hrsg.) ; Wijdicks (Hrsg.): *Disorders of Consciousness* Bd. 90. Elsevier, 2008. – ISSN 0072–9752, S. 369–382

[14] Berry, Eric ; Chen, Yen-Chi ; Cisewski-Kehe, Jessi ; Fasy, Brittany T.: Functional Summaries of Persistence Diagrams. In: *arXiv e-prints* (2018), Apr, S. arXiv:1804.01618

[15] Bhaskar, Dhananjay ; Zhang, William Y. ; Wong, Ian Y.: Topological Data Analysis of Collective and Individual Epithelial Cells using Persistent Homology of Loops. (2020), mar, S. arXiv:2003.10008

[16] Billings, Jacob ; Saggar, Manish ; Hlinka, Jaroslav ; Keilholz, Shella ; Petri, Giovanni: Simplicial and topological descriptions of human brain dynamics. In: *Network Neuroscience* 5 (2021), jun, Nr. 2, S. 549–568. – ISSN 2472–1751

[17] Biswal, Bharat B.: Resting state fMRI: A personal history. In: *NeuroImage* 62 (2012), Nr. 2, S. 938 – 944. – ISSN 1053–8119

[18] Biswal, Bharat B. ; Kylen, Joel V. ; Hyde, James S.: Simultaneous assessment of flow and BOLD signals in resting-state functional connectivity maps. In: *NMR in Biomedicine* 10 (1997), jun, Nr. 4-5, S. 165–170. – ISSN 0952–3480

[19] Boccaletti, S. ; Latora, V. ; Moreno, Y. ; Chavez, M. ; Hwang, D.-U.: Complex networks: Structure and dynamics. In: *Physics Reports* 424 (2006), Nr. 4-5, S. 175–308. – ISSN 0370–1573

[20] Bodien, Y G. ; Chatelle, C ; Edlow, B L.: Functional Networks in Disorders of Consciousness. In: *Seminars in Neurology* 37 (2017), Nr. 5, S. 485–502

[21] Boly, M. ; Phillips, C. ; Tshibanda, L. ; Vanhaudenhuyse, A. ; Schabus, M. ; Dang-Vu, T. ; Moonen, G. ; Hustinx, R. ; Maquet, S.: Intrinsic Brain

Activity in Altered States of Consciousness: How Conscious Is the Default Mode of Brain Function? In: *Annals of the New York Academy of Sciences* 1129 (2008), S. 119–129. – ISSN 1749–6632

[22] Boly, Melanie ; Seth, Anil ; Wilke, Melanie ; Ingmundson, Paul ; Baars, Bernard ; Laureys, Steven ; Edelman, David ; Tsuchiya, Naotsugu: Consciousness in humans and non-human animals: Recent advances and future directions. Front. In: *Frontiers in psychology* 4 (2013), oct, S. 625

[23] Brier, M.R. ; Thomas, J.B. ; Fagan, A.M. ; Hassenstab, J. ; Holtzman, D.M. ; Benzinger, T.L. ; Morris, J.C. ; Ances, B.M.: Functional connectivity and graph theory in preclinical Alzheimer's disease. In: *Neurobiology of Aging* 35 (2014), S. 757–768

[24] Bruno, M. A. ; Laureys, S. ; Demertzi, A.: Chapter 17 - Coma and disorders of consciousness. In: Bernat, James L. (Hrsg.) ; Beresford, H. R. (Hrsg.): *Ethical and Legal Issues in Neurology* Bd. 118. Elsevier, 2013. – ISSN 0072–9752, S. 205 – 213

[25] Bruno, Marie-Aurélie ; Vanhaudenhuyse, Audrey ; Thibaut, Aurore ; Moonen, Gustave ; Laureys, Steven: From unresponsive wakefulness to minimally conscious PLUS and functional locked-in syndromes: recent advances in our understanding of disorders of consciousness. In: *Journal of Neurology* 258 (2011), Nr. 7, S. 1373–1384. – ISSN 0340–5354

[26] Buckner, Randy L. ; Andrews-Hanna, Jessica R. ; Schacter, Daniel L.: The Brain's Default Network. In: *Annals of the New York Academy of Sciences* 1124 (2008), Nr. 1, S. 1–38. – ISSN 1749–6632

[27] Bullmore, E. ; Sporns, O.: The economy of brain network organization. In: *Nature Reviews Neuroscience* 13 (2012), Nr. 5, S. 336–349

[28] Bullmore, Ed ; Sporns, Olaf: Complex brain networks: graph theoretical analysis of structural and functional systems. In: *Nature Reviews Neuroscience* 10 (2009), mar, Nr. 3, S. 186–198. – ISSN 1471–003X

[29] Cacciola, Alberto ; Naro, Antonino ; Milardi, Demetrio ; Bramanti, Alessia ; Malatacca, Leonardo ; Spitaleri, Maurizio ; Leo, Antonino ; Muscoloni, Alessandro ; Cannistraci, Carlo V. ; Bramanti, Placido ; Calabrò, Rocco S. ; Anastasi, Giuseppe P.: Functional Brain Network Topology Discriminates between Patients with Minimally Conscious State and Unresponsive Wakefulness Syndrome. In: *Journal of clinical medicine* 8 (2019), mar, Nr. 3, S. 306. – ISSN 2077–0383

[30] Cai, Yuexin ; Xie, Mingwei ; Su, Yun ; Tong, Zhaopeng ; Wu, Xiaoyan ; Xu, Wenchao ; Li, Jiahong ; Zhao, Fei ; Dang, Caiping ; Chen, Guisheng ; Lan, Liping

; Shen, Jun ; Zheng, Yiqing: Aberrant Functional and Causal Connectivity in Acute Tinnitus With Sensorineural Hearing Loss. In: *Frontiers in Neuroscience* 14 (2020), S. 592. – ISSN 1662–453X

[31] Calhoun, V.D. ; Adali, T. ; Pearlson, G.D. ; Pekar, J.J.: Group ICA of functional MRI data: seperability, stationarity, and inference. In: *Proceedings of International Conference on ICA and BSS*, 2001

[32] Cao, B ; Guo, Y ; Guo, Y ; Xie, Q ; Chen, L ; Huang, H ; Yu, R ; Huang, R: Time-delay structure predicts clinical scores for patients with disorders of consciousness using resting-state fMRI. In: *NeuroImage: Clinical* 32 (2021)

[33] Carlsson, G.: Topology and data. In: *Bulletin of the American Mathematical Society* 46 (2009), Nr. 2, S. 255–308

[34] Carpio, A ; Bonilla, L L. ; Mathews, J C. ; Tannenbaum, A R.: Fingerprints of cancer by persistent homology. In: *bioRxiv* (2019), jan, S. 777169

[35] Cassidy, B. ; Bowman, F. D. ; Rae, C. ; Solo, V.: On the Reliability of Individual Brain Activity Networks. In: *IEEE Transactions on Medical Imaging* 37 (2018), Feb, Nr. 2, S. 649–662. – ISSN 0278–0062

[36] Cha, Sung-Hyuk: Comprehensive Survey on Distance/Similarity Measures Between Probability Density Functions. In: *International Journal of Mathematical Models and Methods in Applied Sciences* 1 (2007), 01, S. 300–307

[37] Chai, Xiaoqian J. ; Berken, Jonathan A. ; Barbeau, Elise B. ; Soles, Jennika ; Callahan, Megan ; Chen, Jen-Kai ; Klein, Denise: Intrinsic Functional Connectivity in the Adult Brain and Success in Second-Language Learning. In: *The Journal of Neuroscience* 36 (2016), jan, Nr. 3, S. 755 LP – 761

[38] Corbetta, Maurizio ; Patel, Gaurav ; Shulman, Gordon L.: The reorienting system of the human brain: from environment to theory of mind. In: *Neuron* 58 (2008), may, Nr. 3, S. 306–324. – ISSN 1097–4199

[39] Crone, Julia S. ; Soddu, Andrea ; Höller, Yvonne ; Vanhaudenhuyse, Audrey ; Schurz, Matthias ; Bergmann, Jürgen ; Schmid, Elisabeth ; Trinka, Eugen ; Laureys, Steven ; Kronbichler, Martin: Altered network properties of the fronto-parietal network and the thalamus in impaired consciousness. In: *NeuroImage: Clinical* 4 (2014), S. 240 – 248. – ISSN 2213–1582

[40] Cruse, D. ; Monti, M.M. ; Owen, A.M.: Neuroimaging in disorders of consciousness: Contributions to diagnosis and prognosis. In: *Future Neurology* 6 (2011), Nr. 2, S. 291–299

[41] Damoiseaux, J. S. ; Rombouts, S. A. R. B. ; Barkhof, F. ; Scheltens, P. ; Stam, C. J. ; Smith, S. M. ; Beckmann, C. F.: Consistent resting-state networks across healthy subjects. In: *Proceedings of the National Academy of Sciences* 103 (2006), Nr. 37, S. 13848–13853

[42] De Martino, Federico ; Gentile, Francesco ; Esposito, Fabrizio ; Balsi, Marco ; Di Salle, Francesco ; Goebel, Rainer ; Formisano, Elia: Classification of fMRI independent components using IC-fingerprints and support vector machine classifiers. In: *NeuroImage* 34 (2007), Nr. 1, S. 177–194. – ISSN 1053–8119

[43] De Pasquale, F. ; Sabatini, U. ; Della Penna, S. ; Sestieri, C. ; Caravasso, C.F. ; Formisano, R. ; PÃ©ran, P.: The connectivity of functional cores reveals different degrees of segregation and integration in the brain at rest. In: *NeuroImage* 69 (2013), S. 51–61

[44] Demertzi, A. ; Soddu, A. ; Laureys, S.: Consciousness supporting networks. In: *Current Opinion in Neurobiology* 23 (2013), Nr. 2, S. 239–244

[45] Demertzi, A. ; Vanhaudenhuyse, A. ; Brédart, S. ; Heine, L. ; di Perri, C. ; Laureys, S.: Looking for the self in pathological unconsciousness. In: *Frontiers in Human Neuroscience* (2013), Nr. SEP

[46] Demertzi, Athena ; Gómez, Francisco ; Crone, Julia S. ; Vanhaudenhuyse, Audrey ; Tshibanda, Luaba ; Noirhomme, Quentin ; arie Thonnard ; Charland-Verville, Vanessa ; Kirsch, Murielle ; Laureys, Steven ; Soddu, Andrea: Multiple fMRI system-level baseline connectivity is disrupted in patients with consciousness alterations. In: *Cortex* 52 (2014), Nr. 0, S. 35–46. – ISSN 0010–9452

[47] Desikan, Rahul S. ; SÃ©gonne, Florent ; Fischl, Bruce ; Quinn, Brian T. ; Dickerson, Bradford C. ; Blacker, Deborah ; Buckner, Randy L. ; Dale, Anders M. ; Maguire, R. P. ; Hyman, Bradley T. ; Albert, Marilyn S. ; Killiany, Ronald J.: An automated labeling system for subdividing the human cerebral cortex on MRI scans into gyral based regions of interest. In: *NeuroImage* 31 (2006), Nr. 3, S. 968 – 980. – ISSN 1053–8119

[48] Destrieux, Christophe ; Fischl, Bruce ; Dale, Anders ; Halgren, Eric: Automatic parcellation of human cortical gyri and sulci using standard anatomical nomenclature. In: *NeuroImage* 53 (2010), Nr. 1, S. 1 – 15. – ISSN 1053–8119

[49] Di Perri, C. ; Stender, J. ; Laureys, S. ; Gosseries, O.: Functional neuroanatomy of disorders of consciousness. In: *Epilepsy and Behavior* 30 (2014), S. 28–32. – ISSN 15255050

[50] Di Perri, Carol ; Amico, Enrico ; Heine, Lizette ; Annen, Jitka ; Martial, Charlotte ; Larroque, Stephen K. ; Soddu, Andrea ; Marinazzo, Daniele ; Laureys, Steven: Multifaceted brain networks reconfiguration in disorders of consciousness uncovered by co-activation patterns. In: *Human Brain Mapping* 39 (2018), jan, Nr. 1, S. 89–103. – ISSN 1065–9471

[51] Di Perri, Carol ; Bahri, Mohamed A. ; Amico, Enrico ; Thibaut, Aurore ; Heine, Lizette ; Antonopoulos, Georgios ; Charland-Verville, Vanessa ; Wannez, Sarah ; Gómez, Francisco ; Hustinx, Roland ; Tshibanda, Luaba ; Demertzi, Athena ; Soddu, Andrea ; Laureys, Steven: Neural correlates of consciousness in patients who have emerged from a minimally conscious state: a cross-sectional multimodal imaging study. In: *The Lancet Neurology* 15 (2016), S. 830–842. – ISSN 1474–4422

[52] Di Perri, Carol ; Thibaut, Aurore ; Heine, Lizette ; Soddu, Andrea ; Demertzi, Athena ; Laureys, Steven: Measuring consciousness in coma and related states. In: *World Journal of Radiology* 6 (2014), S. 589–597. – ISSN 1949–8470

[53] Ding, Hao ; Ming, Dong ; Wan, Baikun ; Li, Qiang ; Qin, Wen ; Yu, Chunshui: Enhanced spontaneous functional connectivity of the superior temporal gyrus in early deafness. In: *Scientific Reports* 6 (2016), Nr. 1, S. 23239. – ISSN 2045–2322

[54] Edelsbrunner, Herbert ; Harer, John: Persistent homology-a survey. In: *Discrete & Computational Geometry - DCG* 453 (2008), 01

[55] Edelsbrunner, Herbert ; Harer, John: *Computational Topology - an Introduction.* 1. American Mathematical Society, 2010. – I–XII, 1–241 S. – ISBN 978–0–8218–4925–5

[56] Ellis, Cameron T. ; Lesnick, Michael ; Henselman-Petrusek, Gregory ; Keller, Bryn ; Cohen, Jonathan D.: Feasibility of topological data analysis for event-related fMRI. In: *Network Neuroscience* 3 (2019), jul, Nr. 3, S. 695–706. – ISSN 2472–1751

[57] Enciso-Olivera, César O. ; nez Rubiano, Edgar G. O. ; Casanova-Libreros, Rosángela ; Rivera, Diana ; Zarate-Ardila, Carol J. ; Rudas, Jorge E. ; Pulido, Cristian ; Gómez, Francisco ; no, Darwin E. Martínez-Ria ; Guerrero, Natalia ; Hurtado, Mayra A. ; Aguilera-Bustos, Natalia ; Hernández-Torres, Clara P. ; Hernández, José ; noz, Jorge H. Marín-Mu Structural and Functional Connectivity of the Ascending Arousal Network for Prediction of Outcome in Patients with Acute Disorders of Consciousness. In: *Scientific Reports* accepted (2021), Nr. preprint

[58] Falcone, Jean-Luc ; Albuquerque, Paul: A Correlation-Based Distance. In: *arXiv e-prints* (2004), Februar, S. cs/0402061

[59] Fernández-Espejo, Davinia ; Bekinschtein, Tristan ; Monti, Martin M. ; Pickard, John D. ; Junque, Carme ; Coleman, Martin R. ; Owen, Adrian M.: Diffusion weighted imaging distinguishes the vegetative state from the minimally conscious state. In: *NeuroImage* 54 (2011), Nr. 1, S. 103–112. – ISSN 1053–8119

[60] Fernández-Espejo, Davinia ; Soddu, Andrea ; Cruse, Damian ; Palacios, Eva M. ; Junque, Carme ; Vanhaudenhuyse, Audrey ; Rivas, Eva ; Newcombe, Virginia ; Menon, David K. ; Pickard, John D. ; Laureys, Steven ; Owen, Adrian M.: A role for the default mode network in the bases of disorders of consciousness. In: *Annals of Neurology* 72 (2012), Nr. 3, S. 335–343. – ISSN 1531–8249

[61] Filippi, Massimo ; Spinelli, Edoardo G. ; Cividini, Camilla ; Agosta, Federica: Resting State Dynamic Functional Connectivity in Neurodegenerative Conditions: A Review of Magnetic Resonance Imaging Findings. In: *Frontiers in neuroscience* 13 (2019), jun, S. 657. – ISSN 1662–4548

[62] Filler, Aaron: The History, Development and Impact of Computed Imaging in Neurological Diagnosis and Neurosurgery: CT, MRI, and DTI. In: *Nature Precedings* (2009)

[63] Fins, Joseph J.: Chapter 15 - Neuroethics and Disorders of Consciousness: A Pragmatic Approach to Neuropalliative Care. In: Laureys, Steven (Hrsg.) ; Gosseries, Olivia (Hrsg.) ; Tononi, Giulio (Hrsg.): *The Neurology of Conciousness (Second Edition)*. Second Edition. San Diego : Academic Press, 2016. – ISBN 978–0–12–800948–2, S. 241–252

[64] Fox, Michael D. ; Raichle, Marcus E.: Spontaneous fluctuations in brain activity observed with functional magnetic resonance imaging. In: *Nature Review Neuroscience* 8 (2007), S. 700–711. – ISSN 1471–003X

[65] Frantzidis, C.A. ; Vivas, A.B. ; Tsolaki, A. ; Klados, M.A. ; Tsolaki, M. ; Bamidis, P.D.: Functional disorganization of small-world brain networks in mild Alzheimer's disease and amnestic Mild cognitive impairment: An EEG study using Relative Wavelet Entropy (RWE). In: *Frontiers in Aging Neuroscience* 6 (2014), Nr. AUG

[66] Fraschini, M. ; Hillebrand, A. ; Demuru, M. ; Didaci, L. ; Marcialis, G.L.: An EEG-based biometric system using eigenvector centrality in resting state brain networks. In: *IEEE Signal Processing Letters* 22 (2014), Nr. 6, S. 666–670

[67] Friston, K.: Chapter 2 - Statistical parametric mapping. In: Friston, Karl (Hrsg.) ; Ashburner, John (Hrsg.) ; Kiebel, Stefan (Hrsg.) ; Nichols, Thomas (Hrsg.) ; Penny, William (Hrsg.): *Statistical Parametric Mapping*. London : Academic Press, 2007. – ISBN 978–0–12–372560–8, S. 10 – 31

[68] Friston, K. J. ; Frith, C. D. ; Liddle, P. F. ; Frackowiak, R. S. J.: Functional Connectivity: The Principal-Component Analysis of Large (PET) Data Sets. In: *J Cereb Blood Flow Metab* 13 (1993), Nr. 1, S. 5–14. – ISSN 0271–678X

[69] Gamboa, O.L. ; Tagliazucchi, E. ; Von Wegner, F. ; Jurcoane, A. ; Wahl, M. ; Laufs, H. ; Ziemann, U.: Working memory performance of early MS patients correlates inversely with modularity increases in resting state functional connectivity networks. In: *NeuroImage* 94 (2014), S. 385–395

[70] Garyfallidis, Eleftherios ; Brett, Matthew ; Amirbekian, Bagrat ; Rokem, Ariel ; Van Der Walt, Stefan ; Descoteaux, Maxime ; Nimmo-Smith, Ian: Dipy, a library for the analysis of diffusion MRI data. In: *Frontiers in Neuroinformatics* 8 (2014), S. 8. – ISSN 1662–5196

[71] Geerligs, L ; Henson, R N. ; Cam-CAN ; Cam-CAN: Functional connectivity and structural covariance between regions of interest can be measured more accurately using multivariate distance correlation. In: *NeuroImage* 135 (2016), S. 16–31

[72] Ghrist, Robert: Barcodes: The persistent topology of data. 45 (2008), 02, S. 61–75

[73] Giacino, Joseph T. ; Kalmar, Kathleen ; Whyte, John: The {JFK} Coma Recovery Scale-Revised: Measurement characteristics and diagnostic utility. In: *Archives of Physical Medicine and Rehabilitation* 85 (2004), Nr. 12, S. 2020–2029. – ISSN 0003–9993

[74] Giacino, J.T. ; Fins, J.J. ; Laureys, S. ; Schiff, N.D.: Disorders of consciousness after acquired brain injury: The state of the science. In: *Nature Reviews Neurology* 10 (2014), Nr. 2, S. 99–114

[75] Giusti, Chad ; Ghrist, Robert ; Bassett, Danielle S.: Two's company, three (or more) is a simplex: Algebraic-topological tools for understanding higher-order structure in neural data. (2016), jan, S. arXiv:1601.01704

[76] Giusti, Chad ; Pastalkova, Eva ; Curto, Carina ; Itskov, Vladimir: Clique topology reveals intrinsic geometric structure in neural correlations. In: *Proceedings of the National Academy of Sciences* 112 (2015), Nr. 44, S. 13455–13460

[77] Greicius, Michael D. ; Srivastava, Gaurav ; Reiss, Allan L. ; Menon, Vinod: Default-mode network activity distinguishes Alzheimer's disease from healthy aging: Evidence from functional MRI. In: *Proceedings of the National Academy of Sciences* 101 (2004), Nr. 13, S. 4637–4642. – ISSN 0027–8424

[78] Grötschel, M. ; Holland, O.: Solving matching problems with linear programming. In: *Mathematical Programming* 33 (1985), Dec, Nr. 3, S. 243–259. – ISSN 1436–4646

[79] Guldenmund, P. ; Vanhaudenhuyse, A. ; Sanders, R. D. ; Sleigh, J. ; Bruno, M. A. ; Demertzi, A. ; Bahri, M. A. ; Jaquet, O. ; Sanfilippo, J. ; Baquero, K. ; Boly, M. ; Brichant, J. F. ; Laureys, S. ; Bonhomme, V.: Brain functional connectivity differentiates dexmedetomidine from propofol and natural sleep. In: *British Journal of Anaesthesia* 119 (2017), Oct, S. 674–684

[80] Guldenmund, Pieter ; Demertzi, Athena ; Boveroux, Pierre ; Boly, Melanie ; Vanhaudenhuyse, Audrey ; Bruno, Marie-Aurélie ; Gosseries, Olivia ; Noirhomme, Quentin ; Brichant, Jean-FranÃ§ois ; Bonhomme, Vincent ; Laureys, Steven ; Soddu, Andrea: Thalamus, Brainstem and Salience Network Connectivity Changes During Propofol-Induced Sedation and Unconsciousness. In: *Brain Connectivity* 3 (2013), Apr, S. 273–285. – ISSN 2158–0014

[81] Hafkemeijer, Anne ; Möller, Christiane ; Dopper, Elise ; Jiskoot, Lize ; Schouten, Tijn ; van Swieten, John ; van der Flier, Wiesje ; Vrenken, Hugo ; Pijnenburg, Yolande ; Barkhof, Frederik ; Scheltens, Philip ; van der Grond, Jeroen ; Rombouts, Serge: Resting state functional connectivity differences between behavioral variant frontotemporal dementia and Alzheimer's disease. In: *Frontiers in Human Neuroscience* 9 (2015), S. 474. – ISSN 1662–5161

[82] Hannawi, Y. ; Lindquist, M.A. ; Caffo, B.S. ; Sair, H.I. ; Stevens, R.D.: Resting brain activity in disorders of consciousness: A systematic review and meta-analysis. In: *Neurology* 84 (2015), Nr. 12, S. 1272–1280

[83] Heine, L. ; Demertzi, A. ; Laureys, S. ; Gosseries, O.: Consciousness: And Disorders of Consciousness. In: Toga, Arthur W. (Hrsg.): *Brain Mapping*. Waltham : Academic Press, 2015. – ISBN 978–0–12–397316–0, S. 1067–1073

[84] Heine, Lizette ; Soddu, Andrea ; Gómez, Francisco ; Vanhaudenhuyse, Audrey ; Tshibanda, Luaba ; Thonnard, Marie ; Charland-Verville, Vanessa ; Kirsch, Murielle ; Laureys, Steven ; Demertzi, Athena: Resting state networks and consciousness. Alterations of multiple resting state network connectivity in physiological, pharmacological and pathological consciousness states. In: *Frontiers in Psychology* 3 (2012), Nr. 295, S. 1–12. – ISSN 1664–1078

[85] van den Heuvel, Martijn P. ; Sporns, Olaf: A cross-disorder connectome landscape of brain dysconnectivity. In: *Nature Reviews Neuroscience* 20 (2019), Nr. 7, S. 435–446. – ISSN 1471–0048

[86] van den Heuvel, Martijn ; Mandl, Rene ; Hulshoff Pol, Hilleke: Normalized Cut Group Clustering of Resting-State fMRI Data. In: *PLoS ONE* 3 (2008), 04, Nr. 4, S. e2001

[87] van den Heuvel, M.P. ; Hulshoff Pol, H.E.: Exploring the brain network: A review on resting-state fMRI functional connectivity. In: *European Neuropsychopharmacology* 20 (2010), Nr. 8, S. 519–534

[88] van den Heuvel, M.P. ; Sporns, O.: An anatomical substrate for integration among functional networks in human cortex. In: *Journal of Neuroscience* 33 (2013), Nr. 36, S. 14489–14500

[89] van den Heuvel, M.P. ; Sporns, O.: Network hubs in the human brain. In: *Trends in Cognitive Sciences* 17 (2013), Nr. 12, S. 683–696

[90] Hirschberg, Ron ; Giacino, Joseph T.: The Vegetative and Minimally Conscious States: Diagnosis, Prognosis and Treatment. In: *Neurologic Clinics* 29 (2011), Nr. 4, S. 773–786. – Disorders of Consciousness. – ISSN 0733–8619

[91] Hoffman, E.J. ; Huang, S.-C. ; Phelps, M.E.: Quantitation in positron emission computed tomography: 1. effect of object size. In: *Journal of Computer Assisted Tomography* 3 (1979), Nr. 3, S. 299–308

[92] Huang, Lixuan ; Zheng, Yan ; Zeng, Zisan ; Li, Muyan ; Zhang, Ling ; Gao, Yang: Fractional Amplitude of Low-Frequency Fluctuations and Functional Connectivity in Comatose Patients Subjected to Resting-State Functional Magnetic Resonance Imaging. In: *Annals of Indian Academy of Neurology* 22 (2019), Nr. 2, S. 203–209. – ISSN 0972–2327

[93] Islambekov, Umar ; Gel, Yulia R.: Unsupervised space-time clustering using persistent homology. In: *Environmetrics* 30 (2019), Nr. 4, S. e2539. – e2539 env.2539

[94] Jafri, Madiha J. ; Pearlson, Godfrey D. ; Stevens, Michael ; Calhoun, Vince D.: A method for functional network connectivity among spatially independent resting-state components in schizophrenia. In: *NeuroImage* 39 (2008), Feb, S. 1666–1681. – ISSN 1053–8119

[95] Jang, Joon H. ; Kim, Jae-Hun ; Yun, Je-Yeon ; Choi, Soo-Hee ; An, Seung C. ; Kang, Do-Hyung: Differences in Functional Connectivity of the Insula Between Brain Wave Vibration in Meditators and Non-meditators. In: *Mindfulness* 9 (2018), Nr. 6, S. 1857–1866. – ISSN 1868–8527

[96] Joyce, Karen E. ; Laurienti, Paul J. ; Burdette, Jonathan H. ; Hayasaka, Satoru: A New Measure of Centrality for Brain Networks. In: *PLOS ONE* 5 (2010), 08, Nr. 8, S. 1–13

[97] Kandeepan, Sivayini ; Rudas, Jorge ; Gomez, Francisco ; Stojanoski, Bobby ; Valluri, Sreeram ; Owen, Adrian M. ; Naci, Lorina ; Nichols, Emily S. ; Soddu,

Andrea: Modeling an auditory stimulated brain under altered states of consciousness using the generalized Ising model. In: *NeuroImage* 223 (2020), dec, S. 117367. – ISSN 1095–9572 (Electronic)

[98] Kirsch, Muriëlle ; Guldenmund, Pieter ; Ali Bahri, Mohamed ; Demertzi, Athena ; Baquero, Katherine ; Heine, Lizette ; Charland-Verville, Vanessa ; Vanhaudenhuyse, Audrey ; Bruno, Marie-AurÃ©lie ; Gosseries, Olivia ; Di Perri, Carol ; Ziegler, Erik ; Brichant, Jean-FranÃ§ois ; Soddu, Andrea ; Bonhomme, Vincent ; Laureys, Steven: Sedation of Patients With Disorders of Consciousness During Neuroimaging: Effects on Resting State Functional Brain Connectivity. In: *Anesthesia & Analgesia* 124 (2017). – ISSN 0003–2999

[99] Koch, Christof ; Massimini, Marcello ; Boly, Melanie ; Tononi, Giulio: Neural correlates of consciousness: Progress and problems. In: *Nature Reviews Neuroscience* 17 (2016), S. 307–321

[100] Kono, Kai T. ; Takeuchi, Tsutomu T. ; Cooray, Suchetha ; Nishizawa, Atsushi J. ; Murakami, Koya. *A Study on the Baryon Acoustic Oscillation with Topological Data Analysis*. jun 2020

[101] Kristensen, Line B. ; Wang, Lin ; Petersson, Karl M. ; Hagoort, Peter: The Interface Between Language and Attention: Prosodic Focus Marking Recruits a General Attention Network in Spoken Language Comprehension. In: *Cerebral Cortex* 23 (2012), 07, Nr. 8, S. 1836–1848. – ISSN 1047–3211

[102] Larson-Prior, Linda J. ; Zempel, John M. ; Nolan, Tracy S. ; Prior, Fred W. ; Snyder, Abraham Z. ; Raichle, Marcus E.: Cortical network functional connectivity in the descent to sleep. In: *Proceedings of the National Academy of Sciences* 106 (2009), Nr. 11, S. 4489–4494

[103] Laureys, S. ; Schiff, N.D.: Coma and consciousness: Paradigms (re)framed by neuroimaging. In: *NeuroImage* 61 (2012), Nr. 2, S. 478–491

[104] Laureys, Steven ; Owen, Adrian M. ; Schiff, Nicholas D.: Brain function in coma, vegetative state, and related disorders. In: *The Lancet Neurology* 3 (2004), Nr. 9, S. 537–546. – ISSN 1474–4422

[105] Lauterbur, P.C.: Image Formation by Induced Local Interactions: Examples Employing Nuclear Magnetic Resonance. In: *nature* 242 (1973), März, S. 190–191

[106] Lee, M.H. ; Smyser, C.D. ; Shimony, J.S: Resting-state fMRI: a review of methods and clinical applications. In: *American journal of neuroradiology* 34 (2013), Oct, S. 1866 – 1872. – ISSN 1936–959X

[107] Liu, Chang ; Pu, Weidan ; Wu, Guowei ; Zhao, Jie ; Xue, Zhimin: Abnormal resting-state cerebral-limbic functional connectivity in bipolar depression and unipolar depression. In: *BMC Neuroscience* 20 (2019), Nr. 1, S. 30. – ISSN 1471–2202

[108] Liu, Jiao ; Wang, Qin ; Liu, Feiwen ; Song, Haiyan ; Liang, Xiaofeng ; Lin, Zhengkun ; Hong, Wenjun ; Yang, Shanli ; Huang, Jia ; Zheng, Guohua ; Tao, Jing ; Chen, Li-Dian: Altered functional connectivity in patients with post-stroke memory impairment: A resting fMRI study. In: *Experimental and therapeutic medicine* 14 (2017), sep, Nr. 3, S. 1919–1928. – ISSN 1792–0981

[109] Liu, Xiaozheng ; Chen, Wei ; Tu, Yunhai ; Hou, Hongtao ; Huang, Xiaoyan ; Chen, Xingli ; Guo, Zhongwei ; Bai, Guanghui ; Chen, Wei: The Abnormal Functional Connectivity between the Hypothalamus and the Temporal Gyrus Underlying Depression in Alzheimer's Disease Patients. In: *Frontiers in aging neuroscience* 10 (2018), feb, S. 37. – ISSN 1663–4365

[110] Lohmann, Gabriele ; Margulies, Daniel S. ; Horstmann, Annette ; Pleger, Burkhard ; Lepsien, Joeran ; Goldhahn, Dirk ; Schloegl, Haiko ; Stumvoll, Michael ; Villringer, Arno ; Turner, Robert: Eigenvector Centrality Mapping for Analyzing Connectivity Patterns in fMRI Data of the Human Brain. In: *PLOS ONE* 5 (2010), 04, Nr. 4, S. 1–8

[111] Lord, Louis-David ; Expert, Paul ; Fernandes, Henrique M. ; Petri, Giovanni ; Van Hartevelt, Tim J. ; Vaccarino, Francesco ; Deco, Gustavo ; Turkheimer, Federico ; Kringelbach, Morten L.: Insights into Brain Architectures from the Homological Scaffolds of Functional Connectivity Networks. In: *Frontiers in Systems Neuroscience* 10 (2016), S. 85. ISBN 1662–5137

[112] Lum, P. Y. ; Singh, G. ; Lehman, A. ; Ishkanov, T. ; Vejdemo-Johansson, M. ; Alagappan, M. ; Carlsson, J. ; Carlsson, G.: Extracting insights from the shape of complex data using topology. In: *Scientific Reports* 3 (2013), Februar, S. 1236–

[113] Lutsep, H.L. ; Albers, G.W. ; DeCrespigny, A. ; Kamat, G.N. ; Marks, M.P. ; Moseley, M.E.: Clinical utility of diffusion-weighted magnetic resonance imaging in the assessment of ischemic stroke. In: *Annals of Neurology* 41 (1997), Nr. 5, S. 574–580

[114] Malagurski, Brigitta ; PÃ©ran, Patrice ; Sarton, Benjamine ; Vinour, Hélène ; Naboulsi, Edouard ; Riu, Béatrice ; Bounes, Fanny ; Seguin, Thierry ; Lotterie, Jean A. ; Fourcade, Olivier ; Minville, Vincent ; Ferré, Fabrice ; Achard, Sophie ; Silva, Stein: Topological disintegration of resting state functional connectomes in coma. In: *NeuroImage* 195 (2019), S. 354–361. – ISSN 1053–8119

[115] Manno, Edward M.: Coma and Disorders of Consciousness. In: Bhardwaj, Anish (Hrsg.) ; Mirski, Marek A. (Hrsg.): *Handbook of Neurocritical Care*. Springer New York, 2010. – ISBN 978–1–4419–6841–8, S. 277–286

[116] Mao, Xing-gang ; Xue, Xiao-yan ; Wang, Ling ; Wang, Liang ; Li, Liang ; Zhang, Xiang: Hypoxia Regulated Gene Network in Glioblastoma Has Special Algebraic Topology Structures and Revealed Communications Involving Warburg Effect and Immune Regulation. In: *Cellular and Molecular Neurobiology* 39 (2019), Nr. 8, S. 1093–1114. – ISSN 1573–6830

[117] Martínez, Darwin E. ; Martínez, Johann H. ; Rudas, Jorge E. ; Demertzi, Athena ; Heine, Lizette ; Tshibanda, Luaba ; Soddu, Andrea ; Laureys, Steven ; Gómez, Francisco: Functional resting state networks characterization through global network measurements for patients with disorders of consciousness. In: *Computing Colombian Conference (10CCC), 2015 10th*, 2015, S. 8

[118] Martínez, Darwin E. ; Martínez, Johann H. ; Rudas, Jorge E. ; Demertzi, Athena ; Heine, Lizette ; Tshibanda, Luaba ; Soddu, Andrea ; Laureys, Steven ; Gómez, Francisco: A graph based characterization of functional resting state networks for patients with disorders of consciousness. In: *Image, Signal Processing and Artificial Vision (STSIVA), 2015 XX Symposium on*, 2015, S. 8

[119] Martínez, Darwin E. ; Rudas, Jorge ; Demertzi, Athena ; Charland-Verville, Vanessa ; Soddu, Andrea ; Laureys, Steven ; Gómez, Francisco: Reconfiguration of large-scale functional connectivity in patients with disorders of consciousness. In: *Brain and Behavior* 10 (2020), jan, Nr. 1, S. e1476. – ISSN 2162–3279

[120] Mazaika, P.K. ; Hoeft, F. ; Glover, G.H. ; Reiss, A.L.: Methods and Software for fMRI Analysis of Clinical Subjects. In: *NeuroImage* 47 (2009), Nr. Supplement 1, S. S58

[121] McKeown, M. J. ; Makeig, S. ; Brown, G. G. ; Jung, T. ; Kindermann, S. S. ; Bell, A. J. ; Sejnowski, T. J.: Analysis of fMRI data by blind separation into independent spatial components. In: *Human Brain Mapping* 6 (1998), S. 160–188

[122] Mencarelli, L ; Biagi, M C. ; Salvador, R ; Romanella, S ; Ruffini, G ; Rossi, S ; Santarnecchi, E: Network mapping of connectivity alterations in disorder of consciousness: Towards targeted neuromodulation. In: *Journal of Clinical Medicine* 9 (2020), Nr. 3

[123] Moreno-Ayure, Michela ; Páez, Cristian ; López-Arias, María A ; Mendez-Betancurt, Johan L. ; Ordóñez-Rubiano, Edgar G. ; Rudas, Jorge ; Pulido, Cristian ; Gómez, Francisco ; Martínez, Darwin ; Enciso-Olivera, Cesar O. ;

Rivera-Triana, Diana P. ; Casanova-Libreros, Rosangela ; Aguilera, Natalia ; Marín-Muñoz, Jorge H.: Establishing an acquisition and processing protocol for resting state networks with a 1.5 T scanner: A case series in a middle-income country. In: *Medicine* 99 (2020), jul, Nr. 28, S. e21125–e21125. – ISSN 1536–5964

[124] Muñoz-López, M ; Insausti, R ; Mohedano-Moriano, A ; Mishkin, M ; Saunders, R C.: Anatomical pathways for auditory memory II: information from rostral superior temporal gyrus to dorsolateral temporal pole and medial temporal cortex. In: *Frontiers in neuroscience* 9 (2015), may, S. 158. – ISSN 1662–4548

[125] NITRC. *NITRC: Neuroimaging Tools & Resources Collaboratory*. 2020

[126] Ogawa, Seiji ; Sung, Yul-Wan: Selected Topics Relating to Functional MRI Study of the Brain. In: *The Keio Journal of Medicine* 68 (2019), Nr. 4, S. 73–86

[127] Olson, Ingrid R. ; McCoy, David ; Klobusicky, Elizabeth ; Ross, Lars A.: Social cognition and the anterior temporal lobes: a review and theoretical framework. In: *Social cognitive and affective neuroscience* 8 (2013), feb, Nr. 2, S. 123–133. – ISSN 1749–5024

[128] Owen, Adrian M.: Disorders of Consciousness. In: *Annals of the New York Academy of Sciences* 1124 (2008), mar, Nr. 1, S. 225–238. – ISSN 0077–8923

[129] Pape, Theresa Louise-Bender ; Mallinson, Trudy ; Guernon, Ann: Psychometric Properties of the Disorders of Consciousness Scale. In: *Archives of Physical Medicine and Rehabilitation* 95 (2014), Nr. 9, S. 1672–1684. – ISSN 0003–9993

[130] Ribeiro de Paula, Demetrius ; Ziegler, Erik ; Abeyasinghe, Pubuditha M. ; Das, Tushar K. ; Cavaliere, Carlo ; Aiello, Marco ; Heine, Lizette ; di Perri, Carol ; Demertzi, Athena ; Noirhomme, Quentin ; Charland-Verville, Vanessa ; Vanhaudenhuyse, Audrey ; Stender, Johan ; Gómez, Francisco ; Tshibanda, Jean-Flory L. ; Laureys, Steven ; Owen, Adrian M. ; Soddu, Andrea: A method for independent component graph analysis of resting-state fMRI. In: *Brain and Behavior* 7 (2017), Nr. 3, S. e00626. – ISSN 2162–3279

[131] Penny, William (Hrsg.) ; Friston, Karl (Hrsg.) ; Ashburner, John (Hrsg.) ; Kiebel, Stefan (Hrsg.) ; Nichols, Thomas (Hrsg.): *Connectivity*. 1. Herausgeber : Elsevier, 2011. – ISBN 978–0–08–046650–7

[132] Petri, G ; Expert, P ; Turkheimer, F ; Carhart-Harris, R ; Nutt, D ; Hellyer, P J. ; Vaccarino, F: Homological scaffolds of brain functional networks. In: *Journal of The Royal Society Interface* 11 (2014), dec, Nr. 101, S. 20140873

[133] Pfurtscheller, G. ; Aranibar, A.: Event-related cortical desynchronization detected by power measurements of scalp EEG. In: *Electroencephalography and Clinical Neurophysiology* 42 (1977), Nr. 6, S. 817–826

[134] Power, Jonathan D. ; Barnes, Kelly A. ; Snyder, Abraham Z. ; Schlaggar, Bradley L. ; Petersen, Steven E.: Spurious but systematic correlations in functional connectivity MRI networks arise from subject motion. In: *NeuroImage* 59 (2012), Nr. 3, S. 2142 – 2154. – ISSN 1053–8119

[135] Preti, Maria G. ; Bolton, Thomas A W. ; Ville, Dimitri Van D.: The dynamic functional connectome: State-of-the-art and perspectives. In: *NeuroImage* 160 (2017), S. 41–54. – ISSN 1053–8119

[136] Raichle, Marcus E. ; MacLeod, Ann M. ; Snyder, Abraham Z. ; Powers, William J. ; Gusnard, Debra A. ; Shulman, Gordon L.: A default mode of brain function. In: *Proceedings of the National Academy of Sciences* 98 (2001), Nr. 2, S. 676–682

[137] Redcay, E. ; Moran, J.M. ; Mavros, P.L. ; Tager-Flusberg, H. ; Gabrieli, J.D.E. ; Whitfield-Gabrieli, S.: Intrinsic functional network organization in high-functioning adolescents with autism spectrum disorder. In: *Frontiers in Human Neuroscience* (2013), Nr. SEP

[138] Ropper, A.H. ; Samuels, M.A.: Coma and Related Disorders of Consciousness. In: Victor's, Adams (Hrsg.): *Principles of Neurology*. 10. New York : McGraw-Hill, 2014. – 17. Coma and Related Disorders of Consciousness. – ISBN 978–0071499927, Kapitel 17, S. 339–361

[139] Rosazza, C. ; Minati, L.: Resting-state brain networks: Literature review and clinical applications. In: *Neurological Sciences* 32 (2011), S. 773–785

[140] Rubin, Emily B. ; Bernat, James L.: Ethical Aspects of Disordered States of Consciousness. In: *Neurologic Clinics* 29 (2011), Nr. 4, S. 1055–1071. – Disorders of Consciousness. – ISSN 0733–8619

[141] Rubinov, M. ; Bullmore, E.: Fledgling pathoconnectomics of psychiatric disorders. In: *Trends in Cognitive Sciences* 17 (2013), Nr. 12, S. 641–647

[142] Rubinov, Mikail ; Sporns, Olaf: Complex network measures of brain connectivity: Uses and interpretations. In: *NeuroImage* 52 (2010), Nr. 3, S. 1059 – 1069. – ISSN 1053–8119

[143] Rudas, J. ; Guaje, J. ; Demertzi, A. ; Heine, L. ; Tshibanda, L. ; Soddu, A. ; Laureys, S. ; Gómez, F.: A method for functional network connectivity using

distance correlation. In: *Engineering in Medicine and Biology Society (EMBC), 2014 36th Annual International Conference of the IEEE*, 2014. – ISSN 1557–170X, S. 2793–2796

[144] Rudas, Jorge ; Martínez, Darwin ; Castellanos, Gabriel ; Demertzi, Athena ; Martial, Charlotte ; Carriére, Manon ; Aubinet, Charlène ; Soddu, Andrea ; Laureys, Steven ; Gómez, Francisco: Time-Delay Latency of Resting-State Blood Oxygen Level-Dependent Signal Related to the Level of Consciousness in Patients with Severe Consciousness Impairment. In: *Brain Connectivity* 10 (2020), mar, Nr. 2, S. 83–94. – ISSN 2158–0014

[145] Saggar, Manish ; Sporns, Olaf ; Gonzalez-Castillo, Javier ; Bandettini, Peter A. ; Carlsson, Gunnar ; Glover, Gary ; Reiss, Allan L.: Towards a new approach to reveal dynamical organization of the brain using topological data analysis. In: *Nature Communications* 9 (2018), Nr. 1, S. 1399. – ISSN 2041–1723

[146] Sakoglu, U. ; Pearlson, G. ; Kiehl, K. ; Wang, Y. ; Michael, A. ; Calhoun, V.: A method for evaluating dynamic functional network connectivity and task-modulation: application to schizophrenia. In: *MAGMA* 23 (2010), Dec, Nr. 5-6, S. 351–366

[147] Salch, Andrew ; Regalski, Adam ; Abdallah, Hassan ; Suryadevara, Raviteja ; Catanzaro, Michael J. ; Diwadkar, Vaibhav A.: From mathematics to medicine: A practical primer on topological data analysis (TDA) and the development of related analytic tools for the functional discovery of latent structure in fMRI data. In: *PLOS ONE* 16 (2021), aug, Nr. 8, S. e0255859

[148] Santarnecchi, E. ; Rossi, S. ; Rossi, A.: The smarter, the stronger: Intelligence level correlates with brain resilience to systematic insults. In: *Cortex* 64 (2015)

[149] Sarasso, Simone ; Casali, Adenauer G. ; Casarotto, Silvia ; Rosanova, Mario ; Sinigaglia, Corrado ; Massimini, Marcello: Consciousness and complexity: a consilience of evidence. In: *Neuroscience of Consciousness* (2021), aug. – ISSN 2057–2107

[150] Schiff, Nicholas D.: Central Thalamic Contributions to Arousal Regulation and Neurological Disorders of Consciousness. In: *Annals of the New York Academy of Sciences* 1129 (2008), 5, Nr. 1, S. 105–118. – ISSN 1749–6632

[151] Schmidt, A. ; Diwadkar, V.A. ; Smieskova, R. ; Harrisberger, F. ; Lang, U.E. ; McGuire, P. ; Fusar-Poli, P. ; Borgwardt, S.: Approaching a network connectivity-driven classification of the psychosis continuum: A selective review and suggestions for future research. In: *Frontiers in Human Neuroscience* 8 (2015), Nr. JAN, S. 1–16

[152] Schnakers, Caroline ; Chatelle, Camille ; Majerus, Steve ; Gosseries, Olivia ; De Val, Marie ; Laureys, Steven: Assessment and detection of pain in noncommunicative severely brain-injured patients. In: *Expert Review of Neurotherapeutics* 10 (2010), Nr. 11, S. 1725–1731

[153] Schnakers, Caroline ; Laureys, Steven: *Coma and Disorders of Consciousness*. 1. London : Springer, 2012. – ISBN 9781447124405

[154] Schnakers, Caroline ; Majerus, Steve ; Giacino, Joseph ; Vanhaudenhuyse, Audrey ; Bruno, Marie-Aurelie ; Boly, Melanie ; Moonen, Gustave ; Damas, Pierre ; Lambermont, Bernard ; Lamy, Maurice ; Damas, François ; Ventura, Manfredi ; Laureys, Steven: A French validation study of the Coma Recovery Scale-Revised (CRS-R). In: *Brain Injury* 22 (2008), Nr. 10, S. 786–792

[155] Singh, Gurjeet ; Memoli, Facundo ; Carlsson, Gunnar: Topological Methods for the Analysis of High Dimensional Data Sets and 3D Object Recognition. In: Botsch, M. (Hrsg.) ; Pajarola, R. (Hrsg.) ; Chen, B. (Hrsg.) ; Zwicker, M. (Hrsg.): *Eurographics Symposium on Point-Based Graphics*, The Eurographics Association, 2007. – ISBN 978–3–905673–51–7

[156] Snider, S B. ; Edlow, B L.: MRI in disorders of consciousness. In: *Current opinion in neurology* 33 (2020), Nr. 6, S. 676–683

[157] Song, Limei ; Ge, Yanming ; Long, Jinfeng ; Dong, Peng: Altered Intrinsic and Casual Functional Connectivities of the Middle Temporal Visual Motion Area Subregions in Chess Experts. In: *Frontiers in Neuroscience* 14 (2020), S. 1203. – ISSN 1662–453X

[158] Sporns, O.: The non-random brain: Efficiency, economy, and complex dynamics. In: *Frontiers in Computational Neuroscience* (2011), Nr. FEBRUARY

[159] Sporns, O.: Structure and function of complex brain networks. In: *Dialogues in Clinical Neuroscience* 15 (2013), Nr. 3, S. 247–262

[160] Sporns, O. ; Chialvo, D.R. ; Kaiser, M. ; Hilgetag, C.C.: Organization, development and function of complex brain networks. In: *Trends in Cognitive Sciences* 8 (2004), Nr. 9, S. 418–425

[161] Stender, Johan ; Gosseries, Olivia ; Bruno, Marie-Aurélie ; Charland-Verville, Vanessa ; Vanhaudenhuyse, Audrey ; Demertzi, Athena ; Chatelle, Camille ; Thonnard, Marie ; Thibaut, Aurore ; Heine, Lizette ; Soddu, Andrea ; Boly, Melanie ; Schnakers, Caroline ; Gjedde, Albert ; Laureys, Steven: Diagnostic precision of PET imaging and functional MRI in disorders of consciousness: a clinical validation study. In: *The Lancet* 384 (2014), Nr. 9942, S. 514–522

[162] Strogatz, S.H.: Exploring complex networks. In: *Nature* 410 (2001), Nr. 6825, S. 268–276

[163] Székely, Gábor J. ; Rizzo, Maria L. ; Bakirov, Nail K.: Measuring and Testing Dependence by Correlation of Distances. In: *The Annals of Statistics* 35 (2007), Nr. 6, S. 2769–2794. – ISSN 00905364

[164] Taylor, P.N. ; Kaiser, M. ; Dauwels, J.: Structural connectivity based whole brain modelling in epilepsy. In: *Journal of Neuroscience Methods* 236 (2014), S. 51–57

[165] Teasdale, G ; Jennett, B: Assessment of coma and impaired consciousness. A practical scale. In: *Lancet (London, England)* 2 (1974), jul, Nr. 7872, S. 81–84. – ISSN 0140–6736 (Print)

[166] Teasdale, G ; Jennett, B: Assessment and prognosis of coma after head injury. In: *Acta neurochirurgica* 34 (1976), Nr. 1-4, S. 45–55. – ISSN 0001–6268 (Print)

[167] Tononi, G ; Sporns, O ; Edelman, G M.: A measure for brain complexity: relating functional segregation and integration in the nervous system. In: *Proceedings of the National Academy of Sciences* 91 (1994), Nr. 11, S. 5033–5037

[168] Tononi, Giulio ; Koch, Christof: The Neural Correlates of Consciousness. In: *Annals of the New York Academy of Sciences* 1124 (2008), Nr. 1, S. 239–261. – ISSN 1749–6632

[169] Tononi, Giulio ; Koch, Christof: Consciousness: here, there and everywhere? In: *Philosophical Transactions of the Royal Society of London B: Biological Sciences* 370 (2015), Nr. 1668. – ISSN 0962–8436

[170] Toussaint, P.-J. ; Maiz, S. ; Coynel, D. ; Doyon, J. ; Messé, A. ; de Souza, L.C. ; Sarazin, M. ; Perlbarg, V. ; Habert, M.-O. ; Benali, H.: Characteristics of the default mode functional connectivity in normal ageing and Alzheimer's disease using resting state fMRI with a combined approach of entropy-based and graph theoretical measurements. In: *NeuroImage* 101 (2014), S. 778–786

[171] Tralie, Christopher ; Saul, Nathaniel ; Bar-On, Rann: Ripser.py: A Lean Persistent Homology Library for Python. In: *Journal of Open Software* 3 (2018), Nr. 29, S. 925–928

[172] Turken, A. ; Dronkers, N.: The Neural Architecture of the Language Comprehension Network: Converging Evidence from Lesion and Connectivity Analyses. In: *Frontiers in Systems Neuroscience* 5 (2011), S. 1. – ISSN 1662–5137

[173] Uddin, L.Q. ; Mooshagian, E. ; Zaidel, E. ; Scheres, A. ; Margulies, D.S. ; Kelly, A.M.C. ; Shehzad, Z. ; Adelstein, J.S. ; Castellanos, F.X. ; Biswal,

B.B. ; Milham, M.P.: Residual functional connectivity in the split-brain revealed with resting-state functional MRI. In: *NeuroReport* 19 (2008), S. 703 – 709. – ISSN 0959–4965

[174] Uddin, Lucina Q. ; Nomi, Jason S. ; Hébert-Seropian, Benjamin ; Ghaziri, Jimmy ; Boucher, Olivier: Structure and Function of the Human Insula. In: *Journal of clinical neurophysiology : official publication of the American Electroencephalographic Society* 34 (2017), jul, Nr. 4, S. 300–306. – ISSN 1537–1603

[175] Uludağ, Kâmil ; Uğurbil, Kâmil: Physiology and Physics of the fMRI Signal. In: Uludag, Kamil (Hrsg.) ; Ugurbil, Kamil (Hrsg.) ; Berliner, Lawrence (Hrsg.): *fMRI: From Nuclear Spins to Brain Functions*. Boston, MA : Springer US, 2015, Kapitel 8, S. 163–213

[176] Van Dellen, E. ; Douw, L. ; Hillebrand, A. ; de Witt Hamer, P.C. ; Baayen, J.C. ; Heimans, J.J. ; Reijneveld, J.C. ; Stam, C.J.: Epilepsy surgery outcome and functional network alterations in longitudinal MEG: A minimum spanning tree analysis. In: *NeuroImage* 86 (2014), S. 354–363

[177] Vanhaudenhuyse, Audrey ; Noirhomme, Quentin ; Tshibanda, Luaba J.-F. ; Bruno, Marie-Aurelie ; Boveroux, Pierre ; Schnakers, Caroline ; Soddu, Andrea ; Perlbarg, Vincent ; Ledoux, Didier ; Brichant, Jean-François ; Moonen, Gustave ; Maquet, Pierre ; Greicius, Michael D. ; Laureys, Steven ; Boly, Melanie: Default network connectivity reflects the level of consciousness in non-communicative brain-damaged patients. In: *Brain* 133 (2010), Nr. 1, S. 161–171. – ISSN 0006–8950

[178] Vuksanović, V.a b. ; Hövel, P.a b.: Functional connectivity of distant cortical regions: Role of remote synchronization and symmetry in interactions. In: *NeuroImage* 97 (2014), S. 1–8

[179] Wang, R. ; Lin, P. ; Liu, M. ; Wu, Y. ; Zhou, T. ; Zhou, C.: Hierarchical Connectome Modes and Critical State Jointly Maximize Human Brain Functional Diversity. In: *Physical Review Letters* 123 (2019), Nr. 3

[180] Watts, Duncan J. ; Strogatz, Steven H.: Collective dynamics of small-world networks. In: *Nature* 393 (1998), S. 440–442. – ISSN 0028–0836

[181] Welch, B. L.: The generalisation of student's problems when several different population variances are involved. In: *Biometrika* 34 (1947), S. 28–35. – ISSN 0006–3444

[182] Whyte, John: Rancho Los Amigos Scale. In: Kreutzer, Jeffrey S. (Hrsg.) ; DeLuca, John (Hrsg.) ; Caplan, Bruce (Hrsg.): *Encyclopedia of Clinical Neuropsychology*. Springer New York, 2011. – ISBN 978–0–387–79947–6, S. 2110–2110

[183] Wig, G.S.: Segregated Systems of Human Brain Networks. In: *Trends in Cognitive Sciences* 21 (2017), Nr. 12, S. 981–996

[184] Woolrich, Mark W. ; Jbabdi, Saad ; Patenaude, Brian ; Chappell, Michael ; Makni, Salima ; Behrens, Timothy ; Beckmann, Christian ; Jenkinson, Mark ; Smith, Stephen M.: Bayesian analysis of neuroimaging data in FSL. In: *NeuroImage* 45 (2009), Nr. 1, Supplement 1, S. S173–S186. – ISSN 1053–8119

[185] Wu, Guo-Rong ; Liao, Wei ; Stramaglia, Sebastiano ; Ding, Ju-Rong ; Chen, Huafu ; Marinazzo, Daniele: A blind deconvolution approach to recover effective connectivity brain networks from resting state fMRI data. In: *Medical Image Analysis* 17 (2013), Nr. 3, S. 365–374. – ISSN 1361–8415

[186] Xie, Xiaoping ; Cao, Zhitong ; Weng, Xuchu: Spatiotemporal nonlinearity in resting-state fMRI of the human brain. In: *NeuroImage* 40 (2008), Nr. 4, S. 1672–1685. – ISSN 1053–8119

[187] Xiong, Hang ; Guo, Rong-Juan ; Shi, Hua-Wei: Altered Default Mode Network and Salience Network Functional Connectivity in Patients with Generalized Anxiety Disorders: An ICA-Based Resting-State fMRI Study. In: *Evidence-Based Complementary and Alternative Medicine* 2020 (2020), S. 4048916. – ISSN 1741–427X

[188] Xu, Yaping: Altered brain functional connectivity and correlation with psychological status in patients with unilateral pulsatile tinnitus. In: *Neuroscience Letters* 705 (2019), jul, S. 235–245. – ISSN 18727972

[189] Xue, K. ; Luo, C. ; Zhang, D. ; Yang, T. ; Li, J. ; Gong, D. ; Chen, L. ; Medina, Y.I. ; Gotman, J. ; Zhou, D. ; Yao, D.: Diffusion tensor tractography reveals disrupted structural connectivity in childhood absence epilepsy. In: *Epilepsy Research* 108 (2014), Nr. 1, S. 125–138

[190] Ylipaavalniemi, Jarkko ; VigÃ¡rio, Ricardo: Analyzing consistency of independent components: An fMRI illustration. In: *NeuroImage* 39 (2008), Nr. 1, S. 169–180. – ISSN 1053–8119

[191] Yoo, K ; Rosenberg, M D. ; Noble, S ; Scheinost, D ; Constable, R T. ; Chun, M M.: Multivariate approaches improve the reliability and validity of functional connectivity and prediction of individual behaviors. In: *NeuroImage* 197 (2019), S. 212–223

[192] Yu, Q. ; Erhardt, E.B. ; Sui, J. ; Du, Y. d. ; He, H. ; Hjelm, D. ; Cetin, M.S. ; Rachakonda, S. ; Miller, R.L. ; Pearlson, G. ; Calhoun, V.D.: Assessing dynamic brain graphs of time-varying connectivity in fMRI data: Application to healthy controls and patients with schizophrenia. In: *NeuroImage* 107 (2015), S. 345–355

[193] Yu, Q. ; Sui, J. ; Kiehl, K.A. ; Pearlson, G. ; Calhoun, V.D.: State-related functional integration and functional segregation brain networks in schizophrenia. In: *Schizophrenia Research* 150 (2013), Nr. 2-3, S. 450–458

[194] Zhang, Huayu ; Zhao, Yue ; Cao, Weifang ; Cui, Dong ; Jiao, Qing ; Lu, Weizhao ; Li, Hongyu ; Qiu, Jianfeng: Aberrant functional connectivity in resting state networks of ADHD patients revealed by independent component analysis. In: *BMC Neuroscience* 21 (2020), Nr. 1, S. 39. – ISSN 1471–2202

[195] Zhang, Jin-Tao ; Yao, Yuan-Wei ; Li, Chiang-Shan R. ; Zang, Yu-Feng ; Shen, Zi-Jiao ; Liu, Lu ; Wang, Ling-Jiao ; Liu, Ben ; Fang, Xiao-Yi: Altered resting-state functional connectivity of the insula in young adults with Internet gaming disorder. In: *Addiction Biology* 21 (2016), may, Nr. 3, S. 743–751. – ISSN 1355–6215

[196] Zhou, J. ; Seeley, W.W.: Network dysfunction in Alzheimer's disease and frontotemporal dementia: implications for psychiatry. In: *Biological Psychiatry* 75 (2014), S. 565–573

[197] Zhu, Feiyin ; Tang, Liying ; Zhu, Peiwen ; Lin, Qi ; Yuan, Qing ; Shi, Wenqing ; Li, Biao ; Ye, Lei ; Min, Youlan ; Su, Ting ; Shao, Yi: Resting-state functional magnetic resonance imaging (fMRI) and functional connectivity density mapping in patients with corneal ulcer. In: *Neuropsychiatric disease and treatment* 15 (2019), jul, S. 1833–1844. – ISSN 1176–6328